The Robustness of Energy Systems

A novel method to explore the impact of uncertainties on Energy System Design Optimization Models

J.L. Fraiture

TU Delft

ORTEC
OPTIMIZE YOUR WORLD

The Robustness of Energy Systems

Master thesis submitted to Delft University of Technology

in partial fulfilment of the requirements for the degree of

MASTER OF SCIENCE

in **Engineering and Policy Analysis**

Faculty of Technology, Policy and Management

by

Julie Fraiture

Student number: 4260627

To be defended in public on March 17, 2020

Graduation committee

Chairperson	: Dr. ir. J.H. Kwakkel, Section Policy Analysis
First Supervisor	: Dr. ir. E.J.L. Chappin, Section Energy and Industry
External Supervisor	: Ir. I. van Beuzekom, ORTEC B.V.

Executive Summary

To achieve the goal of decreasing greenhouse gas emissions as stated in the Paris Agreement, it is necessary to largely increase the deployment of renewable energy sources for the production of energy. Without infrastructural changes, the current energy system is not able to accommodate this energy transition. A long-term view is necessary in the design of energy systems to ensure that investment and operational decision-making leads to robust real-world energy systems that deliver this transition goal. Energy system planners and decision makers rely on Energy System Optimization Models in assisting these long-term design decisions. However, the long-term development of the energy system is characterized by a combination of factors that are uncertain, such as technology innovations, resource availability and socio-economic dynamics. This introduces uncertainty into the model outcomes. Optimization usually provides a single 'optimal' outcome which misrepresents the underlying uncertainties and the large set of possible futures. This uncertainty introduces the need for a method to deal with uncertainty.

The aim of this research is to: *Propose a generically applicable method with which model-owners can be provided insight into the impact of uncertainties on Energy System Design Optimization Model outcomes*. The proposed method consists of three steps: 1) Uncertainty Characterization, 2) Exploratory Modelling, 3) Results Analysis, and is visualized in figure 1. This method deals with uncertainty in Energy System Optimization Design Models by producing insights regarding the model behavior across model runs under uncertainty. When applied to an existing Energy System Optimization Model, this method should help to answer these questions:

- How do the Energy System Designs vary resulting from underlying uncertainties?
- What Energy System Design trade-offs are driven by which underlying uncertainties?

As a proof of concept of the applicability and functionalities of the proposed method, it is applied to a Python-based Energy System Optimization Model that aims to aid decision-making regarding integrated energy system design and operation in urban areas. This Mixed-Integer Linear Programing model solves a greenfield and aggregated case of a medium-sized Dutch city, in which the objective is to identify a least-cost energy system design. To meet the set energy transition goal, the natural gas supply decreases and only PV and wind supply units can be invested in to meet the energy demand up to 2050. In this case, the three energy systems of electricity gas and heat are integrated in the form of network and storage units, and

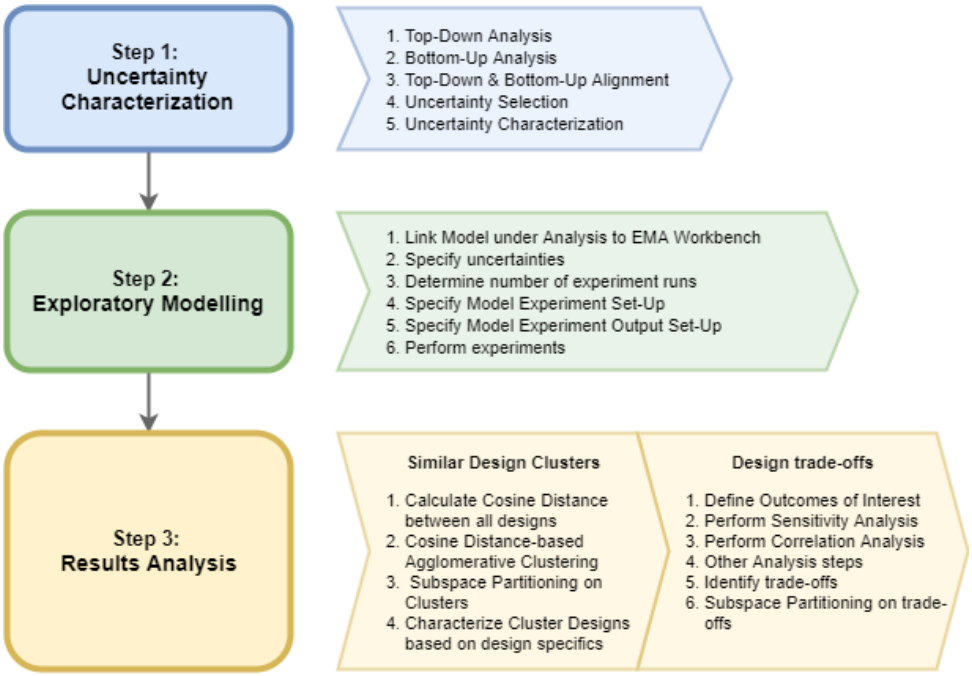

Figure 1: Blockscheme of the proposed method.

the Combined Heat and Power (CHP), Power-2-Gas (P2G), and Heat Pump (HP) conversion technologies.

Effective characterization of uncertainties is crucial for the design of robust energy systems across a wide range of futures. In step 1 of the proof of concept, the following model-parameters are selected as uncertainties to be analyzed: the energy demand development, the discount rate and the technological development rates of PV supply, wind supply, P2G conversion and electricity storage. This selection is based on the analysis of the IMAGE, PROMETHEUS and TIMES energy models, in combination with a variety of relevant scenario planning studies. The most determining uncertainties are the PV supply development rate and demand development, especially the gas reliance.

In step 2) Exploratory Modelling, the selected and characterized uncertainties are integrated into the Energy System Optimization Model under analysis to provide model-based insights rather than precise looking projections. The open source and Python-based Exploratory Modeling and Analysis (EMA) Workbench is used to perform Uncertainty and Sensitivity Analysis. Linking the model under analysis to the Workbench was greatly facilitated by the fact that both are Python-based. With the Workbench, the model is set to solve the case for 800 simulations. During each simulation, the provided uncertainty ranges are sampled with Latin Hypercube Sampling. This results in 800 experiments that each represent a unique set of uncertain parameter value combinations and of outcomes containing the model behavior resulting from that

specific experiment input space. To facilitate the results analysis, each experiment-specific outcome should include *all* design facets, in the same ordering, of the energy system design included in the model under analysis. The total exploratory modelling outcome of the proof of concept has a matrix size of $[3451, 800]$.

The first question, "*How do the Energy System Designs vary resulting from underlying uncertainties?*", is answered as follows. From the total outcome, 6 clusters of experiments resulting in similar energy system design are identified. This is achieved with a novel approach of cosine distance-based agglomerative hierarchical clustering with complete linkage. To characterize the cluster designs, the total outcome is aggregated to the three case-design specifics: the investments in which *technology type* and *time period* and at what *location*. The main cluster variations relate to all three design specifics. Which of the three design specifics portrays the most variation per cluster design, compared to the non-clustered design, is dependent on the underlying uncertainty composition. First, clusters portray the largest variation in technology type investments with a low underlying PV development rate in combination with a demand development that simulates a limited or delayed decrease in gas reliance towards electricity and heat. Second, the largest variation in location-specific investments is portrayed in clusters with a high amount of investments in technology types which are subject to allocation constraints. Third, the largest variation in the time-period of investment is demonstrated in cluster designs which are underlying by either demand development which change very fast towards a different demand mix or by demand development patterns without a decrease in the total gas demand.

The second question, "*What Energy System Design trade-offs are driven by which underlying uncertainties?*", is answered as follows. A general characterization of design elements that are of particular interest is performed with sensitivity analysis and subspace partitioning techniques. Two Energy System Design trade-offs are present in the proof-of-concept: first a consideration between investments in electricity supply from PV or from wind units, and second, a consideration between investments in Combined Heat and Power (CHP) conversion capacity or in gas storage capacity. First, PV supply technology is preferred over wind supply, due to the locational constraints of the latter and the absence of seasonality and day/night patterns. The uncertainty of the PV development rate is the main determining factor in this trade-off. In case of wind supply investments, additional network investments are required to transport the supplied energy to the constrained locations. A lower PV development rate results in a relatively less attractive PV supply technology. As a consequence, the strong reliance on PV supply is alleviated towards increased wind supply investments in case of a lower PV development rate. Second, in case of continued gas reliance or a delayed decrease in gas reliance, additional gas is supplied via conversion of electricity. Then, superfluous gas supply is stored to meet the gas demand in later time periods. This gas demand development induces high investments in P2G, PV and gas storage capacity and low investments in CHP conversion capacity. Conversely, when the gas reliance decreases faster than the intended decrease in gas supply, superfluous gas is converted to meet the increased electricity and heat demand. In this scenario, the investments in CHP conversion capacity are high, as opposed to the low investments in P2G, PV

and gas storage capacity.

Thus, the proof of concept method application to an existing Energy System Design Optimization Model and its simulated case revealed the following main insights. Numerous uncertainties play a role or potentially impact energy systems. To ensure an energy transition towards a sustainable future, the energy system is inevitably changing. The investment patterns reveal that investments towards a changing energy system should be performed at short-term and that supply, conversion and storage units are preferably located where the demand is high. Also, if the gas supply decreases as intended, but the gas demand does not follow, different sources of gas supply must be tapped. Finally, in urban regions, PV supply is expected to be preferred over wind supply if no other sustainable electricity sources are available.

The main conclusion of this research is that the proposed method is useful in providing insight to model-owners on the impact of uncertainties on the outcomes of their Design Optimization Models. A novel approach that is introduced, enables the identification of clusters of similar design. Model-owners can use the insights to 1) identify model specifications (or the lack thereof) that are determining for the model output, and possibly take measures to limit these effects, and to 2) offer their clients (possibly decision-makers) strategy advice. The proposed method is applicable to Energy System Design Optimization Models specifically, and to Design Optimization Models in general. This general applicability is constrained to (Energy System) Design Optimization Models where the 'optimized' outcome, the design, can be formatted as a (high dimensional) vector which contains the value for all potential design components, including the zero values, in a fixed ordering over all experiment runs.

For future research, it is recommended to apply the proposed method to other Design Optimization Models and to models that simulate a less aggregated case, for this research offers a single proof of concept of the method applicability. In doing so, it is recommended to specify an optimality gap value that is as low as possible while maintaining acceptable total computation time. This is expected to result in a higher number of uncertainties that can be identified as significantly underlying for specific model outcomes, or designs.

Preface

This report is the result of my graduation internship at ORTEC B.V. and it serves as my thesis for the Engineering and Policy Analysis master at Delft University of Technology. Looking back at my time in Delft, I am happy to say that I have enjoyed every moment: it has been a wonderful period of my life.

I consider the opportunity to graduate at ORTEC a great experience. Not only did it offer me the possibility to work on a project that combines my interests in both the energy transition and exploratory modelling, it also provided me an inside look into what working in a business environment is like.

First, I would like to thank Iris van Beuzekom who assisted and guided me through this research as my daily supervisor. Thank you for your enthusiasm, critical questions and help in structuring my thesis. Special thanks for your endless devotion in taking the time and flexibility to provide me with feedback.

Next, I would like to thank Jan Kwakkel who was my thesis supervisor at Delft University. In our meetings you always managed to quickly get to the core of my questions and guide me towards new solutions. When the data import from the EMA Workbench to the model was bugged, you immediately took the time to help me solve the issue. Also, I thank Emile Chappin for being critical at all times and helping me focus on the scientific contribution of my work.

My time at ORTEC and my time as a graduate student would not have been the same without my fellow interns and the colleagues from the left back corner of the office. I have appreciated the many laughs we shared. Thank you Tim, for preparing the desired set-up of the model specification in Python. Thank you Jeroen, for providing me with expert input. Special thanks to Noortje and Tessa with whom I could always share my struggles.

Especially, I want to thank my family for their unconditional and unwavering support. Also, I want to thank my friends who were always willing to distract me. Last but not least, I want to thank Jaap for coaching me and always making me smile.

Julie Fraiture, March 2nd, 2020

Contents

Abbreviations

CART	Classification nd Regression Tree
CHP	Combined Heat and Power
E	Electricity
EMA	Exploratory Modelling and Analysis
ESD	Energy System Design
ESDOM	Energy System Design Optimization Model
ESM	Energy System Model
ESOM	Energy System Optimization Model
G	Gas
GSA	Global Sensitivity Analysis
H	Heat
HP	Heat Pump
IQR	Inter Quantile Range
LHS	Latin Hypercube Sampling
LP	Linear Programming
MEuro	Million Euro
MILP	Mixed-Integer Linear Programming
MIP	Mixed-Integer Programming
MIPGap	Mixed-Integer Programming optimality Gap
PJ	Peta Joule
PRIM	Patient Rule Induction Algorithm
PV	Photovoltaic
P2G	Power-to-Gas
RDM	Robust Decision Making
RES	Renewable Energy Sources
SA	Sensitivity Analysis
SDG	Sustainable Development Goal
UA	Uncertainty Analysis

List of Figures

List of Tables

Chapter 1

Introduction

In this introduction to the research, first, challenges for energy systems related to the energy transition are described (section 1.1). Second the optimization modelling of energy systems is introduced in section 1.2, followed by an elaboration on the presence of and difficulties associated with uncertainties related to these Energy System Optimization Models (section 1.3). In section 1.4 the scientific knowledge gap is elaborated upon followed by the formulation of the aim of this research (section 1.5). Finally, the scope of this research and the structure of this report are introduced (sections 1.6 and 1.7).

1.1 Energy Systems and the Energy Transition

The large-scale emission of greenhouse gases (GHG) causes global warming and climate change (IPCC, 2014; Rice et al., 2016). This has undesirable effects such as sea level rise, increased occurrence of severe weather events, shortage of freshwater availability and a decline in biodiversity (IPCC, 2014, 2019). By signing the Paris Agreement, 195 countries have committed to deep reduction of GHG emissions to address climate change (UNFCCC. Conference of the Parties (COP), 2015). The emission reduction target of the European Union (EU) is an 80 to 95 percent decrease by 2050 (EU climate action).

The increased deployment of Renewable Energy Sources (RES) for the production of energy is a way to commit to decreasing GHG emissions. As most RES supply energy in the form of electricity, the European electricity generation is expected to increase with a factor 2.5 towards 2050 (DNV GL, 2018). The electricity share in the final energy demand is projected to increase from only 20 percent now to almost 50 percent in 2050 (DNV GL, 2018). Incidentally, these numbers are just one vision on these critical developments and other researchers take on even more ambitious numbers.

However, two challenges arise in the electrical energy system having to accommodate this large-scale generation of electricity by RES (van Beuzekom et al., n.d.). The first being the *energy carrier mismatch* between the supply and the lagging demand of electrical energy. The second is the *temporal mismatch* associated with the considerably fluctuating and intermit-

tent energy production of RES, depending on weather conditions. Due to these mismatches, the current energy system will oftentimes not be reliable in meeting the demand. These mismatches stress the need for flexible energy systems that are reliable and lead to reduced carbon emissions through deployment of renewable energy capacities (IIESI, 2016).

Consequently, a long-term view is necessary in the design of energy systems. This long-term view will ensure that investment and operational decision-making leads to robust real-world energy systems that deliver these transition goals (McCallum et al., 2019). This is complicated by the scale, complexity and cost of energy system expansion.

1.2 Energy System Optimization Models

To face these challenges in complex decision making, energy system planners and policy makers rely on Energy System Models (ESMs) (McCallum et al., 2019). Modelling has been an important part of the energy domain in assisting these long-term energy design and policy decisions, and in providing insight into how energy systems might evolve in the future (Mavromatidis et al., 2018). Also, modelling can be used to analyse the behaviour of sustainability transitions, for example on how new systems might replace established systems, and the associated pathways (Moallemi & Köhler, 2019).

Models that support infrastructural decision-making, such as Energy System Models, should account for long-term risks and the long-term environment, needs, alternatives and constraints (Hallegatte, Lempert, & Brown, 2012; Störmer et al., 2009; Ranger, Reeder, & Lowe, 2013). All decisions made in infrastructure projects, during the whole life-cycle, are afflicted by uncertainty (Larsson Ivanov, Honfi, Santandrea, & Stripple, 2019). Due to the long life times of infrastructure, decisions that impact energy infrastructure (usually assumed to be greater than 30 years) have long-term consequences and can shape development for decades or centuries (Störmer et al., 2009). In addition, because of this long-term life cycle and the considerable uncertainties related to this, investment planning is challenging for high-valued assets present in energy systems (Moallemi, Elsawah, Turan, & Ryan, 2019). What is more, the uncertainty in future risk and projections grows at longer prediction lead times (Haasnoot, Kwakkel, Walker, & ter Maat, 2013). Both the long life-time of energy infrastructure and the uncertainty in future conditions increase the importance of good and robust energy systems design and investment planning (Moallemi et al., 2019; DeCarolis, Babaee, Li, & Kanungo, 2016).

The family of Energy System Models can be grouped into four categories: Energy System Optimization Models, Energy System Simulation Models, Power Systems and Electricity Market Models and Mixed-Methods Scenarios (Pfenninger, Hawkes, & Keirstead, 2014). The definition given by Pfenninger et al. for Energy System Optimization Models (ESOMs) is: Models covering the entire energy system, primarily using optimization methods, with the primary aim of providing normative scenarios of how the system could evolve. This makes ESOMs particularly relevant for long-term energy system planning studies, such as for the design and

operation of future energy systems (McCallum et al., 2019; Pfenninger et al., 2014; Mavromatidis et al., 2018; IIESI, 2016; Mancarella, 2014). Well-known examples of established Energy System Optimization Models are MARKAL, TIMES, MESSAGE and OSeMOSYS.

1.3 Uncertainties in Energy System Optimization Models

One of the main challenges in constructing Energy System Optimization Models (ESOMs), is the handling of uncertainty (E3MLab/ICCS, 2017; Pfenninger et al., 2014; DeCarolis et al., 2017). The long-term development of the energy system is characterized by a combination of factors that are uncertain, such as technology innovations, resource availability, and socio-economic dynamics (DeCarolis et al., 2017; Guivarch, Lempert, & Trutnevyte, 2017). The projections of these developments vary largely among different studies (Witt, Dumeier, & Geldermann, 2020).

Two types of uncertainties abound in ESOMs: parametric and structural uncertainty (Zhang, Tang, & Chen, 2019; Mavromatidis et al., 2018; DeCarolis et al., 2017). Model-parameter uncertainty refers to imperfect knowledge of ESOM input parameter values, that arise due to for example lack of data and/or assumptions. These uncertainties are also referred to as external uncertainties (Stewart & Durbach, 2016). Structural uncertainty, or internal uncertainty, refers to uncertainty in the form of the mathematical relations describing the energy system development and operation within the model (Witt et al., 2020).

In optimization, it is common practice to consider a single input variable representative value for objects with a diverse set of potential values in the real world, for example the capacity, conversion efficiency or investment costs (Nejlaoui, Houidi, Affi, & Romdhane, 2013). The set of potential values for these objects in the real world arises from variations in for instance material properties, geographical locations and geometry. In assuming a single value it is assumed that all uncertainty is resolved ex ante, whereas decision makers need to act or time needs to pass before uncertainty is resolved (DeCarolis et al., 2017). Because of the importance and uncertainty of these specified parameter values, ESOMs are usually neither certain nor objective (Pfenninger et al., 2014; Thompson & Smith, 2019; Almassalkhi & Towle, 2016). Also, this model input uncertainty introduces uncertainty into the model outcomes (McCallum et al., 2019).

1.4 Scientific Knowledge Gap

All in all, there is high system uncertainty and complexity in Energy System Optimization Models (ESOMs) while the stakes for decision making in energy systems are high (Pye, Sabio, & Strachan, 2015). In other words, in an area where decision makers should have great assurance in model-based results, this very assurance is complicated by the system - and future

uncertainties.

In a system that is characterized by such future uncertainties as the energy system, the use of optimization models can be misleading. This is because ESOMs provide a single 'optimal' outcome which misrepresents the large set of possible futures. In long-term energy projections, effort should be put in to quantify the model sensitivities and uncertainties. Nevertheless, even with a rigorous meticulous uncertainty analysis, it is unattainable to account for all uncertainties due to the high dimensional decision space.

DeCarolis et al. (2017) have formulated seven guiding principles for ESOM-based analysis. Among which: 'Consider uncertainties that are both endogenous and exogenous to the model and how they can affect conclusions'.

This uncertainty introduces the need for a framework to deal with uncertainty in Energy System Optimization Models to ensure robust real-world model-based energy systems design and operation (Moallemi & Köhler, 2019). Because: "ignoring these uncertainties and developing deterministic designs can render such designs sub-optimal and result in [real-world] system failure" (Zhang et al., 2019). According to Chong, Xu, and Khee Poh (2015), the use of uncertainty analysis offers decision-makers greater assurance in the results generated by simulation tools, since they are provided with more information when evaluating alternative designs. Adequate effort should be devoted to uncertainty characterization and integrating uncertainties into energy system modelling (Mavromatidis et al., 2018).

To this end, uncertainty analysis in Energy System Optimization Models has been carried out with open-source models (Hunter, Sreepathi, & DeCarolis, 2013; Howells et al., 2011; Welsch et al., 2012; Pfenninger et al., 2014) or by extending existing models with stochastic optimization approaches (Kim, Cheon, Ahn, & Choi, 2019; DeCarolis et al., 2016; Pfenninger et al., 2014; Trutnevyte, 2016). Researchers have developed frameworks to deal with uncertainty quantification in specific sub-parts of ESOMs, such as for evaluating the effect of uncertain prospective policy measures, residential energy demand, the (residential) building sector or PV prices (Kim et al., 2019; Radaideh & Kozlowski, 2019; Zhang et al., 2019).

According to DeCarolis et al., "the focus of ESOM-based analysis should be based on producing insights, which requires the identification of patterns across ESOM model runs under uncertainty". The produced insight into ESOM behavior will limit the misleading effect of providing singular model outcomes and will shed light on the impact of uncertainties.

Effective characterization of uncertainties is crucial for the design of robust energy systems across a wide range of futures. However, there is currently no method that systematically combines uncertainty and sensitivity analysis with the aim to provide insight into the behavior of existing Energy System Optimization Models that optimize for Energy System Design: Energy System Design Optimization Models. The applicability of uncertainty analysis to existing models is required in cases where for example a very specific energy system is modelled

or when a decision maker desires the use of an exclusive model, such as in a consulting project.

1.5 Research Aim

Following the recommendation from DeCarolis et al. (2017), the aim of this research is to:

Propose a generically applicable method with which model-owners can be provided insight into the impact of uncertainties on Energy System Design Optimization Model outcomes.

Insight into the variability of optimization model outcomes across uncertainties should aid model-owners in increasing their insight into the model behavior under a large set of experiments, under specific uncertainties, and in identifying the potential vulnerabilities of their model specification.

This improved insight of model-owners into the impact of uncertainties on Energy System Design Optimization Models should allow them to aid decision makers in applying Energy System Design investment plans that are robust across a range of uncertain futures. By considering uncertainties and providing variability predictions instead of the usual point estimates, decision makers would have greater confidence in simulation results (Chong et al., 2015).

This proposition is also in line with the recommendation to develop a method for joint application of the two approaches of (economic) optimization and Robust Decision Making (Matrosov, Padula, & Harou, 2013). Robust Decision Making is a combination of scenario planning and discovery techniques with computation techniques "to support decision makers by helping to identify potential [Energy System Design] strategies that are robust to future unknowns, characterize the vulnerabilities of such strategies, and evaluate trade-offs among alternatives" (Guivarch et al., 2017).

As a proof of concept of the applicability and functionalities of the proposed method, it is applied to a model that aims to aid decision-making regarding *integrated* energy system design and operation (Appendix A). The model solves a case in which the Energy System Design and operation for a medium-sized Dutch city are modelled from the year 2018 to 2050 by using an optimization approach with Mixed-Integer Linear Programming (MILP). The objective is to identify a least-cost energy system design while meeting energy demand up to 2050. Three energy systems are integrated in this case: electricity, gas and heat. The model is designed in the context of an ongoing PhD research at Eindhoven University of Technology, department of Electrical Engineering, and ORTEC B.V. (Van Beuzekom, Gibescu, Pinson, & Slootweg, 2017; van Beuzekom et al., n.d.).

Applying the proposed method to an existing Energy System Design Optimization Model should answer these questions:

- How do the Energy System Designs vary resulting from underlying uncertainties?
- What Energy System Design trade-offs are driven by which underlying uncertainties?

1.6 Research Scope

The method proposed in this research explicitly focuses on providing and uncertainty analysis for *existing* Energy System Design Optimization Models.

Energy System Optimization Models can be split into two basic types: design models and operation models (Mavromatidis et al., 2018). Design models consider the selections, siting and sizing of technologies that will compose an energy system. In doing so, the models consider the operational characteristics and constraints for these technologies, while optimizing for the desired performance criteria. Operation models optimize the operation of generation and storage technologies in an energy system of known structure and capacities along some time horizon. This research aims to provide a method which is applicable to the Energy System Optimization Models that optimize for Energy System Design.

The scope of this research is limited to the analysis of parametric (external) uncertainty.

In a complicated system such as the energy system, a lot of stakeholders are involved (Trutnevyte et al., 2019). Think of for example energy consumers, energy suppliers, policy makers and system operators. To further complicate matters, each of these stakeholders can be split into multiple levels of detail. For example, the stakeholder division of energy consumers can be split into: residential, industrial and commercial users. However, industrial energy consumption differs greatly between coal plants and bio-fuel plants and the energy consumption of residential users depends on the kind of residence, the number and characteristics of its inhabitants and whether or not the residence is properly insulated. This research does not explicitly consider the presence of stakeholders, the interactions between actors or the consequences and dynamics of (multi-)actor decision making. However, due to the analysis of a wide range of uncertainties, it could be that possible stakeholder interactions and consequences are implicitly taken into account.

1.7 Report Structure

The structure of this report is as follows.

First, the proposed method is introduced (chapter 2). Each of the three method steps (Uncertainty Characterization, Exploratory Modelling, Results Analysis) are substantiated. This chapter also introduces the fundamentals of the model to which the method is applied to demonstrate its functionalities. However, this model and the case that is simulated, are intro-

duced explicitly in Appendix A.

Chapters 3, 4 and 5 elaborate on the proof of concept method application to the model under analysis. Chapter 3 describes the application of *Step 1: Uncertainty Characterization* to the model. It is explained that the uncertain key model drivers of which the impact on the model outcome are quantified are selected and characterized by a combined top-down and bottom-up analysis. As part of the top-down analysis, the three established energy systems models IMAGE, TIMES and PROMETHEUS and the analysis of scenario planning studies are described. Followed by the selection and characterization of the following parameters as uncertainties to be analyzed: energy demand development, (technological) development rates, and the discount rate. Next, in chapter 4, as part of *Step 2: Exploratory Modelling*, the experiment set-up and the use of the Exploratory Modelling and Analysis (EMA) Workbench are described. Third, the application of *Step 3: Results Analysis* to the model under analysis is described in chapter 5. First, the description of variation between similar Energy System Design clusters is provided. This clustering is enabled by a novel approach that proposes a cosine distance-based agglomerative clustering of the model outcomes across uncertainties. Second, the identification of trade-offs between Energy System Design investment possibilities is described.

Finally, chapter 6 reflects on the real-world implications of this research and the limitations to the method and to this research. Then, this chapter concludes on the method functionality and provides suggestions for follow-up research.

Chapter 2

Method Description

In this chapter the proposed method is introduced and substantiated. The proposed method consists of three subsequent research steps (figure 2.1):

1. *Uncertainty Characterization;*
2. *Exploratory Modelling;*
3. *Results Analysis.*

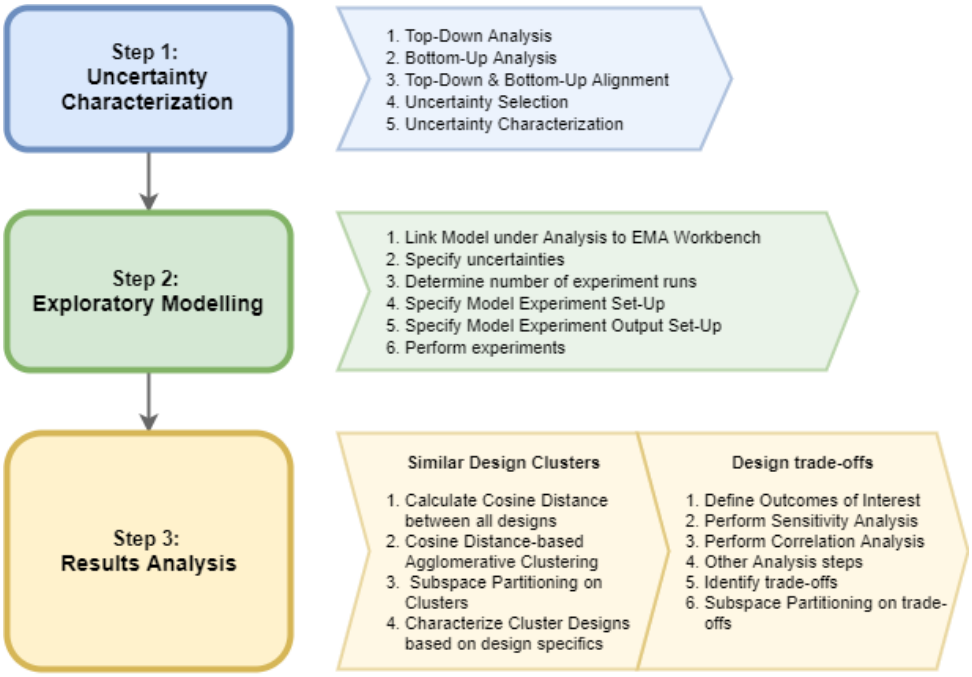

Figure 2.1: Blockscheme of the proposed method.

The method presented in this work relies on a number of well-established research themes and utilizes a range of existing methods to act as a conceptual overarching framework. In some aspects, specific tools can be interchanged with alternatives. The choice for certain method applications, such as the experiment set-up or the choice for specific data visualization and results analysis techniques, is dependent on the properties of the model under analysis and the case that it simulates. Consequently, in this chapter certain method applications are described in a generic manner. In describing the proof of concept method application to an existing model (chapters 3, 4 and 5), these applications are decided upon specifically for the properties of the model under analysis.

2.1 Step 1: Uncertainty characterization

To integrate uncertainty in an Energy System Design Optimization Model (ESDOM), it is important to start with characterizing the uncertainties present in the model under analysis. Such an uncertainty characterization consists of the identification of uncertain parameters and the assignment of an appropriate mathematical representation of their uncertainty (Mavromatidis et al., 2018; Chong et al., 2015). Although the task of uncertainty characterization can itself be seen as uncertain, exploring the nature of uncertainty is significantly more valuable than using deterministic, best-guess values. Failing to identify uncertain parameters or assigning invalid representation of this uncertainty can lead to sub-optimal model outcomes. Therefore, effective characterization and integration of uncertainty into ESDOMs is crucial for the design of robust energy systems across a wide range of futures (Mavromatidis et al., 2018).

The identification of uncertain parameters to be characterized and integrated into the model under analysis consists of two approaches: *bottom-up and top-down*. Because the proposed method is applicable to *existing* models, the prerequisite for uncertainties is applicability to the model. Therefore, the bottom-up approach consists of an analysis of the model-parameters to identify the parameters which are possibly subject to external uncertainty. Thereafter, a top-down approach is employed to identify parameters that are considered to be uncertainties in renowned energy models and scenario planning studies or by the problem owners. Subsequently, the bottom-up and top-down uncertainty parameters are aligned to select the main uncertainties for step 2: Exploratory Modelling. Hence, a scientific basis for the uncertainty parameter selection is provided. Next, the assignment of an appropriate range of the selected model-parameter uncertainties is based on observed data, expert judgement, literature, standards and case studies (Chong et al., 2015).

Renowned energy models and scenario planning studies are proposed as scientific basis for the top-down uncertainty parameter selection, because both deal with uncertainty. In all models, assumptions need to be made for a range of factors that shape the direction and rate of change in key model variables and results (Netherlands Environmental Assessment Agency, 2014). In scenario planning studies, scenarios consisting of a set of parameters that represent (external) uncertainties are used as model input variation to examine the variety of possible futures resulting from different uncertain input (Witt et al., 2020; Stewart & Durbach, 2016). Both such assumptions and scenario key parameters are used to identify uncertainties that can be

related to the model under analysis.

Not all models and studies are relevant for the top-down analysis of the model under analysis. The choice for the models that are studied, is made on the basis of following three criteria:

- **Availability of open-source documentation**: To be able to analyse the treatment of uncertainty in the energy models, availability of open-source documentation is a prerequisite for selection. More specifically, documentation on (parametric) uncertainties must be available.

- **Geographical scale**: Generally, the models can be specified on both a global scale and on the same geographical scale as the model under analysis. It is found that most global-scaled models consist of 'general' equations which are filled with regional-specific data. Even more so, global-scaled models are commonly employed for regional-specific practices. Therefore, it is assumed to be valid to relate the parameters that are deemed uncertain in a global model specification to a lower geographical scale. This with the exception of specifications that are dedicated to developing countries, which usually describe different parameters.

- **Model type**: The design of energy systems can be modelled on a multiplicity of (geographical) scales, (energy) systems, time periods and stakeholders. Preferably, the model considers the same energy systems. Also, parameters describing the same energy system components should be present. Other specifications are of a less influence.

2.2 Step 2: Exploratory Modelling

Following the identification and characterization of model-parameter uncertainties, the uncertainties are integrated into the model under analysis. There are two main methods that can be applied to integrate uncertainties into energy system modelling after uncertainty has been characterized (Mavromatidis et al., 2018):

1. **Uncertainty and Sensitivity Analysis**
   Uncertainty and Sensitivity Analysis is usually performed with Monte Carlo or Latin Hypercube simulations to shed light on the impact of uncertain input on and the drivers of model output. Uncertainty and Sensitivity Analysis can be a useful tool to provide decision-makers with more information about alternative model outcomes as a result of uncertainties. However, Uncertainty and Sensitivity Analysis cannot be used to identify a single optimal model decision for the envisioned energy system. A few examples of the use of Uncertainty and Sensitivity Analysis in the model-based design of energy systems are described by Keirstead and Calderon (2012); Sun, Gu, Wu, and Augenbroe (2014); Ashouri, Petrini, Bornatico, and Benz (2014) and Ren, Gao, and Ruan (2008). A limitation to most uncertainty analysis tools is that they do not facilitate the inclusion of Uncertainty Analysis in the simulation process. Often, a manual changing of inputs is

required each time a simulation is run with a different uncertain parameter value. Subsequently, the processing of the many separately generated output files usually is time consuming (Chong et al., 2015).

2. **Optimization under Uncertainty**
   Optimization under Uncertainty allows to make optimal energy system decisions under uncertainty by including uncertainty with extensions to the model specification. Consequently, although Optimization under Uncertainty introduces uncertainty in the optimization process, it still produces a precise-looking projection which does not provide increased insight into the model behaviour (DeCarolis et al., 2016). The two main approaches for Optimization under Uncertainty are Stochastic Programming and Robust Optimization (Mavromatidis et al., 2018). A drawback of both approaches is the exponential increase of computational requirements with the number of uncertain parameters that are modelled (DeCarolis et al., 2017).

According to DeCarolis et al. (2016), the focus of Energy System Optimization Model-based analysis should lie on providing model-based insights rather than precise looking projections. In other words, singular optimization model projections can be misleading, especially given the presence of uncertainties. Therefore, the Uncertainty and Sensitivity Analysis technique is employed to integrate uncertainties into Energy System Design Optimization Models.

2.2.1 Exploratory Modelling and Analysis Workbench

The Exploratory Modeling and Analysis (EMA) Workbench is employed to perform Uncertainty and Sensitivity Analysis. The EMA Workbench has been developed mainly for model-based decision support (Kwakkel & Pruyt, 2013). Exploratory modelling in general, and the EMA Workbench specifically, have been used for coping with uncertainties in a variety of modelling purposes (Lempert, Popper, & Bankes, 2003). However, the EMA Workbench has not yet been employed to cope with uncertainties in Design Optimization Models, let alone in Energy System Design Optimization Models.

The EMA Workbench is a useful open source library that supports the generation and analysis of results from computational experiments and covers how various uncertainties work through in a model (Kwakkel, 2017). A major advantage of employing this open-source, Python-based Workbench for Uncertainty and Sensitivity Analysis is that it allows the inclusion of Uncertainty Analysis in the simulation process by facilitating a link between the provided uncertainty ranges and the model, without having to alter the model (Kwakkel, 2017). The Workbench samples from a modeller-provided quantitative assumption set that can cover uncertainty ranges and potential policies. Latin Hypercube Sampling is usually employed to systematically sample and explore the provided input space (Kwakkel, 2017). Each exploratory modelling case is composed of a number of *experiments* which each represent a unique set of uncertain parameter value combinations and of *outcomes* which contain the model behaviour

resulting from that specific experiment input space. The analysis part of the Workbench provides tools to systematically investigate the relation between the input space and the resulting model behaviour.

Exploratory Modelling

Most research with the aim to account for uncertainty in their modelling treat (future) uncertainty through a variety of qualitative imaginable scenarios and use the models as a forecast engine (Moallemi & Köhler, 2019; Yáñez, Ortiz, Brunaud, Grossmann, & Ortiz, 2019; Van Vuuren et al., 2012; Xu et al., 2019; Witt et al., 2020; Statharas, Moysoglou, Siskos, Zazias, & Capros, 2019). However, using models as a forecast engine under a set of 'most-likely' imaginable scenarios can only present a biased and simplified version of the real challenge and hence excludes unforeseen events (Moallemi & Köhler, 2019). These scenario types can be formulated as: following trend-lines or using 'what-if' scenarios (Maier et al., 2016). The use of such models and predictions lead to a restricted understanding of future dynamics that can be misleading and hence result in policy formulations with limited robustness.

Exploratory modelling aims to improve the robustness of decision making by, as defined by Bankes (1993), "the use of series of computational experiments to explore the implications of varying assumptions and hypotheses". Exploratory scenarios can be framed (capturing divergent plausible futures) or unframed (not constrained by driving uncertainties) (Maier et al., 2016). Exploratory analysis of a wide range of uncertainties, with limited informative priors, can be used to gain an understanding of model behaviour that is less sensitive to the researcher's initial assumptions or trend-lines because it includes a larger proportion of unforeseen futures (Moallemi & Köhler, 2019). Consequently, the use of exploratory modelling to deal with uncertainties can limit the impact of researcher's bias on results (figure 2.2). Provided the model can deal with a multiplicity of futures, this allows for the analysis of a future that *could* happen instead of that *will* happen (Maier et al., 2016).

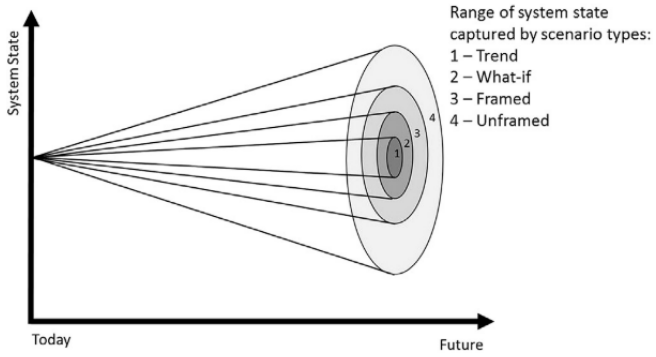

Figure 2.2: Forward-focused scenario types illustrating the allowance for uncertain and divergent figures according to scenario types. Figure retrieved from Maier et al. (2016).

2.2.2 Decision Theory

Through the employment of Exploratory Modelling and Analysis to an optimization model, two different decision aiding techniques are combined.

Decision aiding is defined by Tsoukias et al. (2013) as "the use of a formal and abstract language in order to handle problem situations faced by individuals and/or organizations". Both the use of optimization modelling and exploratory modelling can be described as decision support techniques with the aim to aid real decision makers in real problem situations involved in real decision processes. These modelling techniques aid the translation from (uncertain) information to a formal representation of a real problem situation. Four decision aiding approaches are identified by Tsoukias et al.: normative; descriptive; prescriptive and constructive (table 2.1).

Table 2.1: Differences among decision aiding approaches, retrieved from Tsoukias et al. (2013).

Approach	**Characteristics**	**Process to obtain the model**
Normative	Exogenous rationality, ideal economic behaviour	To postulate
Descriptive	Exogenous rationality, empirical behaviour models	To observe
Prescriptive	Endogenous rationality, coherence with the decision situation	To unveil
Constructive	Learning process, coherence with the decision process	To reach a consensus

The use of Exploratory Modelling, in which parameters are assigned different uncertainty values across experiments, the decision aiding approach is described as *constructive*. The Energy System Design Optimization Model (ESDOM) to which the Exploratory Modelling Approach can be 'linked' in the proposed method , likely employs a different approach. The combination of two different decision aiding approaches in one decision aiding process is valid, because according to Tsoukias et al. 'the differences among the [decision aiding] approaches do not concern the methods used to solve a decision problem'. It is stated that "We can conduct a decision aiding process constructively and end by using a combinatorial optimization approach" (Tsoukias et al., 2013). Nevertheless, they claim that it is essential that the additional decision aiding approach is conducted after the modelled problem has been formulated and the evaluation model has been constructed.

In this research, the constructive approach (EMA) is conducted based on the existing decision aiding process. The uncertainty parameter selection and variation are performed after (and based on) the problem formulation and evaluation model construction, because the proposed method applies to already *existing* ESDOMs. This makes the constructive approach a valid addition to the original optimization approach.

2.2.3 Model Output Set-Up

An exploratory modelling case consists of a number of experiment runs specified by the analyst. Each experiment run results in experiment-specific outcomes due to the unique underlying un-

certainty parameter-values as input.

Each experiment-specific outcome should include *all* facets, in the same ordering, of the energy system design that is included in the model under analysis. This allows the analyst to compare the experiment-specific outcomes and to aggregate the total outcome to all various levels that are part of the model under analysis.

For example, consider a model that specifies energy system design based on three factors: technology unit, location and time period. Then, to include all facets of a model under analysis, the experiment-specific model output should include the number of investments performed in each technology unit at each location and time period. Let the model under analysis consider two technology units ($k = 2$) which can be invested in at two locations ($l = 2$) during two time periods ($m = 2$) analysed with four experiment runs ($n = 4$). This leaves the number of rows, or investment possibilities, of all experiment-specific output vectors to equal $k_{technologyunits} * l_{locations} * m_{timeperiods} = 8$. So, for this example each experiment should result in an experiment-specific output vector of equal ordering and size $[8,]$. Resulting, the total exploratory modelling case outcome should be a matrix, containing the output vectors for each experiment run, with size $[8, 4]$ (table 2.2).

Table 2.2: The model output set-up concept for a fictional model with the number of investments for $k = 2$ technology units, $l = 2$ locations, $m = 2$ time-periods and $n = 4$ experiment runs resulting in a matrix of $klm = 8$ rows and $n = 4$ columns.

	Investment possibilities			Experiment runs			
	Type	**Location**	**Time**	**1**	**2**	**3**	**4**
1	Technology unit 1	Loc 1	Time period 1	1	2	3	5
2	Technology unit 1	Loc 1	Time period 2	0	0	1	9
3	Technology unit 1	Loc 2	Time period 1	0	0	0	0
4	Technology unit 1	Loc 2	Time period 2	0	0	0	0
5	Technology unit 2	Loc 1	Time period 1	1	2	2	1
6	Technology unit 2	Loc 1	Time period 2	0	0	0	5
7	Technology unit 2	Loc 2	Time period 1	0	0	1	0
8	Technology unit 2	Loc 2	Time period 2	0	0	0	0

2.3 Step 3: Results Analysis

Finally, the total experiment case outcome, in the form of a matrix containing the outcome vector for each experiment, is analyzed to provide insight into the impact of uncertainties on the model outcomes. With this result analysis, the following two questions can be answered for the model under analysis:

1. How do the Energy System Designs vary resulting from underlying uncertainties?

2. What Energy System Design trade-offs are driven by which underlying uncertainties?

2.3.1 Energy System Design Variation

In this section, the results analysis section to answer the first question is provided: "*How do the Energy System Designs vary resulting from underlying uncertainties?*" (figure 5.2).

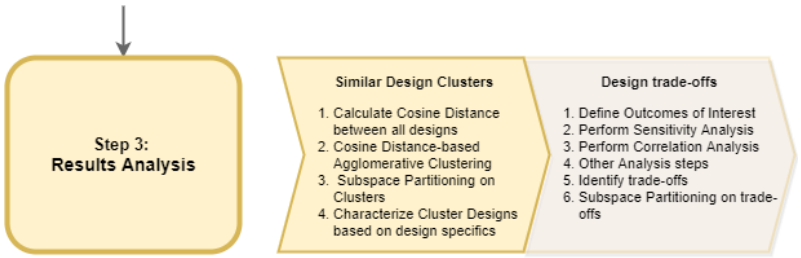

Figure 2.3: Step 3.1 of the proposed method: Results Analysis to identify distinct design characteristics.

As explained before, the total modelling outcome contains each experiment-specific design in the form of an output vector that is part of the total outcome matrix. The large size of this matrix, even in case an aggregated case is modelled, introduces the need for a different approach to analyse the impact of uncertainties on the total design.

The novel approach that is introduced in this section offers tools to analyze the total design. This is done by clustering of the total outcome space, based on the cosine distances between all experiment-specific designs, which represent the design similarity. Thereafter, this cosine distance is provided as input into an agglomerative clustering algorithm with which similar energy system design clusters are identified within the entire outcome space. Characterization of the cluster designs, and using CART subspace partitioning to identify the underlying uncertainties, provides insight into the variation of the model outcomes.

The choices for these specific methods are elaborated upon in the following sections.

Cosine Distance

The cosine distance is a distance metric which produces high quality results across different domains (Zadeh & Goel, 2013). The metric measures the error between two vectors by the cosine of the angle between two non-negative vectors (figure 2.4). A negative vector orientation does not occur, as the number of investments performed cannot be negative. A low cosine distance, near the maximum value 0, indicates that the two vectors have the same dimensional orientation. A cosine distance of 1 occurs when two vectors are most distant with an angle of 90 degrees. The cosine distance excludes the magnitude of the vectors (Qiu, Zhang, Li, Qu, & Tong, 2020).

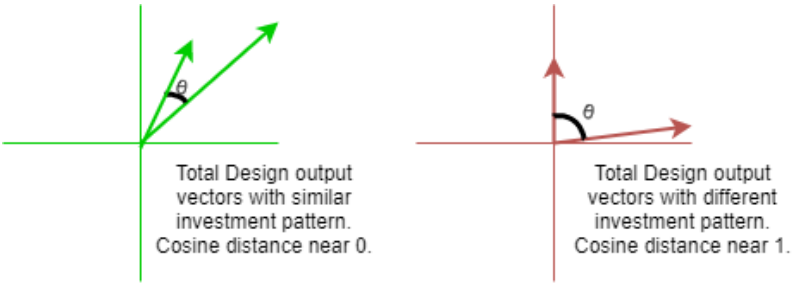

Figure 2.4: Cosine Distance measure between two vectors in a two-dimensional space.

Table 2.3: Cosine distance matrix of the cosine distances between the four experiment-specific output vectors as introduced in table 2.2.

Output vector	**Exp.**	**1**	**2**	**3**	**4**
[1,0,0,0,1,0,0,0]	**1**	0.0	0.0513	0.0871	0.6307
[2,0,0,0,1,0,0,0]	**2**	0.0513	0.0	0.0762	0.5718
[3,1,0,0,2,0,1,0]	**3**	0.0871	0.0762	0.0	0.4156
[5,9,0,0,1,5,0,0]	**4**	0.6307	0.5718	0.4156	0.0

The cosine distance is preferred over other distance metrics, such as the euclidean or manhattan distances, because these measures consider the differences between two 'close' investment possibilities to be equally important as the differences between two 'far' investment possibilities. This limits the feasibility for such distance measures in this research, because the design in this method is represented by a 'fixed' ordering of investment possibilities across experiments. Hence, the distance measure should mainly register the investment *pattern* similarity: whether or not investments are performed in the same design components.

The cosine measure is suitable as it is applicable to high-dimensional and sparse vectors, which is necessary because the total output vectors contain a majority of zero-values. In addition, the measure is not influenced by the total number of investments, but does represent the relative contribution of a certain investment possibility to the total invested. Each investment possibility embodies a dimension in the solution space. Most importantly, because of the measure of orientation in the multi-dimensional space, the cosine distance reflects similar investment patterns between experiment vectors.

The cosine distance is calculated between all experiment designs with the Python SciPy spatial distance library. Following the outcome matrix example as provided in table 2.2, the cosine distance function takes the matrix in the form of dataframe $[n, klm]$ and returns a square matrix with row- and column size equal to the number of experiment runs (nxn) (table 2.3). Cosine distance value with index (n_x, n_y) representing the cosine distance between the experiment design output vectors at row x and column y. A cosine distance between two columns with value 0 indicates the highest design similarity, Consequently, cosine distance value 1 indicates the highest design dissimilarity.

Clustering of Experiments resulting in Similar Designs

To cluster the outcome matrix into clusters of experiments that result in similar Energy System Design, the cosine distance matrix is provided as input into a clustering algorithm. The use of a clustering algorithm is required, because the identification of patterns and variation between designs would be impossible from a one-by-one analysis and comparison of each experiment-specific design.

The use of a hierarchical clustering algorithm is proposed to identify clusters. Hierarchical clustering is preferred over non-hierarchical clustering, because it systematically evaluates all potential groupings. Therefore, it is assumed that hierarchical clustering results in clusters with a higher in-cluster design similarity.

Hierarchical clustering groups data objects into a hierarchical 'tree' of similar clusters. Two types of hierarchical clustering exit: divisive clustering and agglomerative clustering (Podani, 1989). The difference between the two is in the startpoint of the clustering: whether the hierarchical decomposition is formed in a bottom-up (agglomerative) or top-down (divisive) manner 2.5. Agglomerative clustering starts the clustering with each data point as a singleton cluster from which the singleton clusters are recursively combined into larger clusters. In divisive clustering, the entire dataset is considered as one cluster at the start, from which point the cluster is recursively split into smaller clusters. This clustering method is quite sensitive to the initialization, due to the many possible cluster splits at the first step (Shobha & Rangaswamy, 2018). Therefore, the use of agglomerative hierarchical clustering is proposed.

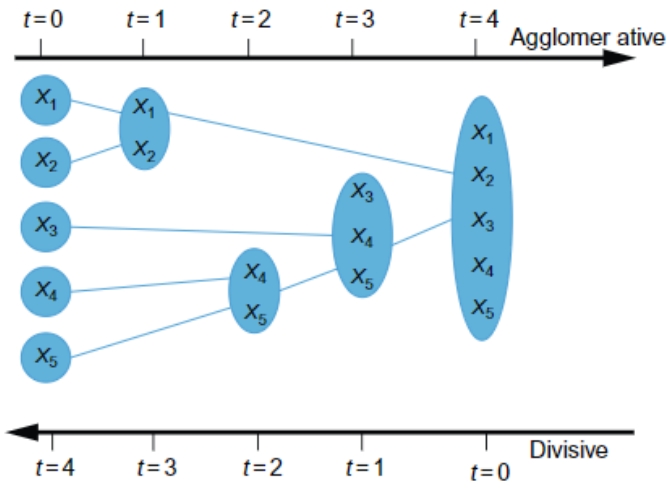

Figure 2.5: Hierarchical clustering algorithms. Figure retrieved from Shobha and Rangaswamy (2018)

In order to identify clusters of similar total designs, the algorithm needs to be provided with a linkage criterion (figure 2.6). The linkage methods differ in how the proximity between any two clusters is defined. Because of the input of the predefined cosine distance matrix into the algorithm, the linkage method possibilities are: single (nearest neighbour), com-

plete (farthest neighbour) and average (Podani, 1989; Li & De Rijke, 2017). Single linkage proximity between two clusters is the proximity between their two closest objects: only the nearest neighbors similarity is controlled. Complete linkage defines the shortest link-distance as the proximity between their two furthest removed objects. Consequently, the clusters that are combined, have the *smallest* farthest distance between any two cluster elements. This results in clusters with extremely 'compact' borders. Finally, with average linkage the proximity between two clusters is the mean of all proximities between the objects of both clusters in comparison. Hence, all datapoints within each of the two clusters have equalized influence on the proximity.

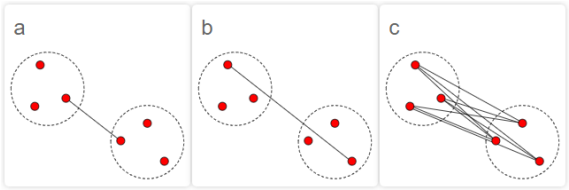

Figure 2.6: Hierarchical clustering linkage methods with (a) single linkage, (b) complete linkage and (c) average linkage to define the shortest-link distance.

To ensure the formation of compact clusters with a high in-cluster design similarity, the complete linkage method is used.

The agglomerative clustering is performed with the *sci-kit-learn.cluster.AgglomerativeClustering* function. The desired number of clusters is visually identified from a dendrogram, which portrays the linkage distance value between all values. The linkage distance value threshold is used to cut-off the number of clusters. This threshold is calculated with the 'default' color_threshold formula: $0.7 * max(Z[:,2])$, where Z is the complete linkage distance matrix resulting from the cosine distance matrix and $Z[i,2]$ the linkage value at the i-th iteration between the clusters with indices $Z[i,0]$ and $Z[i,1]$ (The SciPy community, 2019). It is important to note that the resulting clustering cannot be stated to be mathematical truths, because the clustering is performed based on the criterions as provided by the analyst, such as the specified linkage method and the linkage distance threshold to specify the desired number of clusters.

2.3.2 Energy System Design Trade-Offs

In this section, the results analysis section to answer the second question is provided: "*What Energy System trade-offs are driven by which uncertainties?*" (figure 5.9).

Design elements that are of specific interest for the model under analysis, are selected by the analyst to analyse potential trade-offs between these investment possibilities. These design elements are referred to as Outcomes of Interest and are retrieved by aggregating the total design according to the preferences. For example, the energy capacity invested in per tech-

Figure 2.7: Step 3.2 of the proposed method: Results Analysis to identify design trade-offs.

nology unit could be an interesting design element to provide insight into trade-offs regarding the capacity investments.

Correlation Between Outcomes of Interest

It is recommended to analyse the correlation between the Outcomes of Interest. Strong negative and positive correlations can indicate the presence of a trade-off between investment possibilities.

Characterization of Outcomes of Interest

The choice for tools to further characterize the Outcomes of Interest depends on the model under analysis, its simulated case, and the insights that the analyst wants to provide their clients with. Therefore, no *one* right characterization tool can be proposed here. However, suggestions are provided.

It is recommended to at least perform a sensitivity analysis to identify the sensitivity of Outcomes of Interest to individual uncertain parameters. This sensitivity can provide insight into the determining power of uncertainties in determining the value of Outcomes of Interest (Moallemi & Köhler, 2019). The *ema_workbench.analysis* library in Python contains various options for regional as well as global sensitivity analysis. Generally, global sensitivity analysis is preferred over regional sensitivity analysis because the global sensitivity considers the direct impact of that uncertainty as well as the joint impact due to interactions across their entire feasible space (Pianosi et al., 2016). The results of the sensitivity analysis will aid in identifying which uncertain inputs are the most determining for the model output and specifically for the specified Outcomes of Interest. This yields insight into the combinations of parameters that lead to specific Outcome of Interest values (Kwakkel, 2017; DeCarolis et al., 2017).

To characterize the energy system designs resulting from the various uncertainty inputs, the *ema_workbench.analysis* library offers various tools. For example, probability density plots can be prepared to show the *distribution* of Outcomes of Interest. Also, the Outcomes of

Interest across all experiments can be visualized as investment trajectories over time with line plots to illustrate *how many* (resulting in what costs and capacity) of *what* (which technology unit) is invested *when* (in which time period). Both line plots and distribution visualizations can facilitate the visual identification of interesting 'clusters' for the Outcomes of Interest. In addition, a measure and visualization of the spread of the data can provide valuable insight into the variability of Outcome of Interest values across experiments.

2.3.3 Subspace Partitioning

In both steps of the results analysis, subspace partitioning techniques are proposed to find (orthogonal) subspaces in the model input space (the uncertainty ranges) that are of interest in determining the resulting design characteristics (total design clusters or design elements) (Kwakkel & Jaxa-Rozen, 2016). In other words: which uncertainties and which values of this uncertainty lead to a high proportion of in-cluster outcomes or particular model behaviour.

Two rule induction methods are presented to explore patterns and relationships in exploratory modelling output data: the Patient Rule Induction Method (PRIM) and Classification and Regression Trees (CART). Both algorithms are included in the *ema_workbench.analysis* library. CART is a tree-based algorithm which, as the tree grows, recursively splits the data into smaller nodes of data. CART is suitable to apply to clustered data and is therefore used on the clusters of experiments that result in similar designs. PRIM is a lenient hill climbing optimization algorithm which recursively 'peels away' small proportions of the data based on a rule that is developed on the remaining data. PRIM is employed to identify uncertainty ranges that result in design trade-offs.

2.4 Model under Analysis

In order to demonstrate the functionalities of the proposed method, it is applied as proof of concept to an existing Energy System Optimization Model. The model and its simulated case are introduced extensively in Appendix A. The essential characteristics of both are summarized in this section.

Using a model to illustrate and evaluate the method functionality decreases the level of abstractness by providing specific results. This model is on the forefront of research into Integrated Energy System Optimization Models. Furthermore, the formulation of the model in the Python language facilitates linking the model to the EMA Workbench. Finally, the aggregated character of the case that is simulated by the model limits the computational requirements for both the method step 2: Exploratory Modelling and the Results Analysis.

The model is a Python-based Energy System Optimization Model that aims to aid decision-making regarding *integrated* energy system design and operation in urban areas. Energy Systems Integration connects energy systems by including interactions among these systems with

for example conversion units, which allows to take advantage of the benefits in efficiency and performance of each of the connected energy systems (Mancarella, 2014; Gabrielli, Gazzani, Martelli, & Mazzotti, 2018; Kroposki et al., 2012). This model solves a greenfield and aggregated case of a medium-sized Dutch city, in which the objective is to identify a least-cost energy system design. To meet the set energy transition goal, the natural gas supply decreases and only PV and wind supply units can be invested in to meet the energy demand up to 2050. In this case, the three energy systems of electricity gas and heat are integrated in the form of network and storage units, and the Combined Heat and Power (CHP), Power-2-Gas (P2G), and Heat Pump (HP) conversion technologies (figure 2.8).

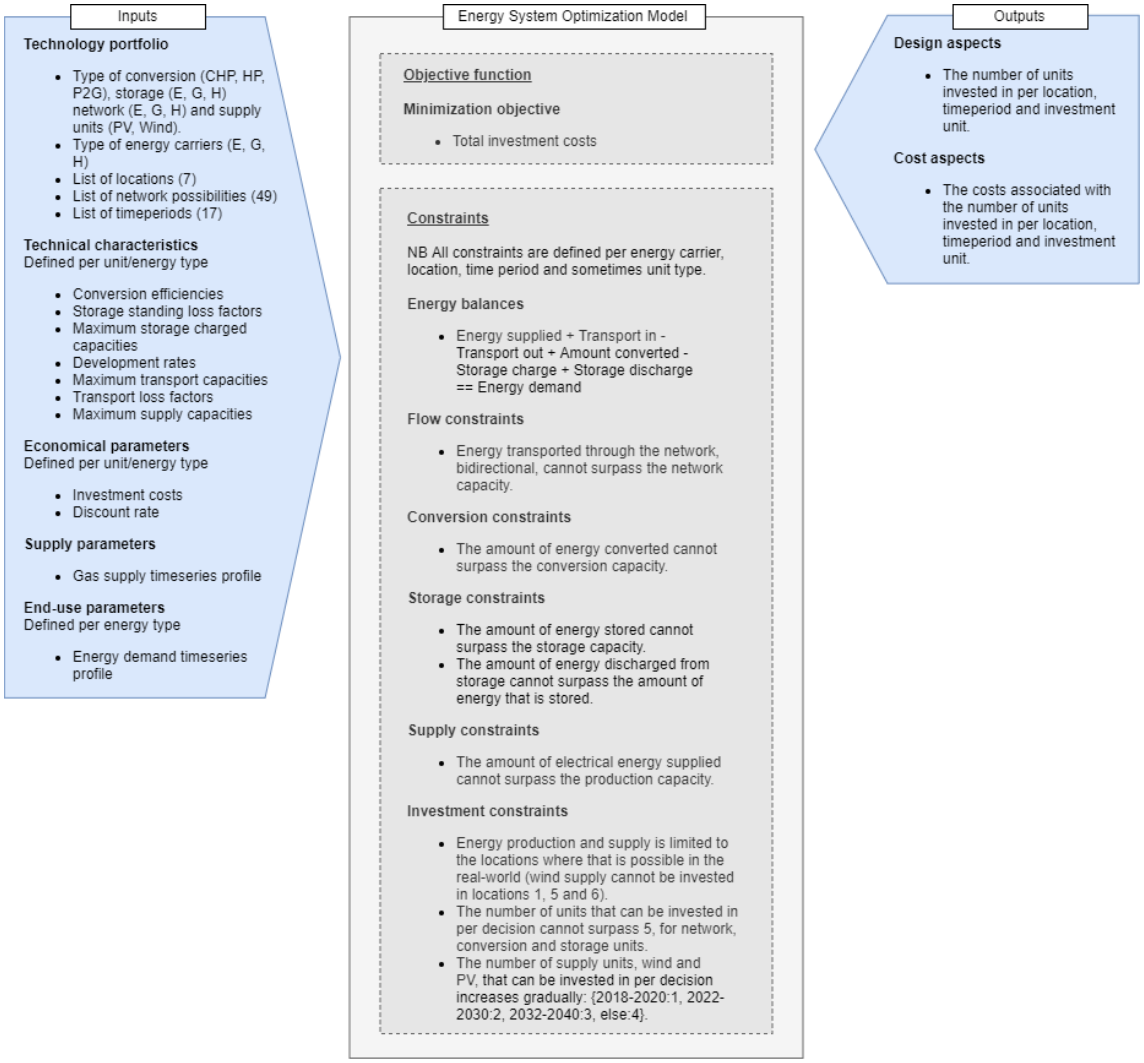

Figure 2.8: Overview of the structure of the analyzed optimization model, and the simulated case, with model inputs, decision variables, outputs, objective function and constraints (figure adapted from Mavromatidis et al. (2018)).

The objective function of the model is to *minimize the total investment costs*. The investment planning consists of the *design* as well as *operation* of the modelled integrated energy system and the model output concerns the number of investments made per investment possibility and the resulting investment costs.

A *branch-and-bound optimization* algorithm is used and the model is written in *Python* (explanation in Appendix A.4). For the specification of this optimization model in Python, the Pyomo software is used in combination with a Gurobi mathematical Mixed Integer Linear Programming (MILP) optimization solver.

The case that is simulated is greenfield. Hence, the model starts investing without 'existing' infrastructure, or brownfield information, being present in the system. The case concerns an aggregated version of the city of Eindhoven in which the total of energy supply/demand relations at 110 locations are combined into 7 locations to limit the computational complexity. Therefore, the model run time with its 'original' data-input and an optimality gap of 7% is limited to approximately 13 to 14 seconds. Decreasing the optimality gap to 5% increases the computation time to approximately 21 to 25 seconds to reach the specified optimality threshold.

The investment possibilities are determined by the three design specifics: technology unit, location and time-period. The *total number of investment possibilities is* 3451, resulting from 11 technology units, 7 locations for non-network investments, 49 edges for network investments between locations and 17 time periods (figure 2.8). The number of decision variables is 11, which involve the technical characteristics and the economical, supply and end-use parameters (figure 2.8). It should be noted that besides the upfront investment costs, costs such as for operation and maintenance or energy prices are not considered.

Chapter 3

Step 1: Uncertainty Characterization

As elaborated upon in chapter 2, any effort to integrate uncertainty into an optimization model starts with uncertainty characterization (figure 3.1). This first step of the proposed method applied to an existing Energy System Design Optimization Model, starts with the top-down analysis, in which renowned energy models and scenario studies are selected and analysed to identify possibly relevant uncertainties. Then this top-down analysis is aligned with the bottom-up analysis to select uncertainties that can actually be related to the model under analysis. Finally, the selected uncertainties are assigned an uncertainty range which is provided as input to the second step of the method: Exploratory Modelling (chapter 4).

Figure 3.1: Step 1 of the proposed method: Uncertainty Characterization.

3.1 Top-Down Analysis

In this section, the analysis of three renowned energy system models and scenario planning studies is described.

Following the three selection criteria that are specified in chapter 2, the IMAGE (Netherlands Environmental Assessment Agency, 2014), PROMETHEUS (E3MLab/ICCS, 2017) and TIMES (Loulou et al., 2016) energy system models are chosen for analysis. These models are introduced in Appendix C.1.1.

In comparing the uncertainty model drivers of the three analysed energy models, it became apparent that the models use different levels of aggregation of model drivers. The TIMES model is quite aggregated and uses just four scenario model drivers. To be more explicit, the TIMES model considers the 'population projections', 'economic development' and 'lifestyle parameters' model drivers as part of the general and aggregated 'Energy service demand' model driver. Whereas PROMETHEUS uses an especially dis-aggregated list of model drivers and formulates eleven inputs. For instance, policies are separated into taxes and subsidies for energy products and CO_2 emission regulations.

Finding a balance between these formulations, the choice is made to use the seven model drivers as formulated in the IMAGE documentation and to relate the TIMES and PROMETHEUS model drivers to these (table 3.1). Consequently, an exact comparison of each model driver for each energy model could not be attained. Therefore, the uncertainty terms used to described the model drivers are not exact copies of the terms used in each energy model.

Table 3.1: Overview of the parameters and variables that are considered to be uncertainties in the three analysed energy models. The notation of an 'X' in a model-column indicates the specification of that uncertainty in the documentation of that energy model.

Uncertainty	**IMAGE**	**PROMETHEUS**	**TIMES**
Climate/energy policies	X		X
Atmospheric composition and climate	X		
Primary (fossil) resources availability		X	X
Econometric estimations		X	
Technological development		X	X
Energy demand	X		X
Energy supply	X		
Energy conversion/efficiency	X	X	
Human development	X		

In addition to the analysis of the three renowned energy system models, an analysis of six scenario planning studies is performed (Witt et al., 2020; Cole et al., 2018; Mcdowall, Trutnevyte, Tomei, & Keppo, 2014; Xu et al., 2019; Huber et al., 2004; Van Vuuren et al., 2012). This analysis resulted in a listing of 15 scenario key factors which, in these studies, are considered as uncertain future values (Appendix table C.1).

3.2 Bottom-Up Analysis

In this section, the model, as introduced in section 2.4 and Appendix A, is analyzed to identify parameters and variables of which the value is potentially subject to external uncertainties and which can be plausibly varied in accordance with the model functionalities.

As specified in section 1.6, this research is scoped to the impact of *external uncertainties* on model parameters and does not consider uncertainties pertaining to the model specification itself. In this section the model-inherent parameters and variables which are potentially subject to external uncertainties are listed. This will enable the selection of uncertainties to be analyzed, because the prerequisite for this is applicability to the model under analysis.

The model under analysis consists of a large amount of parameters and variables which can be split into four categories:

1. Potentially subject to external uncertainties, which;
2. Can be varied in accordance with model functionalities, or;
3. Cannot be varied in accordance with model functionalities;
4. Not subject to (external) uncertainties.

Most of the model-parameters are not subject to external uncertainties. Examples of these model- or case-inherent 'given' parameters are the number of years, the set time-step, the number of locations and the geographical distance between these locations. Other fixed case functionalities are for example the specification of the energy carriers (electricity, gas and heat), the energy conversion units (Combined Heat and Power, Heat Pump and Power-2-Gas) and the energy supply units (wind and PV). Also, the initial investment costs per investment unit are fixed because the first time period lies in the past (the year 2018). Nevertheless, the investment costs *are* varied over time as a function of the initial investment costs, the discount rate and the applicable technological development rates.

An overview of the model parameters that are potentially subject to external uncertainties is provided in Appendix table C.2. Except for the energy demand and gas the supply, which are specified as time series input to the model, these are all constant parameters.

First, most of these parameters are technological property specifications for the investment units: the conversion -, supply-, transport- and storage potential; the transport- and standing losses; and the conversion efficiencies. The values of these technological parameters are all subject to technological development, which is an external uncertainty (Loulou et al., 2016; Netherlands Environmental Assessment Agency, 2014; E3MLab/ICCS, 2017).

Second, two economic parameters are specified: the development- and the discount rate. These rates are used to calculate the time-dependent investment costs per investment unit based on the initial investment costs. In the model, and therefore in this research as well, the development rate represents the decreased cost/technological performance ratio as a result from technological development per investment unit specifically. The unit-specific development rates are added to the generally-specified discount rates to create technology-specific investment cost trajectories over time. Therefore, the development rates are considered to be subject to the external uncertainty of technological development. The discount rate, which is

specified equally for all investment units, is considered to be subject to external uncertainty because a wide range of discount rates is assumed in different studies and the actual rate value is unsure (Steinbach & Staniaszek, 2015). The development of gas supply over time is subject to external uncertainty because it is unsure which energy policy will be implemented, what the natural resource availability is towards the future, and what the potential is of new (renewable) energy sources (Loulou et al., 2016; Netherlands Environmental Assessment Agency, 2014; E3MLab/ICCS, 2017).

Last, the energy demand development over time is considered to be influenced by external uncertainty as a result from for example the interpretation of historical trends, autonomous and policy-induced energy efficiency improvements and the existence of demand saturation levels (Loulou et al., 2016; Netherlands Environmental Assessment Agency, 2014; E3MLab/ICCS, 2017).

As previously mentioned, not all model parameters that are potentially subject to external uncertainties can be varied in accordance with the model functionalities. More specifically, the technological property specifications for the investment units cannot be varied over time (table 3.2). This is due to the mathematical model set-up in which the technological properties are used as constants to calculate, per time step, the *total* potential, losses and efficiency for all units present in the model. Therefore, varying these technological property values over time mathematically implies that the technological properties of the entire unit base are improved: not only the unit base that is invested in in that specific time-step. Such an assumption cannot be supported, because clearly, the technological properties of already installed and existing units cannot be assumed to change over time. Moreover, varying the constants by selecting another technological value from the feasible range in the starting year would make it difficult to compare the outcomes across experiments. This is because the technology units to be invested in would not have the same basic technological properties, with some E storage having for example a hundred-fold storage capacity compared to other E storage units. This would result in the sampling of unrealistic combinations of technological properties for a single unit. Demanding 'realistic' combinations of the algorithm, with for example likely combinations of initial investment costs and conversion potential, would require an alteration of the mathematical model.

This bottom-up model analysis leaves the following model-inherent parameters feasible for variation as a result of external uncertainties: the energy demand time series, the technology unit-specific technological development rates, the gas supply time series and the general discount rate.

Table 3.2: Overview of which of the model-inherent parameters can and cannot be varied as uncertainty in the model resulting from the specific model set-up.

Can be varied	Cannot be varied
Energy demand	Transport potential
Development rate	Transport losses
Gas supply	Conversion potential
Discount rate	Conversion efficiency
	Standing losses
	Storage potential
	Supply potential

3.3 Uncertainty selection

3.3.1 Top-down and Bottom-up Alignment

The energy models and scenario planning studies top-down analysis is aligned with the bottom-up analysis to select uncertainties that can actually be related to the model under analysis. This result of this alignment is visualized in table 3.3. Again, the exact terms used in each study cannot be replicated in comparing studies. For example, for the scenario planning studies the two factors 'Levelized cost of electricity' and 'Technological development' (table C.1) are merged into the 'Development rate' (table 3.3).

Table 3.3: Alignment of the bottom-up analysis (model) with the top-down analysis (energy models & scenario analyses).

	Model	Energy models	Scenario analyses
Energy demand	X	X	X
Development rate	X	X	X
Gas supply	X	X	
Discount rate	X	X	

3.3.2 Uncertainty Selection and Range Specification

Resulting from the alignment, it was decided to vary the following uncertain model-parameters in the exploratory modelling: energy demand, development rates and the discount rate (table 3.4 and table D.3). Additional information is provided in Appendix D.

Demand

According to Isaac and Vuuren (2009), "the main uncertainties in modelling energy demand relate to the interpretation of historical trends, for instance, on the role of structural change, autonomous energy efficiency increases and price-induced efficiency improvements and their

Table 3.4: Specification of the uncertainties to be explored.

Name	Description	Range
Energy Demand Development	The development over time of the total energy demand, split up to represent the electricity, heat and gas demand per location per time period.	12 scenarios
Wind Development Rate	The rate with which the initial investment costs change in addition to the standard discount rate representing the decreased cost/technological performance ratio as a result from wind electricity supply technological development.	[0.022:0.033]
PV Development Rate	The rate with which the initial investment costs change in addition to the standard discount rate representing the decreased cost/technological performance ratio as a result from PV electricity supply technological development.	[0.025:0.075]
Electricity Storage Development Rate	The rate with which the initial investment costs change in addition to the standard discount rate representing the decreased cost/technological performance ratio as a result from electricity storage technological development.	[0.025:0.075]
P2G Conversion Development Rate	The rate with which the initial investment costs change in addition to the standard discount rate representing the decreased cost/technological performance ratio as a result from P2G conversion technological development.	[0.0395:0.1185]
Discount Rate	The rate representing the present value of future technology unit investment costs.	

projection for the future". McCallum et al. (2019) describe the uncertainty related to energy demand development as: "empirical demand curves (by extrapolating and manipulating present-day demand data) are no longer adequate for describing anticipating demands in the future, due to the poorly understood transformation away from traditional demand behavior". The energy demand development is heavily influenced by for example energy efficiency developments, the GDP per capita, policy instruments such as taxes, and population development (Netherlands Environmental Assessment Agency, 2016; Loulou et al., 2016). Due to this uncertainty, and the driving character of the demand parameter, the demand development time-series is considered as uncertainty.

To thoroughly analyse this uncertainty, different demand development scenarios are defined, based on three factors: the total demand in 2050; the energy mix in 2050; and the demand development curve (extensive description in Appendix D). This resulted in 12 demand development timeseries (table D.3) (van Beuzekom et al., n.d.; Witt et al., 2020; Cole et al., 2018;

Table 3.5: Demand development scenarios.

Scenario	Scenario Description
1	Baseline
2	Very high demand
3	Very low demand
4	High demand
5	Low demand
6	High E, Low G, Low H
7	Low E, Low G, High H
8	Low E, High G, Low H
9	Very low E, Very high G, Very low H
10	Fast change
11	Very fast change
12	No change compared to 2018

Marangoni et al., 2017; Xu et al., 2019).

According to DeCarolis et al. (2017), "scenario analysis can be used to address parametric uncertainty by translating scenario assumptions into ESOM input parameters". The total demand in 2050 is specified to be dependent on the change of energy demand resulting from the trade-off between population growth and energy efficiency development. The energy mix considers the share of the electricity, heat and gas to the total energy demand. This is related to the speed of the phase-out of (fossil) gas reliance towards increased renewable electricity and/or heat reliance. Finally, the demand development curve is related to the speed of realization and implementation of currently existing and/or new climate and energy policy targets due to societal and/or political pressure. In developing the demand development it was assumed that the distribution in energy demand per location and in residential, commercial, industrial and transport demand per location remains constant.

Development rates

The development rates for technology units represents the uncertainty in the rate of technological development by accounting for an uncertain change in investment costs per technological performance. By specifying different development rates for these units per experiment, different linear investment costs trajectories are simulated. This way, the investment costs per time period apply only to the units that are actually invested in in that same time period. More explicitly, the algorithm pays a differently developing price per experiment for the same technology unit performance.

As pointed out before, the development rates are technology-specific. It was decided to only incorporate the development rates with a 'base'-value higher than or equal to 2% (table B.7). This threshold is selected because it is assumed that technology units with a faster predicted

future development have a higher probability of uncertain deviations from this presumed development rate value. Consequently, the development rates for the following technology units *are* considered: Power-2-Gas (7.9%), electrical storage (5%), wind supply (2.2%) and solar supply (5%). As a result, the following development rates are *not* considered as uncertainty: Heat Pump (1%), Combined-Heat-Power (0%), gas storage (0%) and heat storage (1.6%). Following the example of Moallemi, de Haan, Kwakkel, and Aye (2017), a range of minus-plus 50% of the estimated (base) value is assumed as the uncertainty range for the development rates (table D.4).

Discount rate

The discount rate reflects the costs and long-term benefits of different future scenarios by representing the change in investment costs (Steinbach & Staniaszek, 2015). Therefore, discount rates are a crucial parameter in energy system analysis. Consequently, the hypothesis is that the model outcomes in terms of investment decisions and especially the investment costs are highly influenced by the assumed discount rate. Next, considering uncertainty on the discount rate implicitly takes into account changes in finance types and policies (Mavromatidis et al., 2018).

Steinbach and Staniaszek (2015) have examined case studies to draw conclusions on the definition of discount rates in energy system analysis. They found that the discount rates used by government agencies as well as in energy scenarios for EU Member States is assumed to be in a range between 1% and 7%. In order to account for the usually high discount rates hurdles and barriers for consumers, the upper range bound is heightened to 15%. Therefore, the range of minus-plus 50% of the estimated (base) value (Moallemi et al., 2017) is expanded to a range between 1% and 15% for the discount rate.

3.4 Uncertainty Characterization: Main Findings

After alignment of the top-down with the bottom-up analysis, it is decided to consider the demand development, P2G, Wind and PV supply and the E storage development rates, and the discount rate as uncertainties in the exploratory modelling.

Chapter 4

Step 2: Exploratory Modelling

In this chapter, the second step of the proposed method as introduced in chapter 2 is discussed (figure 4.1). The exploratory modelling is performed on the Energy System Design Optimization Model under analysis. First, the experiment set-up is described, including certain settings to the model. Second, the specification of the model output is introduced.

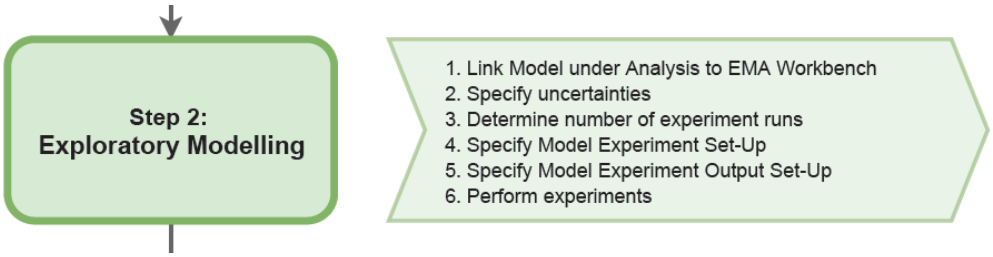

Figure 4.1: Step 2 of the proposed method: Exploratory Modelling.

4.1 Experiment Set-Up

The optimization model requires external data input (figure 2.8). In order to reduce the computational requirements, these 'constant' inputs are imported once and are then provided as input into each experiment from the Workbench. These data are specified in Appendix B. The specified uncertainties are imported into the experiments as real parameters, except for the demand uncertainty which, due to the specification of timeseries, is imported as categorical parameters. These uncertain parameter specifications are introduced in Appendix D.

The exploratory modelling experiment case is executed in parallel with the multiprocessing evaluator. The *ema_workbench.perform_experiments* function is used to sample the specified uncertainties and perform the resulting experiments on the model. The experiment-specific uncertainty input is sampled with Latin Hypercube Sampling (LHS) from the provided uncertainty ranges. LHS is preferred over Monte Carlo sampling because of its efficient layering

process which produces more stable results in reduced computation time (Chong et al., 2015).

The number of experiment runs for k uncertainties should be $> 100 * k$, considering the extra trees global sensitivity analysis technique that is used as part of the results analysis. In this research, $k = 6$ uncertainties are considered. Therefore, the number of runs should be > 600 runs. Therefore, it was chosen to perform 800 experiment runs.

4.1.1 Model Set-Up

Stopping condition

For this study an optimality gap of 7% is specified. As explained in Appendix A.4, the optimality gap can have any value between 0 and 1.0. The lower the specified gap, the closer the optimized solution is to the specified 'Best Bound' and the higher the computational requirements. With a 7% optimality gap, the identified optimal result is guaranteed to be within 7% of the 'Best Bound'. The substantiation for this optimality gap choice is provided in Appendix E.

In addition to the optimality gap of 7%, the stopping condition is supplemented by a maximum computation time specification of 300 seconds. This is implemented to prevent non-converging experiments from running endlessly without reaching the specified optimality gap.

The main stopping condition remains the optimality gap: once a solution with an optimality gap equal to or below 7% is reached, the experiment is considered to be solved to optimality. The percentage of experiments that are solved to optimality is documented to ensure the validity of experiment outcome comparison. With 800 experiment runs, the optimality gap specified to 7% and the maximum computation time of 300 seconds, the percentage of experiments solved to optimality is 100%. This technically rendered the maximum computation time specification unneeded.

Decision-making time horizon

In using models for decision-making, a choice must be made for the time horizon of information that is assumed to be 'known' to decision-makers at the time of their decision-making. Two options are applicable to the model under analysis: using the model as a limited foresight (recursive dynamic) model or as a perfect foresight (clairvoyant) model.

A limited foresight model describes a decision environment where decision-makers do not have information on the full time frame, but on a few years or decades into the future. Thus, sequential decision-making under incomplete information is implied. This offers a good description of the "real-world" decision environment in which decision-makers face high levels of uncertainty with regards to for example future costs, constraints and key developments. This approach can be used to demonstrate pitfalls of short term planning, for example lagging

investments in early time periods (Loulou et al., 2016; Babiker, Gurgel, Paltsev, & Reilly, 2009; Keppo & Strubegger, 2010).

A perfect foresight model, on the other hand, simulates decision-making in each time period with full knowledge of future events. This approach is very useful for providing (socially) optimal and ideal decisions for the modeled problem (Keppo & Strubegger, 2010; Babiker et al., 2009; Loulou et al., 2016). Both decision-making time horizons are valid provided the modeler is well aware of each approach's characteristics (Loulou et al., 2016).

In this research, a perfect foresight modeling approach is employed. Most technology rich energy system models, used for describing the mid- to long-term development of the global or regional energy infrastructure development, are based on a decision-maker with perfect foresight, for example the TIMES, MARKAL and MESSAGE models (Keppo & Strubegger, 2010; Loulou et al., 2016). In addition, the objective of this model is to inform model-owners on the variety of 'optimal' designs under various uncertain future conditions. As explained above, the perfect foresight modeling approach is useful in providing ideal decisions for a modeling problem. Pitfalls of the perfect foresight approach are that it does not reflect the 'short-sightedness' of the decision-maker or the uncertainty present in the decision-making environment (Keppo & Strubegger, 2010; Babiker et al., 2009; Loulou et al., 2016). However, by exploring the impact of uncertainties, the presence of uncertainty in the decision-making environment is inherently acknowledged in this research. This introduces the final argument to use this approach. In energy infrastructural decision-making, the costs are higher and the technology lifetimes are longer than in other decision-making environments. When shorter decision-making time-frames would be simulated, the simulated 'short-sightedness' of decision-makers would lead to some investments never to be made, because these would not be deemed profitable by the model constraints. This is interesting in a decision-making aspect, but not in the main objective of the model under analysis: providing a least-cost integrated Energy System Design.

4.2 Model Output Set-Up

The exploratory modelling experiment case is designed to consist of five output components. The modelling output which is transported back the to the Workbench is a dictionary consisting of these five components. The first being a *ema_workbench.ScalarOutcome* binary vector of whether an experiment case was solved to optimality or not to be able to calculate the percentage of experiments solved to optimality. Then a split is made between non-network and network technology units. This is because the bi-location network investments cannot be combined with the uni-location non-network investments.

For both, a matrix with the number of investments (tables 4.1 and 4.2) and a matrix with the cost of investments is designed and exported according to the set-up explained in section 2.2.3. For the network investments, the matrix size is $[2499, 800]$ and for the non-network investments, the size is $[952, 800]$.

The *total* design matrix is produced by concatenating the network and non-network matrices to a matrix of size $[3451, 800]$. In the table visualizations as example of the total matrices, the first table rows are examples of the specific table composition and ordering, the last few rows present all possibilities for those technology units. The columns $1, 2, ..., 799, 800$ represent the experiment-specific output vectors, with the number of investments per investment possibility.

The Energy System Design of the model under analysis consists of the number of investments *how many units is invested in* for the three design specifics: the technology type *what is invested*; the location *where is it invested*; and the time period *when is it invested*. The number of investments is zero if no investments are made for an investment possibility and above 0 if investments are made, with a maximum of 5 investments per investment possibility (technology unit; location; time period).

Table 4.1: The composition of the number of investments for the non-network investments experiment output matrix. The matrix consists of $klm = 952$ rows and $n = 800$ columns with $k = 8$ non-network technology units, $l = 7$ locations, $m = 17$ time-periods, and $n = 800$ experiment runs.

Type	**Location**	**Time**	**1**	**2**	**...**	**800**
PV	1	2018	1	2	...	1
PV	1	2020	0	0	...	0
...	...	...	...	...	...	...
PV	2	2018	0	0	...	0
...	...	...	...	...	...	...
PV	7	2048	0	0	...	1
PV	7	2050	0	0	...	0
Wind	1:7	2018:2050	...	...	...	...
CHP	1:7	2018:2050	...	...	...	...
HP	1:7	2018:2050	...	...	...	...
P2G	1:7	2018:2050	...	...	...	...
E Storage	1:7	2018:2050	...	...	...	...
G Storage	1:7	2018:2050	...	...	...	...
H Storage	1:7	2018:2050	...	...	...	...

As elaborated upon in chapter 2, the model output should include as much information as possible, to enable the analyst to aggregate the output to any desired Outcome of Interest. An example of the total design matrix, consisting of both the network and non-network investments, aggregated to type results in a matrix size of $[11, 800]$ and is provided in table 4.3. Clearly, the number of rows corresponds with the number of 'items' present in the model for the model-specific to which is aggregated. This aggregation can be performed for the locations and time periods as well. For location-aggregation, the matrix size becomes $[28, 800]$, for the non-network investments can be placed at 7 locations and the bidirectional network investments can be placed at $(7 * (7-1))/2 = 21$ edges. In case of the time-period aggregation, the

Table 4.2: The composition of the number of investments for the network investments experiment output matrix. The matrix consists of $klm = 2499$ rows and $n = 800$ columns with $k = 8$ non-network technology units, $l = 7^2$ locations, $m = 17$ time-periods, and $n = 800$ experiment runs.

Network type	**Location 1**	**Location 2**	**Time**	**1**	**2**	**...**	**800**
Electricity	1	2	2018	0	0	...	0
Electricity	1	2	2020	0	0	...	0
...	...		...	...	...	...	...
Electricity	1	2	2050	0	0	...	0
Electricity	1	3	2018	1	1	...	1
...	...	...	...	...	...	...	...
Electricity	7	6	2048	0	0	...	0
Electricity	7	6	2050	0	0	...	0
Gas	1:7	1:7	2018:2050	...	...	...	...
Heat	1:7	1:7	2018:2050	...	...	...	...

matrix size is $[17, 800]$.

Table 4.3: The composition of the number of investments for the investments output matrix aggregated to type. The matrix consists of k rows and n columns with $k = 11$ technology units and $n = 800$ experiment runs.

Type	**Location**	**Time**	**1**	**2**	**...**	**800**
PV	All	All	17	22	...	7
Wind	All	All	4	4	...	16
CHP	All	All	11	11	...	11
HP	All	All	42	44	...	36
P2G	All	All	6	7	...	19
E Storage	All	All	0	0	...	0
G Storage	All	All	3	3	...	4
H Storage	All	All	0	0	...	0
E Network	All	All	16	16	...	18
G Network	All	All	98	98	...	90
H Network	All	All	0	0	...	2

4.3 Exploratory Modelling: Main Findings

Using the EMA Workbench, written in Python, the model is used to simulate its case for 800 experiment runs. Each experiment run represents a different set of uncertainty inputs, which are sample with Latin Hypercube Sampling. An optimality gap of 7%, in combination with a maximum experiment computation time of 300 seconds, is specified as the stopping condition for each optimization model simulation. The exploratory modelling results in a total outcome

matrix size of $[3451, 800]$, which consists of 800 experiment-specific designs.

Chapter 5

Step 3: Results Analysis

In this chapter the final step of the proposed method is discussed: the results of the exploratory modeling applied to the Energy System Optimization Model (ESOM) (figure 5.1). The aim of this results analysis is to answer two questions with respect to the model under analysis:

- *How do the Energy System Designs vary resulting from underlying uncertainties?*
- *What Energy System Design trade-offs are driven by which underlying uncertainties?*

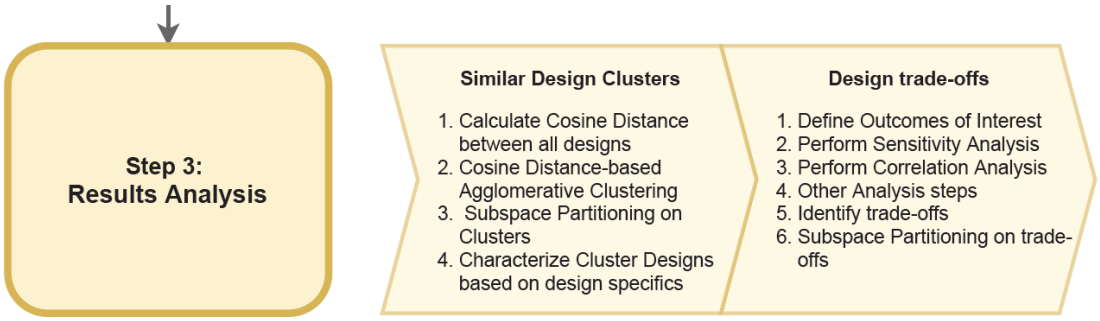

Figure 5.1: Step 3 of the proposed method: Results Analysis.

With the output processing steps, as elaborated upon in chapter 2, the aim is to provide insights valuable to model owners regarding the variability in Energy System Design, the design component trade-offs, and the determining model specifications. The specific results from this proof of concept apply to the case as simulated by the model under analysis.

5.1 Energy System Design Variation

In this section, the results analysis to answer the first question is provided: "*How do the Energy System Designs vary resulting from underlying uncertainties?*". In doing so, the techniques that

are introduced in chapter 2.3.1 are used (figure 5.2).

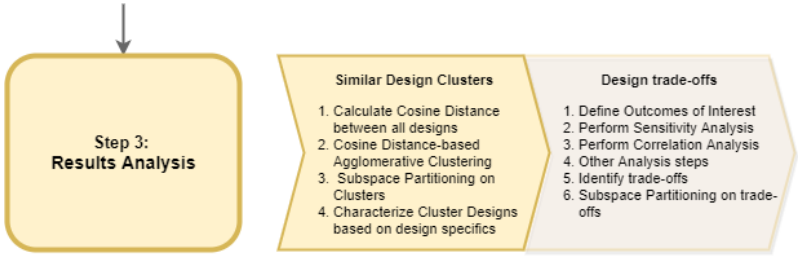

Figure 5.2: Step 3.1 of the proposed method: Results Analysis to identify distinct design characteristics.

The total design matrix is clustered into clusters of experiments that result in similar total energy system designs. The total energy system design is represented by the number of investments per investment possibility for each of the 800 experiments from the total exploratory modelling outcome matrix with size $[3451, 800]$.

To visually identify the desired number of clusters, a dendrogram is produced (figure F.2). This dendrogram portrays the complete linkage distance value between all clusters. These values arise from an agglomerative clustering algorithm with 'complete' linkage performed on the cosine distance matrix. The linkage distance value threshold, which is used to determine the number of clusters, is visualized as the horizontal line in figure F.2 (see section 2.3.1 for the formula). This leads to a linkage distance threshold of 0.252, and a total number of 9 similar design clusters.

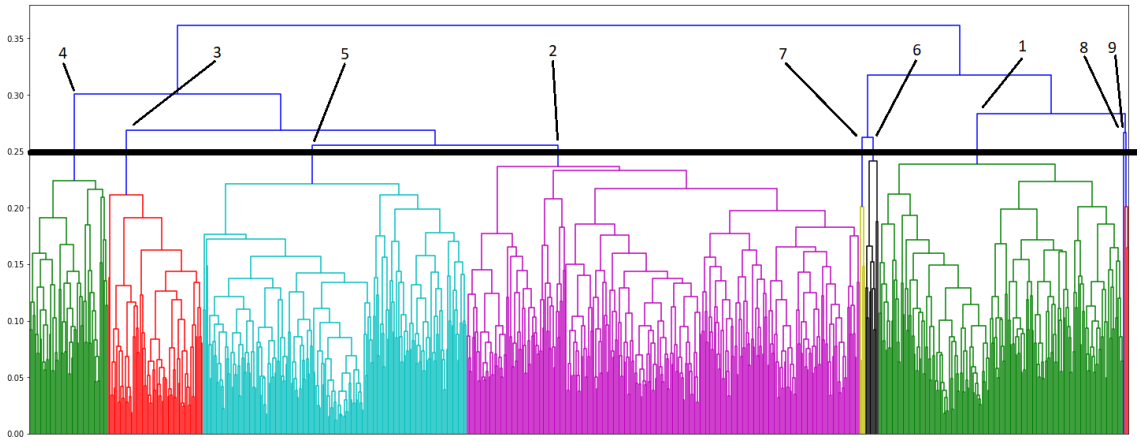

Figure 5.3: Dendrogram of the hierarchical agglomerative clustering of the cosine distance matrix with 'complete' linkage between all experiment outputs for the total design.

Having specified the number of clusters (9), this value is provided as input into the agglomer-

ative clustering algorithm, together with the total design cosine distance matrix ($[800, 800]$). This algorithm results in the assignment of a cluster label $(0, 1, ..., 8)$ to each of the 800 experiments. These cluster labels are further referred to as $(1, 2, ..., 9)$. It is decided to analyse the clusters consisting of more than 1% of all 800 experiments. Three clusters, clusters $7, 8, 9$, consist of less than 1% of the total number of experiments. Therefore, only the six clusters with a sufficient number of in-cluster experiments are further analysed.

5.1.1 Cluster Characterization

Now, the underlying uncertainties and characteristics of the six clusters of similar energy systems design are identified.

First, the underlying uncertainty input ranges resulting in these six clusters of similar designs are identified with the CART subspace partitioning algorithm in CLASSIFICATION mode. This algorithm relates the uncertainty input of each of the 800 experiment runs to the resulting 800 experiment outputs, to which a cluster label $(1, 2, ..., 9)$ is assigned. The algorithm produces a tree (Appendix figure F.3), of which a simplified representation is presented in figure 5.4. To determine which uncertainty ranges are underlying for a specific cluster, the following threshold is adopted: at least 50% of the in-cluster experiments must meet the specified set of underlying uncertainties.

Second, the specific cluster design characteristics are identified by aggregating the total design to the three design specifics (technology type, location and time period). The median and Inter-Quantile Range (IQR) are calculated for each design specific, both for the non-clustered total design (800 experiments) and for each of the six cluster designs. The difference in values between the clusters is visualized with seaborn heatmaps (technology type (figure 5.5), location (figure 5.6) and time period (figure 5.7)). Remarkable cluster design characteristics are interpreted by comparing the median values between the clusters and with the non-clustered characteristics. The IQR represents the in-cluster design similarity. An in-cluster IQR value that is smaller than the associated non-clustered IQR value, indicates a higher in-cluster design similarity.

Resulting from the CART subspace partitioning and the median values for the three design specific aggregates, an overview of the cluster characteristics is provided in table 5.1. The provided cluster characteristics for each of the six clusters entail: the number of in-cluster experiments, the specific uncertainties and their ranges that underlie these cluster designs, and the design characteristics, split into the design specifics: technology type, location and time period. These cluster design characteristics are specified based on comparison of the median values for the cluster designs,with the median values of the non-clustered set of experiments. For each of these clusters, an elaborate characterization is provided in Appendix G.

It seems that the larger a cluster is, in terms of the number of in-cluster experiments, the higher

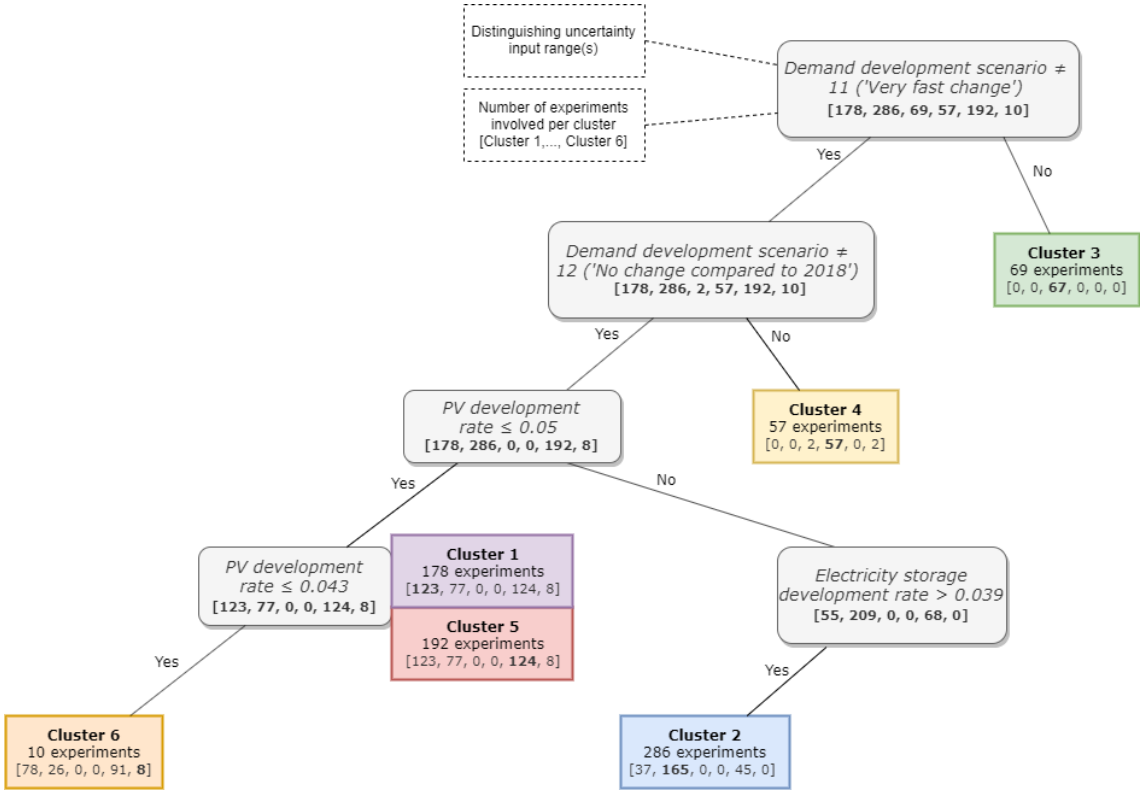

Figure 5.4: Simplified CART tree representation. The tree visualizes the sets of uncertainty input ranges resulting in which clusters of similar energy system design.

the in-cluster design variation. This is confirmed by the observariont that the clusters with a number of in-cluster experiments above 10% of the total number of experiment runs, clusters 1, 2 and 5, portray a lower percentage of in-cluster experiments that meet the specified set of underlying uncertainties (figure 5.4). These three clusters also portray a higher Inter-Quantile Range, especially in the technology type (figure 5.5b) and location (figure 5.6b) design specific aggregations. This is interpreted to illustrate a larger in-cluster design variability, which is as expected for clusters with a higher number of in-cluster experiments. Consequently, this makes it more challenging to draw direct relations between the underlying uncertainties and the resulting, less specific, cluster designs.

5.1.2 General Cluster Design Characteristics

In this section, more general characteristics of the energy system designs across the six clusters are elaborated upon. These general design characteristics are again based on the median values of the clusters aggregated to design specific, as visualized in the previous section: technology type (figure 5.5), location (figure 5.6) and time period (figure 5.7).

Table 5.1: Cluster characteristics for the six similar energy system design clusters. The characteristics are stated in comparison to the non-clustered outcome set representing all 800 experiments. Abbreviations for the uncertainties are: Demand Development Scenario (DDS) and Development Rate (DR).

			Remarkable characteristics compared to non-clustered design		
	# in-cluster	**Underlying uncer-tainties**	**Technology type**	**Location**	**Time-period**
1	178	DDS $\neq 11, 12$. PV DR < 0.05.	High CHP. Low gas storage and gas network.	-	-
2	286	DDS $\neq 11, 12$. PV DR >0.05. E storage DR >0.039.	High PV.	-	-
3	69	DDS 11	High gas storage. Low PV, P2G and CHP.	-	No investments after 2032. High investments in 2024, 2026, 2028 and 2032.
4	57	DDS 12	Very high PV and P2G.	High at 2, 6, 7.	Peak in 2034, High in 2024-2028 and 2036-2044.
5	192	DDS $\neq 11, 12$. PV DR $<= 0.05$.	High gas network. Low HP.	-	-
6	10	DDS $\neq 11, 12$. PV DR $<= 0.043$.	High Wind and P2G. Low PV.	Low at 1, 5, 6.	High in 2036-2044. Low in 2032-2034.

Overall, the IQRs of the clusters are smaller than that of the non-clustered energy system design for all three aggregation levels (figure 5.5b, 5.6b and 5.7b). This confirms that the in-cluster experiments have a higher energy system design similarity compared to the non-clustered design similarity between experiments. Which indicates that using cosine distance-based agglomerative clustering with 'complete' linkage can be successful in identifying clusters of experiments with similar design from a high-dimensional and sparse data set.

General Design Characteristics: Technology type

The total design aggregated to technology type results in an overview of the median total number of investments in each of the 11 technology units, both non-network and network (figure 5.5). In this section, general insights of the technology type-specific characteristics across clusters are provided.

It is observed that the highest number of investments across all clusters is performed in the gas network (figure 5.5a). This high gas network capacity is required to meet the gas demand which is the highest in the first time periods, compared to the electricity and heat demand, across all demand development scenarios (Appendix D). Investing in gas network units is the most cost-efficient solution to transport the supplied gas to the demanding locations. The eventual variability in the number of gas networks invested in across clusters, is explained by a combination of the development of the gas demand towards the future and the location-specific placement of technology units.

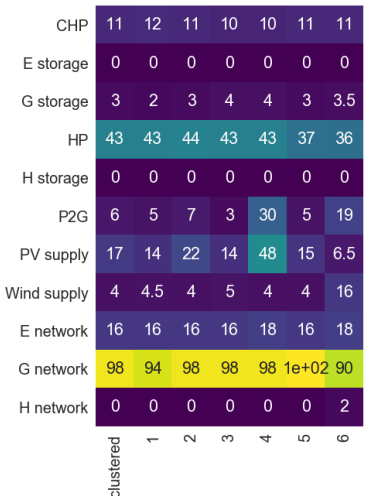

(a) Median number of investments

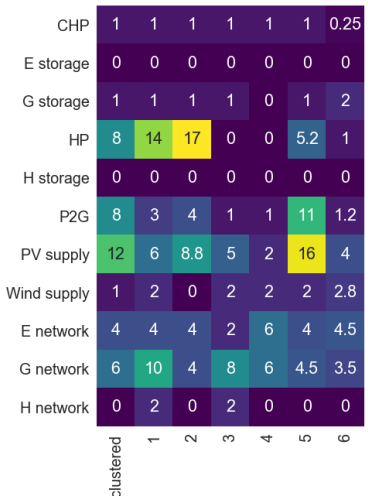

(b) IQR for the number of investments

Figure 5.5: The median and IQR for the number of investments aggregated to the technology units invested in for the non-clustered energy systems design and the six clusters of experiments that resulted in similar total energy system designs.

The next highest number of investments is in Heat Pumps. This can be explained by the fact that it is very energy-efficient to use electricity to gather ambient heat to satisfy the heat demand. In addition, Heat Pump conversion units have the lowest conversion capacity; hence, a higher number of units is required relative to the other conversion units (Appendix table B.9).

The lowest number of investments, or none at all, are performed in electricity storage, heat storage and the heat network. The low occurrence of heat network investments is ascribed to the relatively high associated investment costs and transport losses (Appendix tables B.8 and B.11). Moreover, a large advantage of heat networks and heat storage, which is to compensate seasonal variations, cannot be captured with the annual time periods of the modelled case. The absence of electricity storage capacity investments is an attribute of the annual time step as well. Electricity storage units work with much smaller time steps, such as hours or days, in the real-world. Due to this, the standing losses of electricity storage over a one-year period become too high for electricity storage unit investments to be profitable.

The electricity network investments portray little variation, except for the high number of investments in clusters 4 and 6. In cluster 4, this is explained by the large amount of electrical energy that is to be transported to P2G conversion units in order to meet the high gas demand underlying this cluster. The transport of electricity is preferred over that of gas because of the lower investments costs and the higher transport capacity related to electricity network investments (Appendix tables B.11 and B.8). In cluster 3, the high number of investments in the electricity network is explained by the location-specific constraints of wind supply invest-

ments. Consequently, additional network investments are required to transport the produced electricity to the demanding locations.

Overall, the Power-2-Gas and the PV supply units portray the most variation between the clusters. The number of investments in wind supply is relatively constant, except for the high number of investments in cluster 6. This is explained by the particularly low PV development rate underlying this cluster. The relatively expensive character of high investments in wind supply as opposed to PV supply, due to its location-specific investment constraints, are alleviated for a low PV technological development. The reader is referred to section 5.2 for a more elaborate analysis of these findings. In that section, the underlying reasons for the existence of a trade-off between PV and wind supply investments and the relation between PV and P2G capacity investments are identified.

General Design Characteristics: Location

The total design aggregated to location results in an overview of the median number of *non-network* investments at all seven locations and the number of *network* investments at one of the 21 bi-directional edges between the seven locations (figure 5.6).

Overall, the location-specific placement of network and non-network investments across experiments and clusters is quite similar (figure 5.6b). Most non-network investments are placed at location 6 (figure 5.6a, Node_x). The apparent 'hub' character of location 6 is followed by locations 2 and 7. This locational non-network investment placement follows the percentual contribution to the total demand of the locations (table 5.2).

Table 5.2: Percentual contribution of the 7 locations to the total energy demand. The percentages of the electricity, gas, heat and total demand per location are provided.

Location	Contribution to Total	Electricity	Gas	Heat
1	9.0%	8.61%	9.71%	8.87%
2	16.1%	17.10%	18.08%	14.25%
3	9.0%	8.61%	9.71%	8.87%
4	10.1%	9.23%	9.71%	11.02%
5	10.1%	9.23%	9.71%	11.02%
6	29.7%	30.11%	25.00%	31.72%
7	16.1%	17.10%	18.08%	14.25%
Total	100.0%	100.0%	100.0%	100.0%

In line with this, all locations are connected to location 6 with network investments (figure 5.6, 'Edge_x_x'). The relatively high amount of investments at high-demand locations 7 and 2 are almost exclusively transported from and to highest-demand location 6. The locations with a lower demand, 1, 3, 4 and 5, are not necessarily well connected. However, strong

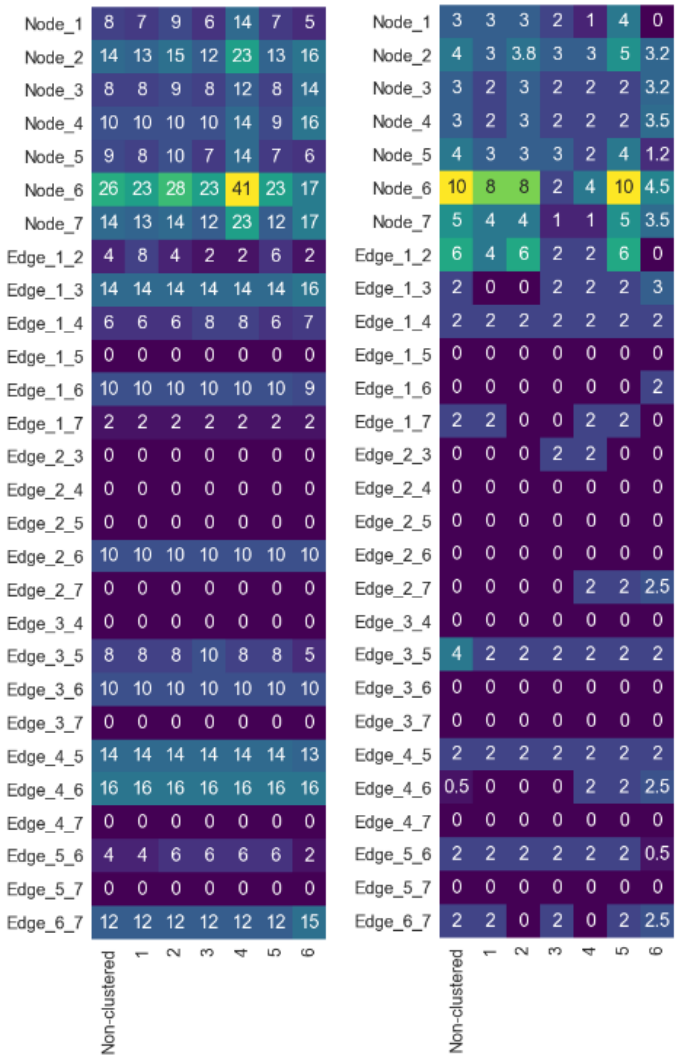

(a) Median number of investments

(b) IQR for the number of investments

Figure 5.6: The median and IQR for the number of investments aggregated to the location of investment for the non-clustered energy systems design and the six clusters of experiments that resulted in similar total energy system designs.

low/low-demand network connections exist between $1-3$, $1-4$, $3-5$ and $4-5$. Otherwise, these lower-demand locations are connected exclusively to location 6 with low/high-demand networks, except for location 1, which has low/high-demand network connections, however more limited, with high-demand locations 2 and 7 as well. The exclusiveness of the low/high-demand network connections between lower-demand location 1 and both high-demand locations 2 and 6 is explained by it being the shortest low/high-demand edge distance. In other words, the other lower-demand locations have a longer edge distance to these high-demand

Table 5.3: The network distance in kilometers between all seven locations.

[km]	1	2	3	4	5	6	7
1	0						
2	2.8825	0					
3	2.3394	3.1535	0				
4	1.9911	4,8737	3.4704	0			
5	4.461	7.3088	5.2187	2.5366			
6	5.0739	7.1747	7.3157	4.2135	5.139	0	
7	3.4563	3.2841	5.3733	4.7446	7.1819	4.778	0

locations. This model preference for the shortest edge distance for low/high-demand network connections is alleviated for location 6, which apparently has a sufficiently high energy demand to compensate for the longer edge distance for low/high-demand network connection placement.

In none of the experiments, (bidirectional) network investments are performed between locations $1-5$, $2-4$, $2-5$, $3-4$, $3-7$, $4-7$ and $5-7$. The absence of low/low-demand network connections between locations $1-5$ and $3-4$ and low/high-demand network connections between locations $2-4$, $2-5$, $3-7$, $4-7$ and $5-7$ are a result of the edge distance. For all these network connections, the edge distance is, for one of both edge locations, the longest of the total of six edge distances in which that location is involved (table B.3).

General Design Characteristics: Time period

The total design aggregated to the time period of investment is portrayed as an overview of the total median number of investments, non-network and network, for all time periods except for the first (2018) (figure 5.7).

As mentioned earlier, the greenfield character of the model causes a 'baseload' of investments to be performed in the first time period (figure 5.13). Because of the large size of this baseload, the presence and differences between smaller investments in later time periods are poorly registered by the cosine distance algorithm. This is visualized in figure 5.8.

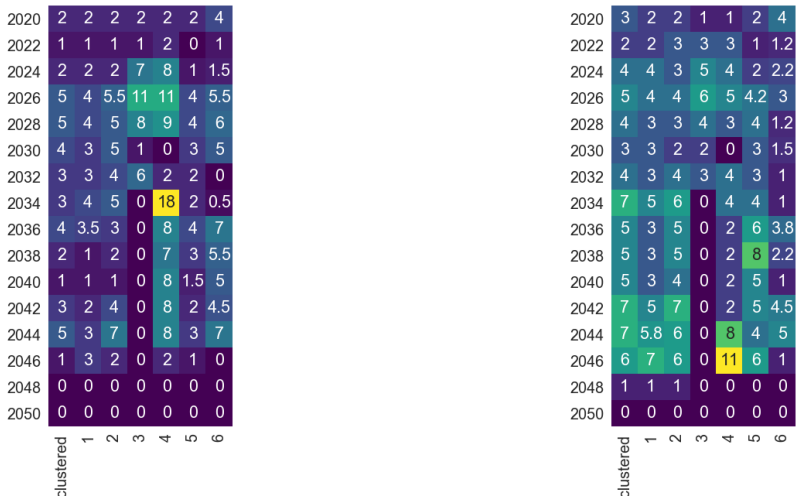

(a) Median number of investments

(b) IQR for the number of investments

Figure 5.7: The median and IQR for the number of investments aggregated to the time period of investment for the non-clustered energy systems design and the six clusters of experiments that resulted in similar total energy system designs.

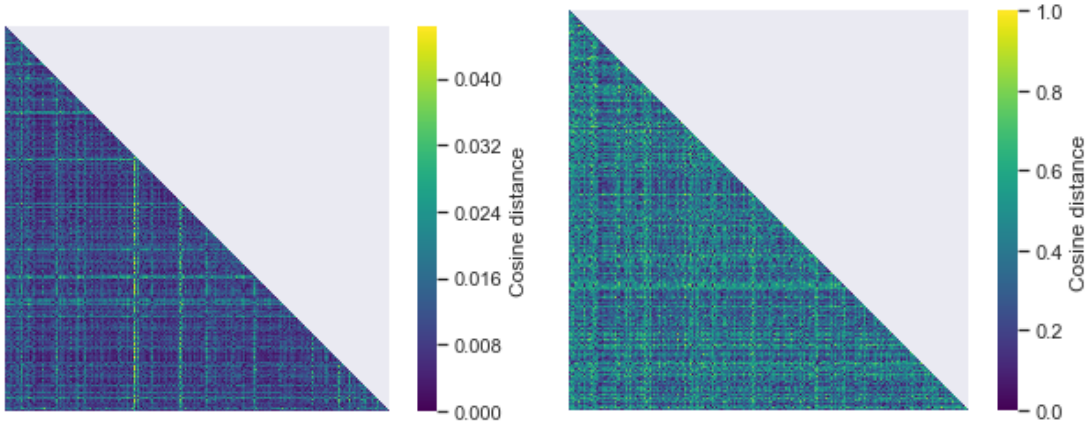

(a) Time period aggregation

(b) Time period aggregation without 2018

Figure 5.8: Seaborn heatmap of the cosine distance values between all experiment outputs for the design aggregated to time period. (b) The 2018 time period counts are removed. The number of rows and columns is equal to the number of experiments (800).

The cosine distance matrix with the distance values between the total design, aggregated to time period, between all 800 experiment runs is presented in the form of a *seaborn* heatmap. A higher distance between experiments is depicted yellow and a lower distance is darker blue on the heatmap. The heatmap that includes the first time period (figure 5.13a), por-

trays much lower distances and identified differences between experiments compared to the heatmap which represents the cosine distance matrix where the first time period is omitted (figure 5.13b). Therefore, it was decided to portray the total design aggregated to time period *without* the starting year 2018 (figure 5.7).

The time periods in which the 'bulk' of investments is performed varies across clusters (figure 5.7b). Over all 800 experiments the main 'bulk' of investments, besides the 'baseload' in 2018, is performed between 2026 and 2044. Overall, the median number of investments that is performed in the final two time-periods is zero. This follows logically from the baseload in the first time period and the final time period in 2050. Clusters 1, 2 and 5 portray a time period-specific design similar to that of the non-clustered experiment set. Cluster 6 portrays a similar pattern, but higher median number of investments per time period. The time period-specific design of clusters 3 and 4 notably deviates from the other (non-)clusters. This is elaborated upon in Appendix G.

5.1.3 Energy System Design Variation: Main Findings

The most important finding from this section is that the use of a cosine-distance based agglomerative hierarchical clustering algorithm with 'complete' linkage in this case is successful in identifying clusters of similar energy system design from the high dimensional data set. In addition, it is demonstrated that the explored uncertainties result in clusters of energy system designs with distinct characteristics. Furthermore, these characteristics are traced back to the underlying uncertainty input. In addition, it is shown that clusters with a number of in-cluster experiments lower than 10% of the total number of experiments, result in clusters with more distinguishable and unique energy system design characteristics. Moreover, these characteristics are better deducible to a set of underlying uncertainties.

5.2 Energy System Design Trade-offs

This section provides the results analysis to answer the second question posed: "*What Energy System trade-offs are driven by which uncertainties?*". The method as described in chapter 2.3.2 is used (figure 5.9). First, it is specified between which design elements trade-offs are identified. Second, various data analysis techniques are employed to identify trade-offs between the specified design elements. Finally, this section provides general characteristics of the analyzed design elements.

Figure 5.9: Step 3.2 of the proposed method: Results Analysis to identify trade-offs between design elements.

5.2.1 Outcomes of Interest

To provide insight into Energy System Designs trade-offs, resulting from the impact of uncertainties, Energy System Designs *elements* that are specifically relevant for the model under analysis, are analyzed. These are called: Outcomes of Interest. In this proof-of-concept, the model targets local governments and energy system operators. Therefore, outcomes of specific interest to the model owners are:

- the required energy capacity to be invested in per technology unit;
- the associated costs, under the variety of futures considered, to meet the energy demand.

Therefore, the Outcomes of Interest are specified as the *cumulative capacity invested in for each of the technology units* considered in the model: wind and PV supply units, Electricity, Gas and Heat storage units, Combined Heat and Power (CHP), Heat Pump (HP) and Power-2-Gas (P2G) conversion units and Electricity, Gas and Heat network units. The three network types are aggregated to one Outcome of Interest: the total network unit capacity invested in. Besides these, the cumulative total investment costs and cumulative total number of investments are presented.

The cumulative capacity invested in per Outcome of Interest provides a direct insight into the amount of energy invested in per experiment per technology unit over all locations and time periods. The energy capacity value per unit, PetaJoules (PJ), is equal across all experiments. Therefore, the capacity invested in is chosen as the main Outcome of Interest. On the contrary, the investment costs per technology unit per time period are calculated with the discount rate and development rates, which are varied as uncertainties. Consequently, the output in monetary values cannot be compared one-on-one between experiments, without considering the uncertainty input. Nevertheless, because the costs are an important outcome to the decision makers targeted by the model-owner, these are provided as well.

It must be noted that the electricity storage capacity invested in is excluded from further analysis, due to the absence of investments in this Outcome of Interest across all 800 experiments. As explained before, the absence of electricity storage investments is ascribed to the annual time steps of the modelled case.

5.2.2 Design Trade-offs

To demonstrate the sensitivity of the Outcomes of Interest to the uncertainties, or in other words, the determining power of the uncertainties for each Outcomes of Interest, an Extra-Trees feature scoring sensitivity analysis is performed (figure 5.10). The Extra-Trees technique is employed because, compared to Sobol indices and linear regression, it requires relatively limited computational resources, does not assume linearity and lacks a restrictive assumption for unimodal symmetry (Kwakkel & Jaxa-Rozen, 2016). In this visualization, the Outcomes of Interest are portrayed on the x-axis and their feature scores to the uncertainties on the y-axis are portrayed with a color range. A bright yellow score indicates a higher sensitivity and the more dark blue, the lower the sensitivity of the Outcome of Interest to that uncertainty. It should be noted that the feature scores have no statistical value: the scores are only significant in comparison to each other.

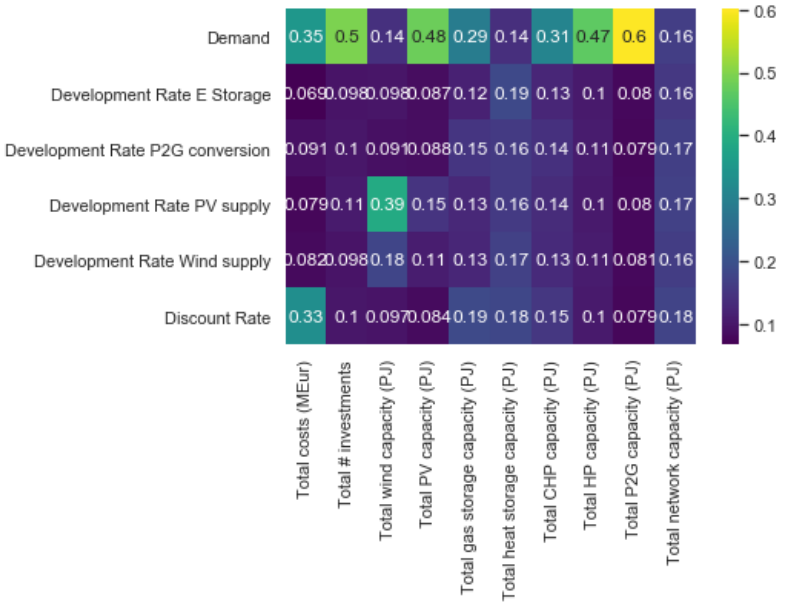

Figure 5.10: Extra-Trees based feature scoring of the sensitivity of the outcomes of interest to each uncertainty. Yellow indicates a relatively high sensitivity and a relatively low sensitivity is indicated with dark blue.

Overall, the energy demand development uncertainty has the highest determining power for most Outcomes of Interest (figure 5.10). This is as expected, because the demand development is the most determining factor for the required energy capacity to be invested in in the model. However, not all demand development scenarios have an equally determining power, which will be elaborated on later in this chapter. Given the direct relation of the discount rate on the investment cost trajectory over time, the high determining power of this uncertainty to the total investment costs is as expected as well.

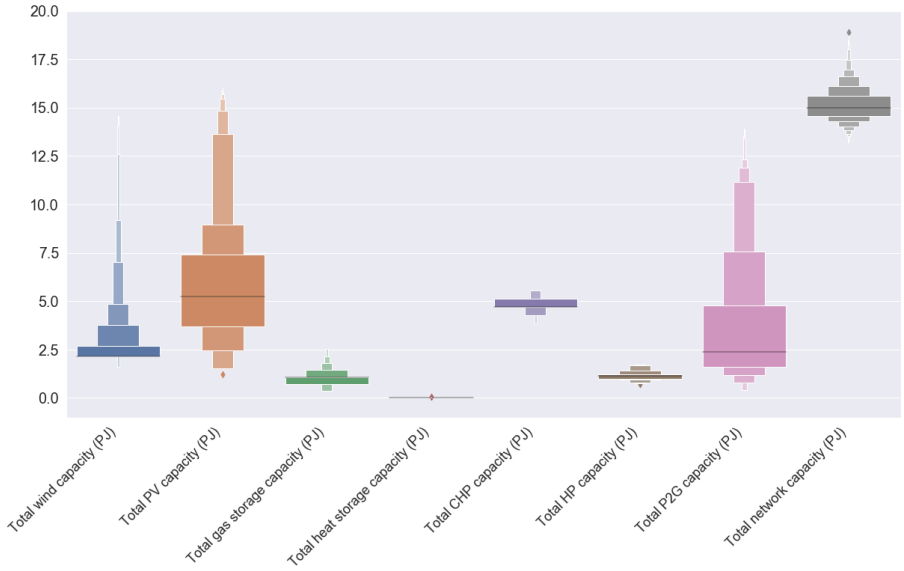

Figure 5.11: Seaborn boxenplot portraying the distribution and the shape of that distribution of the cumulative capacities invested in across experiments per Outcome of Interest (PJ).

In addition to the sensitivity of Outcomes of Interest, their value distribution, and the shape of that distribution, are visualized with a seaborn boxenplot (figure 5.11). The 'longer' the spread of the distribution, the higher the Outcome of Interest value variability across experiments. The 'width' of the boxes represents the number of experiments resulting in an y-axis value range corresponding to that box. The horizontal black line in one of the boxes per Outcome of Interest represents the median value across all experiments. A 'short' box indicates that the Outcome of Interest has a more fixed required capacity to be invested in across the uncertainties considered. Overall, the deterministic optimal solutions, in terms of some Outcomes of Interest, are shown to be varied seriously by the parameter uncertainties.

Furthermore, to indicate the presence of trade-offs between these investment possibilities, strong positive and negative correlations between Outcomes of Interest are used. An aggregated correlation matrix with the correlation between all Outcomes of Interest is visualized with a heatmap to provide a more direct insight into the findings (figure 5.12). A diverging color bar is used to stress the difference between positive (red), neutral (white) and negative correlations (blue).

The most noteworthy correlations are addressed in the following sections. The underlying uncertainties resulting in these trade-offs are identified with PRIM subspace partitioning. A more elaborate description of this analysis step is provided in Appendix H.4.

- Negative correlation between the capacity invested in PV or in wind supply units.
- Positive correlation between the cumulative P2G conversion and PV supply capacities (the P2G conversion capacity invested in is positively correlated with all but one, but

this is the strongest);

- Negative correlation between the cumulative CHP conversion and gas storage capacities (the CHP conversion capacity invested in is negatively correlated to all but one Outcomes of Interest, however, this is the strongest);

Design Trade-off: PV versus Wind Supply

A clear trade-off between investments in either PV supply or wind supply capacity is distinguished, for which the PV development rate is most determining, especially in case of the wind supply capacity (figure 5.10). In this trade-off, the model portrays a clear preference for PV over wind supply technology investments (figure 5.11.

This PV supply preference is a result of both the lack of seasonal and day/night patterns in the model and the locational constraints for wind supply investments (figure 2.8). First, due to the absence of seasonality and day/night patterns, the model assumes the energy supply performance of PV supply units over time to be more reliable than in it is in reality. Second, and most

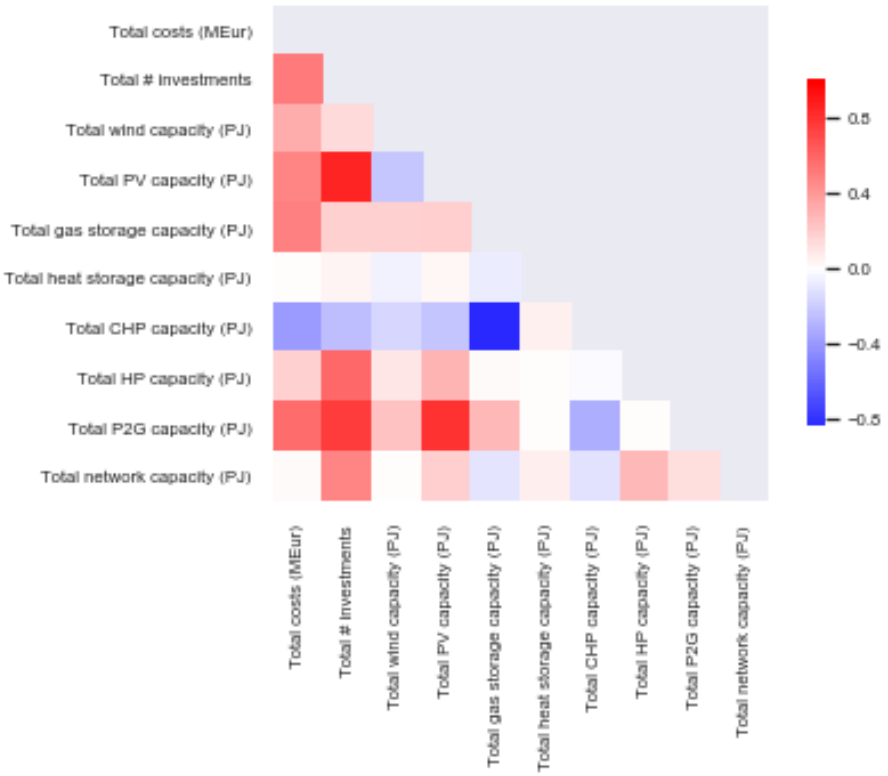

Figure 5.12: Seaborn heatmap of the correlation between the Outcomes of Interest. Darker red indicates a more positive correlation and a negative correlation is indicated with darker blue. The more white the color, the more neutral the correlation.

determining, the model has locational constraints for wind supply placement at locations $1, 5$ and 6. The electricity demand at location 6 is over 30% of the total electricity demand over all seven locations (Appendix table B.2). Therefore, due to these constraints, additional electricity network investments are required to meet the demand at the constrained locations in case of wind supply investments. Consequently, although the supply capacities per investment of PV and wind are comparable (Appendix table B.11 and B.10), investing in wind supply capacity is more expensive. Due to the objective function to minimize the total investment costs, this leads to preferred PV supply investments, provided the PV development rate is sufficiently high. As a result, it was as expected that 1) the PV development rate is most determining, and more determining than the wind supply development rate, for the wind supply capacity invested in in this model and 2) that the model has a preference for PV supply capacity investments.

This trade-off and the determining power of the PV development rate are induced by the models preference for PV supply capacity over wind capacity (figure 5.12). The PV development rate 'tipping point', resulting in either a relatively high capacity of PV supply or of wind supply investments, is identified with PRIM subspace partitioning to have a value of 0.04 or 4%. Generally, if the PV development rate is < 0.04, the wind supply investments are relatively high and the PV supply investments are lower and vice versa.

Design Trade-off: P2G Conversion & PV Supply

The capacity investments in P2G conversion and PV supply technology are strongly positively correlated and both are strongly determined by the energy demand development uncertainty as opposed to their respective technological development rates (figures 5.12 and 5.10).

This is as expected, because with the decreasing gas supply, P2G conversion of electrical energy to gas is considered as the sole source of gas 'supply' in the model. Subsequently, the models 'energy balance constraint' requires the energy demand to be met by the supply (figure 2.8). The P2G technology being the sole source of gas 'supply' in the model is also what explains the strong positive correlation between PV supply and P2G conversion technology, which converts the PV supplied electricity to gas. As a result from the above mentioned model preference for PV supply, the positive correlation between P2G conversion and wind electricity supply is less pronounced. The strong dependence of both the required cumulative P2G conversion and PV supply capacities to be invested in, and the periods of investment on the (gas) demand development, is also what causes the large spread in P2G and PV capacity investments across experiments. These are also a function of the spread in demand development scenarios (figure 5.11).

The determining underlying uncertainty ranges are identified with PRIM subspace partitioning. The demand development scenario 'No change compared to 2018' is dominantly determining for both the P2G and the PV capacity investments to be exceptionally high (> 12.5 PJ).

As expected, the experiments resulting in a cumulative capacity invested in $< Q1$ PJ for both the P2G and PV technologies, are determined by the demand development scenario 'Very low demand'.

Trade-off: CHP Conversion versus Gas Storage

The strongest negative correlation is distinguished between CHP conversion and gas storage capacity investments and both are comparably determined by the energy demand development uncertainty (figures 5.12 and 5.10). Both the CHP conversion and the gas storage investments are discretely distributed across experiments and portray a relatively limited spread in outcome across experiments (figure 5.11).

The negative correlation between CHP conversion and gas storage capacities invested in, is explained by their respective properties, which are functional in opposing scenarios. CHP conversion units convert superfluous gas to electricity and heat, when the demand development scenarios do not portray continued gas reliance. Due to the demand-supply balancing constraint of the model, which requires the 'end-sum' of energy present in the system to be 0, this is preferred over investing in supply and HP conversion units to deliver electricity and heat. Because of the lack of continued gas reliance in these scenarios, CHP conversion of the superfluous gas is preferred over storage. As opposed, investments in gas storage capacity are required to store superfluous gas when the demand development scenarios portray a continued gas reliance towards the future. In such cases, the gas that is superfluous now, is stored for later time periods as opposed to converting it to electricity or heat to consume now, due to the relatively high investment costs of P2G conversion technology compared to gas storage investment costs.

This substantiation is supported by the demand development scenarios underlying respectively high CHP and low gas storage investments and vice versa, as retrieved by PRIM subspace partitioning techniques. The gas demand development scenarios with a fast change from gas reliance to electricity and heat reliance, result in the experiments with the highest quantile CHP conversion and lowest quantile gas storage capacities invested in. On the other hand, the scenarios with high continued gas reliance or with a delayed drop in gas reliance, 'No change compared to 2018' and 'Very fast change', result in the experiments with the lowest quantile CHP capacity and highest quantile gas storage investments. This corresponds with the high P2G and PV capacity investments for this demand scenario which also relates to the positive correlation of P2G, PV and gas storage capacity and the negative correlation of these with the CHP capacity invested in (figure 5.12). Apparently, when the demand composition will not decrease or change, in combination with the intended decreasing gas supply, superfluous electricity production is required to convert to gas with P2G units and subsequently stored. Depending on the PV development rate, this superfluous electricity production is supplied by either PV units (PV development rate $>= 0.04$) or by wind units (PV development rate < 0.04). In this scenario, CHP conversion is evidently not desired, as the gas supply is

insufficient to meet the demand.

5.2.3 General Findings on Outcomes of Interest

In addition to the specific trade-offs between investments in different technology unit capacities, additional remarkable general findings are formulated for the Outcomes of Interest.

The complete set of uncertainties is equally, and to equally limited extent, determining for the heat storage and network capacities invested in. As described before, a large advantage of heat networks and storage, which is to compensate seasonal variations, cannot be captured with the annual modelled time periods. A variation in underlying uncertainties does not change the resulting absence of investments in these technology units. The low general sensitivity of network capacity investments to the uncertainties is induced by the greenfield character of the case studied in the model under analysis. This leads to a 'baseload' of investments in the first time period across all experiments, which is *especially* high for network investments (figure 5.13b). There is some variation in the amount of investments in the baseload, which mainly stems from the network capacity being a combination of the three network units of electricity, gas and heat. Also, due to the perfect foresight modelling approach, the network capacity baseload responds to the required capacity resulting from the uncertainties, but this variation is quite limited. Furthermore, the wind supply and gas storage (non-network) capacity investments are mostly baseload investments as well (Appendix H.2). The impact of uncertainties becomes increasingly important over longer time periods. As a result, the low determining power of uncertainties on the network investments, which are performed in the first time period, is as expected.

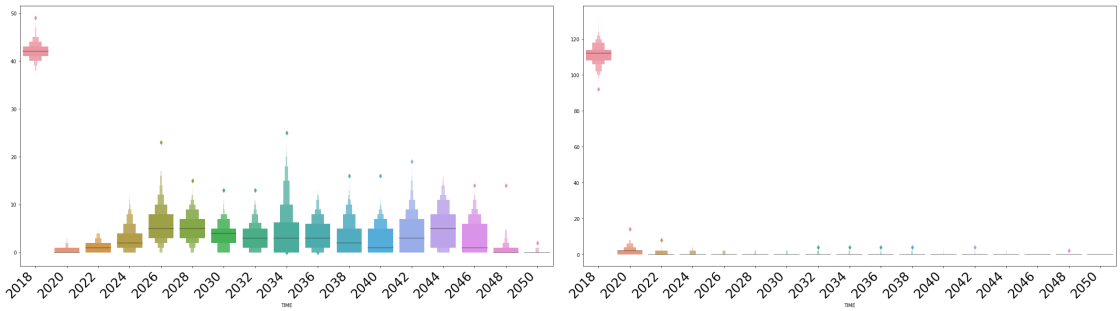

(a) Non-network investments time period aggregation (b) Time period aggregation for network investments

Figure 5.13: Seaborn boxplot of number of investments over all experiments aggregated to time period including the 2018 time period for both network and non-network investments.

A more quantitative characterization of the Outcomes of Interest compared to figures 5.11 and 5.12, is provided in table 5.4. The distribution of most Outcomes of Interest is not Gaussian (normally) distributed, but discretely (Appendix H.2, probability density plots). Consequently,

the standard deviation is not suitable to represent the data spread. Therefore, the 50% (median), 25% (Q1) and 75% (Q3) quantiles are used. The median is used to indicate which investment options are most commonly invested in across the experiments. The data spread, represented by the Inter Quantile Range (IQR), is used as a measure for Outcome of Interest data variability across experiments resulting from uncertainties. Note that the IQR can only be compared across Outcomes of Interest which are expressed in the same unit (table 5.4).

Table 5.4: The specifics per Outcome of Interest sub-section in the form of the median, 25% and 75% quantile borders, Inter Quantile Range (IQR), representing the data spread across experiments, and the minimum capacity invested in.

Outcome of Interest	**Median**	**Q1: 25% quantile**	**Q3: 75% quantile**	**IQR**	**Minimum**
Total costs (MEur)	223.54	214.85	237.29	22.44	202.21
Total # investments	203	191	218	27	156
Total wind capacity (PJ)	2.16	2.16	2.7	0.54	1.62
Total PV capacity (PJ)	5.25	3.71	7.42	3.71	1.236
Total gas storage capacity (PJ)	1.08	0.72	1.08	0.36	0.36
Total heat storage capacity (PJ)	0	0	0	0	0
Total CHP capacity (PJ)	4.69	4.69	5.11	0.43	3.83
Total HP capacity (PJ)	1.15	0.99	1.20	0.21	0.72
Total P2G capacity (PJ)	2.38	1.59	4.76	3.18	0.40
Total network capacity (PJ)	14.99	14.56	15.60	1.04	13.16

As expected from the high sensitivity to the demand development uncertainty and the positive correlation, the PV supply and P2G conversion capacities portray the largest data spread across experiments (table 5.4). In line with this, the Outcomes of Interest which are less determined by the demand development, the wind supply, gas storage, heat storage and CHP conversion, portray a limited data spread with a discrete distribution (table 5.4 and figure 5.11).

The HP conversion capacity invested in seemingly deviates from this pattern as it is as sensitive to the demand development as the PV supply, but unexpectedly portrays a small instead of a larger IQR. Actually, in this case, the use of the IQR as a measure for data spread is somewhat misleading, because the required HP conversion capacity across all experiments is simply a very low value. Relative to this low value, a large variation of values is represented by the IQR. This is in line with the high sensitivity to the demand development. The high variation is made apparent in comparing the (discretely distributed) probability density functions of CHP and HP conversion capacities invested in (figure 5.14). The CHP conversion capacity invested in portrays just five potential values in a total range of 2 PJ across all experiments, whereas the HP conversion capacity invested in shows a much larger number of potential values in a range 1 PJ, which confirms the larger variation of potential values within the small range.

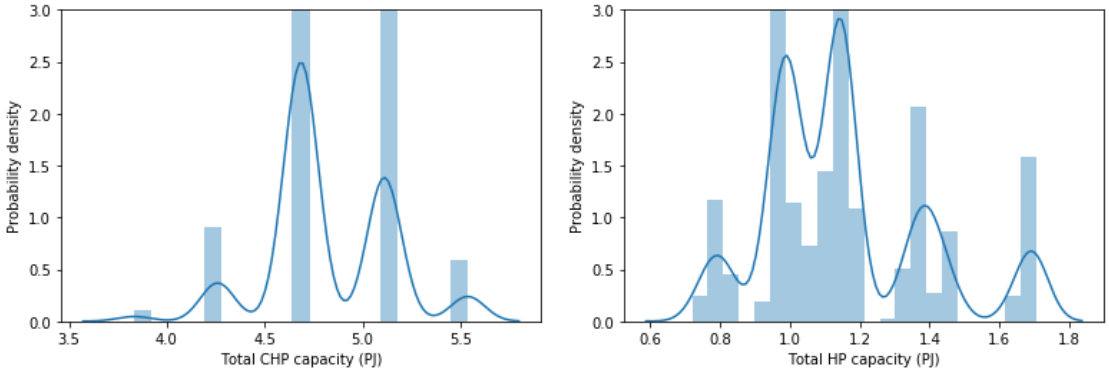

(a) CHP (b) HP

Figure 5.14: Kernel Density Estimate comparison of the probability density of the Outcome of Interest values across all experiments for the CHP and HP conversion capacities invested in.

5.2.4 Energy System Design Trade-offs: Main Findings

All in all, the PV development rate value and the demand development, especially the gas reliance, are the most determining uncertainties for the model investment considerations. The PV supply is preferred over wind supply, due to the location-specific constraints for wind supply and the related additionally required network investments. This trade-off is determined by the value of the PV development rate. The demand development, and especially the gas reliance, are determining for whether the model performs investments in either P2G units, PV supply and gas storage or CHP conversion units. Supplied gas is only converted to electricity and heat if the future gas demand is limited.

Chapter 6

Discussion, Conclusions and Reflection

This chapter elaborates on the proposed method and the results demonstrated in previous chapters. In this research, a method is proposed with which the impact of uncertainties on Energy System Design Optimization Model outcomes can be simulated and analyzed to provide insight to model-owners. The method consists of three steps: Uncertainty Characterization, Exploratory Modelling and Results Analysis. This research also entails a proof of concept of the method functionality by application of the method to an existing Energy System Design Optimization Model. This model optimizes a least-cost investment strategy for the design and operation of an integrated energy system case-study for a medium-sized Dutch city that includes the systems of electricity, gas and heat.

First, a discussion on the real-world implications of this research is provided. This is followed by the limitations to which the method and this research are subject. Next, remarks for the use of the proposed method by model-owners or analysts are provided. Then, the conclusions provide answers to the questions posed, based on the proof of concept method application to an ESDOM and its simulated case study. Furthermore, the method functionality in meeting the aim of this research is concluded upon. Finally, recommendations for future research are posed.

6.1 Implications of this Research

In this section, insights from this research are translated to broader implications. The build-up of this section transitions from the implications of this research from a narrow to a broad spectrum. First, implications for the presence and analysis of uncertainties with respect to Energy System Optimization Models are discussed. Followed by the specification of implications for the modelling of Energy System Designs and for the role of energy systems in the energy transition. Finally, implications for Design Optimization Models and their model-owners in general are discussed.

6.1.1 Implications for the Analysis of Uncertainty in Energy System Optimization Models

In this research the demand development, technological development and the discount rate are analyzed as determining uncertainties for the modelled energy system design. It is expected that these uncertainties are generically applicable and important to other energy systems as well, because these are not specifically related to the electricity, gas and heat systems in an urban environment at medium-sized Dutch city level. Nevertheless, it is not recommended to duplicate these uncertainties and their ranges one-on-one to other energy system design analyses. The uncertainties that are relevant to analyze further, and their applicable ranges, are expected to vary case-by-case. Therefore, an uncertainty characterization, as described in the first step of the proposed research method, should always be performed.

Energy systems are highly complex and as such, is is difficult to strike the right balance in the level of detail of an uncertainty analysis. A highly detailed analysis provides specific insights into the impact of uncertainties. However, this also requires the model to be a sufficiently representative version of reality in order to translate detailed conclusions to the real-world. Also, such an analysis risks missing the bigger picture. A high level uncertainty analysis allows the analyst to draw broader conclusions on general expected patterns. However, this is less relevant when a specific situation is modelled and it risks missing important details. Consequently, it is recommended for the analyst to base the considered level of detail on both communicated findings with the model-owner or client, which can be for instance a (local) government or a network operator, and on the level of detail of the model under analysis.

Using the analysis of several external parametric uncertainties, this research illustrates the large impact of uncertainties on the long-term planning of energy systems in transition. Given the fact that a much wider scoping of uncertainties exists, such as for example stakeholder behavior, decision-making and weather patterns, this research outlines the importance of considering the impact of uncertainties in energy system planning.

6.1.2 Implications for the use of (Optimization) Modelling for Energy Systems Design

This research has shown that the proposed exploratory modelling method was successful in performing a thorough uncertainty analysis on an Energy System Design Optimization Model. Because of the large number of experiment runs, with different scenarios, the model behavior is analysed more thoroughly. Of course, even in an uncertainty analysis where many diverging uncertainty scenarios are explored, the model specification and relations remain determining for the results. Consequently, the exploratory insights that are gained, are generally specific to the model and the case study that are analyzed. In this research for example, besides revealing interesting results on the subject matter of the case study, the uncertainty analysis confirmed the impact of the specified modelling time step and the greenfield character of the case that is simulated by the model under analysis. The uncertainty analysis can confirm or reveal such

potential limitations of their model specification to model-owners.

A model inherently requires scoping, simplifications and the setting of system-boundaries to make it solvable. Hence, as stated by Box and Draper (1987): "Essentially, all models are wrong, but some are useful". Therefore, in designing a real-world energy system using model-based results, these results should always be perceived in light of the model limitations and assumptions in relation to the real-world surroundings and their potential impact to the considered energy system. This advice is relevant for all geographical model scopes. Two examples from this research are provided to illustrate that model-based results cannot be translated one-on-one to the real-world situation. First, consider the locational placement of supply investments. Due to the system-boundary setting in the model, the supply units should be placed within the system and should meet the energy demand present in that system or should otherwise be stored in case of superfluous supply. However in the real-world, especially in densely populated regions, energy demand or supply sources can be found present outside of the system-boundaries as drawn in the model as well. Thus, in real-world cases with a high amount of imported/exported energy, the number of required storage and supply units would be lower compared to the model-based analysis. Now, the second example demonstrates a lower level influence at neighborhood scale. In the real-world, the demographic composition of neighborhoods is subject to change due to for instance gentrification and segregation. The development of demographic compositions can have a direct relation to energy demand developments, for example as a result of a changing average number of residents per household. However, in models where a case is studied in which the total of locations is aggregated to limit computational requirements, the effects of such neighborhood-scale developments are not captured. Hence, in both examples, if a model-owner requires such insights to provide to their client, additional (separate) analyses would be required.

Now, consider the highly uncertain future developments for the large variety of factors that potentially impact the Energy System Designs simulated with (Optimization) Models. Also consider that in this research it is shown that the optimized outcomes from the model under analysis, for the studied outcomes of interest, vary considerably across the different uncertainty inputs. This again implies that the one-on-one real-world implementation of a single optimized Energy System Design Model outcome, without having performed a sufficient uncertainty analysis, almost certainly results in a design that is not robust towards the variety of possible futures.

Also, although an uncertainty analysis explores a range of uncertain parameter values, the actual implementation and representation of these uncertain parameters remains dependent on the model specification. Modelling approaches that assume linearity require simplification of transition characteristics, which are often non-linear dynamics. Nevertheless, the linearity assumption allows to model more system characteristics under limited computational requirements, as compared to nonlinear modelling. In this research, this challenge is illustrated with the models inability to implement varying technological development curves, which are usually s-shaped over time. This could lead to both under- and overestimating the development

of technologies over time.

The following paragraphs relate to 'extensions' of models that can be made to result in outcomes that are better translatable to the real-world. In interpreting these recommendations, it should be noted that existing optimization models could already reach their computational limitations due to mathematical complexity. For example, the model under analysis is already considered to be strongly NP-hard. In addition, Pfenninger et al. (2014) state that, if prediction is the goal, simple energy models are often equally strong in their predictive power as complex ones, so that model simplifications not necessarily constrain its functionality. Model-owners who work with models that are already NP-hard and who desire to extend their model, could instead use for instance iterative optimization. With such an approach, different levels of detail, in for example the time step, are solved subsequently instead of simultaneously, to limit the additional computational requirements while increasing the models complexity.

It is recommended to include different levels of time steps in the modelling of (Energy System) Designs. As elaborated upon earlier, this research illustrates the determining effect of the relatively large modelled time step on the considerations resulting in specific Energy System Design outcomes. Remember for example the electricity storage technology units, which were not invested in due to the simulated large storage losses resulting from the one-year time step. Specification of a smaller time step, such as per day or even smaller, would allow the specification of a smaller storage loss for electricity storage units rendering investments in this technology type profitable. Or remember the preference for PV supply over wind supply units. The specification of smaller time steps, which would allow the incorporation of determining patterns, such as seasonality and day/night, would result in a more realistic supply capacity over time for both supply technologies.

In line with the previous paragraph, this research marks the relevance of using brownfield data in the modelled cases, which include the existing infrastructure, to produce realistic Energy Systems Designs with the proposed method. As illustrated, the greenfield character of the modelled case under analysis results in a baseload of investments in the starting year, which serves to 'fill' the system with the required, or 'existing' infrastructure (figure 6.1). In combination with the perfect foresight modelling approach, which induces investments with a future-oriented perspective, the interesting baseload investments, which are additional to the 'existing' infrastructure, cannot be distinguished from the less interesting investments, which should form the 'existing' infrastructure. Without knowledge on which investments are supposed to be 'new' infrastructure and which represent 'existing' infrastructure, it is impossible to provide advice on which investments should be performed to end-up with a robust design. It is recommended to avoid this issue by producing a brownfield starting point for the model, by running the greenfield model in 2018 with a limited foresight approach of two years. The investments required for that first time step are the 'existing' infrastructure, or the brownfield, which subsequently can be used as input to the remaining time periods $2020 - 2050$, which are run with a perfect foresight modelling approach.

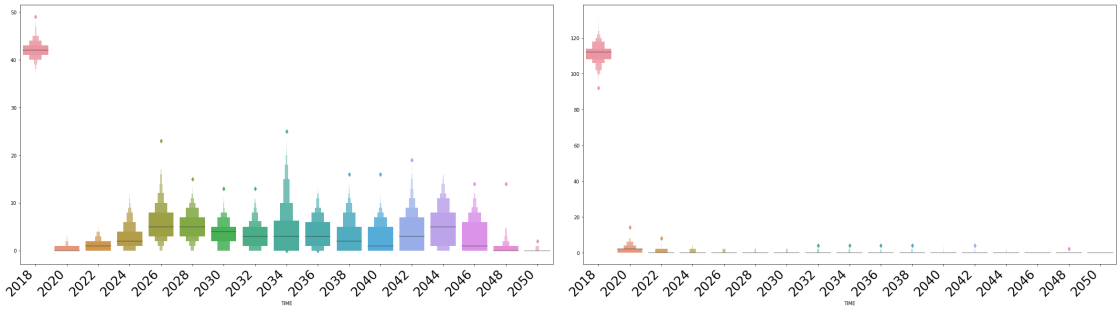

(a) Non-network investments time period aggregation (b) Time period aggregation for network investments

Figure 6.1: Seaborn boxplot of number of investments over all experiments aggregated to time period including the 2018 time period for both network and non-network investments.

6.1.3 Implications for Energy Systems in the Energy Transition

If there is one thing that has been shown with this research, it is that the energy system is inevitably changing. Even (or especially) with a non-changing energy consumption pattern, significant investments and system adjustments are required to maintain an energy system that is reliable towards the future, with an energy transition towards renewable energy. With energy systems being affected by such a variety of changing factors: politics, individual behavior patterns and the energy transition, it is impossible to keep the energy system as it is.

Also, the investment patterns resulting from the large variety of scenarios of the uncertainties studied, revealed that investments should be performed soon. A peak in investments in the years $2026 - 2028$ could clearly be observed in the model under analysis which performs a least-cost optimization. Of course, more analyses must be performed and more models must be studied to draw definitive conclusions on what this implies. However, for now it is interpreted that investments are required within a limited time-frame, to ensure a reliable energy system with limited (societal) investment costs. Therefore, it is key for modellers, decision makers and investors to act fast to prevent that eventually the society pays for a stalled transition to a future-proof system.

Now, some lessons on the specific design characteristics of energy systems are drawn from this research.

First, this research shows that, if a decrease in local natural gas supply remains desired, it is key to provide another source of gas supply. In the proof of concept, a great dependence on Power-2-Gas (P2G) conversion capacity is portrayed across most possible futures. In this, the modelled energy balance constraint (energy supply must meet the energy demand), was dominant over the P2G technological development rate. This is as expected, with P2G technology being the sole remaining source of gas supply, in combination with the assumed quick and constant decrease in natural gas supply. Nevertheless, this emphasizes that either our gas dependence should decrease much faster or the gas supply should be maintained; either

sustainable, with for example P2G technology (if feasible), or by importing natural gas from other countries. Measures to decrease our gas dependence could be for example larg-scale isolation of residences and other buildings, subsidised transfer from gas reliance to electricity reliance and stimulation of technological development of other sources of gas production, such as biogas produced with algae, waste (water) or methane.

The proof of concept, which models an urban environment, portrays a strong preference for PV over wind supply. Naturally, this preference arises with the constraints and limitations of the model under analysis, such as the production dependence on sun radiation, the lack of additional costs in general and of locational constraints for PV supply, and the consideration of just a single capacity type. Nevertheless, in reality, PV supply requires very limited costs of operation and maintenance in comparison to different technology units. On top of that, PV supply units can be placed easily in densely populated areas, for example on rooftops. Therefore, it is expected that the preference for PV supply over wind will hold for urban energy systems.

In translating model-based energy infrastructural placements, it is important to keep in mind that citizens might not be all-accepting in such energy infrastructural investments. This challenge is demonstrated by societal uprises involved with the placement of onshore wind supply units in the Netherlands. To improve acceptance, citizens must be involved in the process of actual investments and supported in the realization of investments. Otherwise, the envisioned energy system design is likely to be thwarted by population protests. Also, to prevent protests about the distribution of the burdens and the benefits (distributive justice), compensation could be considered.

The relative importance and driving character of the energy demand development is expected to be generally applicable to energy systems. This is perhaps the most important lesson that model-owners can communicate to decision makers. It is hypothesized that if policies are deployed to urge energy consumers towards a more desired energy demand pattern, for example with a lower total demand and decreased gas reliance, such changing demand development patterns could serve as a determining power for Energy System Design investments, and potentially even technological development patterns.

6.1.4 Implications for Design Optimization Models

It is expected that the proposed method, and cosine distance-based clustering technique specifically, is applicable to *Design* Optimization Models in general. In this case, Design Optimization Models are defined as: *An optimization model in which a fixed set of parameter values (design specifics) need to be determined to achieve the best measurable performance (objective function), possibly under given constraints.* This general applicability is a result from: the model-specific selection of uncertainties, the model-specific experiment design, the open-source character of the EMA Workbench, which provides support for models developed in various modelling

packages and environments, the model-specific selection of design specifics, and the broad suitability and variety of the results analysis tools.

The general applicability of the proposed method is constrained to Design Optimization Models where the 'optimized' outcome, the design, can be formatted as a (high dimensional) vector which contains the value for all potential design components, including the zero values, in a fixed ordering over all experiment runs. The method, the cosine distance function in particular, is expected to be functional with non-integer-values as well as integer-values. This implies that the values, other than the number of investments, can concern a technical unit specification as well, such as the density, provided that all design components present in the vector are specified in the same technical unit, such as kg/m^3. Furthermore, it is expected that the proposed method performs successfully for optimization models which do not employ a Mixed Integer Linear Programming (MILP) algorithm as well. For the method to be functional, it is essential for the model under analysis to produce a single 'optimal' design which can be compared across model runs. The mathematical procedure of how such as design is obtained is not relevant in this matter.

It is imagined that the method could be applied to non-Energy System Design Optimization Models such as: the design of water infrastructure; the design of mechanical structures for the minimization of for example stress concentration or heat accumulation; or the design of energy systems on a different geographical scale. With these potential use cases, instead of the technology type being composed of 11 technology type possibilities such as in the proof of concept model, these technology type possibilities could for example be a pump, dike and water locks or length, width, height, volume and density.

6.1.5 Implications for Design Optimization Model-Owners

This results of this research have been presented to an optimization modelling expert to further substantiate the functionality, added value for the industry and the general applicability to Design Optimization Models of the proposed method. The expert works as an energy analytics consultant at ORTEC B.V. and has expertise in developing (Design) Optimization Models, and in using optimized results to provide consulting services to clients. The expert was not involved in any step of this research and is therefore considered to be an independent party. The expert's quotes are used to provide anecdotal evidence to outline implications of this research and the proposed method for potential model-owners: "*I really think that this method has very concrete and useful use cases in the industry*" and "*If I regard the work that I do, this [method] is very relevant. Many people run into the issue of how to relate the impact of uncertainty in the input to the resulting output*" .

Overall comments on the method: "*I find it [the method] a very intuitive way to regard scenarios. This is a true issue in the industry, because such a large proportion of optimization model input is variable. I find the translation of* 800 *experiment runs to clusters of similar outputs, the*

most important aspect of the method. This is so relevant because looking at clusters instead of at single runs, allows the identification of patterns of model-behavior and identifying the causes of these behaviors. Knowledge on such concrete causes, is relevant information which I can provide to my clients, decision makers.".

On the uncertainty characterization: "*In optimization, we usually use a single point value as input. The greatest challenge related to this is, is the assignment of a fixed set of potential values to these, while we know that this single point value is in fact subject to uncertainty and part of a surface of potential input values.*". On the tree visualization of CART subspace partitioning: "*The clustering technique and the tree are very insightful and useful in identifying which specific scenarios [uncertainty ranges] are indicative to specific model output.*". "*It is very interesting to be able to see, in retrospect, which of the specified uncertainty scenarios are most determining in reaching an outcome and in generating certain output behavior. This is something that normally requires a lot of work to acquire.*".

On the identification of clusters of similar output behavior from the high dimensional outcome space: "*What I consider to be very strong about this method is the possibility to identify trends, even trends which arise from a very small number of experiments. When these trends are known, this can be related to the behavior we see across all experiments.*"

On the applicability of the method to one of the experts current projects: "*In one of my projects, we model every single day of the year* 2050*. It would be interesting to see what design choices and trade-offs, such as the sizing of installments such as battery and gas storage units, result from the choices for characteristics that are modelled for such a year. Uncertainty inputs for that model could be the installment costs and the selected capacities. Now, we separately run thousands of scenarios, and then in retrospect we have to almost guess which values cause tipping points. That is a very relevant challenge, which people now try to solve by just running more scenarios and taking a median for each outcome. This clustering of similar outcomes and the identification of uncertainties causing the behavior could aid in this challenge.*"

6.2 Limitations of the Method and this Research

Although the results from applying the proposed method to an existing Energy System Optimization Model are shown to provide valuable insights and lessons, the method, the simulated case study and results are subject to limitations. To be able to draw conclusions on the method functionality and this research, this section provides a reflection on the limitations of the proposed method and of this research in general, which includes the limitations related to applying the method to the chosen model under analysis.

6.2.1 Limitations of the Proposed Method

Limitations to Step 1: Uncertainty Characterization

In this step, a top-down and bottom-up analysis are combined to identify and characterize the selection of uncertainties relevant to the model under analysis and the scoping.

First, it should be noted that both the surroundings that impact energy systems, and the energy systems themselves, are subject to constant development. Therefore, the uncertainties to be analyzed that impact energy systems, identified with application of the proposed method, cannot be assumed to remain applicable for extended periods of time. This indicates that application of the proposed method in a different time period, say in a few years, is bound to produce different results. This concerns both the importance of different types of uncertainties and their relevant ranges.

The literature review-based top-down approach is not expected to be suitable for the analysis of all types of uncertainties. In reviewing literature it can be a challenge to select the most valuable sources among the vast amount of information available. Also, it was challenging to find models with adequate open-source uncertainty documentation. Specific circumstances influencing an energy system under analysis, such as the potential implementation of relevant policies, such as a carbon dioxide emission tax, the threat of a citizen uprise to higher energy prices, or the ban of a certain type of energy supply, can prove to be more relevant than the (parametric) uncertainties considered in this research. However, such specific circumstances cannot be retrieved or characterized from a general literature review of renowned Energy System Models and scenario planning studies. To retrieve more specific knowledge on uncertainties, expert input could be employed instead of, or in addition to, the literature-review based top-down approach.

Moreover, the literature review-based top-down approach has the potential to become quite time-intensive if no adequate scoping steps are taken. In this research, the search for energy models suitable for the top-down analysis in relation to the ESOM under analysis, first resulted in a listing of over 30 models used worldwide for a diversity of (sub)topics in the energy and climate field, dedicated to varying geographical and modelling scales and different levels of detail (Krey et al., 2019; Integrated Assessment Modeling Consortium, 2016; Connolly, Lund, Mathiesen, & Leahy, 2010). This was solved by deciding to limit the number of analysed models to three. This variation in models was assumed to provide scientific basis and leave enough time to adequately perform the analyses. Nevertheless, it is expected that a more extensive analysis results in a more diverse set of potential uncertainties.

The set of three main uncertainties, of which the impact is analyzed, does not represent the full scope of uncertainties that impact such an energy system in the real-world. This implies that inclusion of a more complete set of uncertainties would influence the exploratory modelling results. However, the consideration of a truly complete set of uncertainties is impossible to accomplish and would subsequently result in a more complicated analysis of results. Further-

more, it is important to strike a balance between the amount of detail in the results and the added value of increasingly detailed results to model-owners, and with respect to the level of detail in the model under analysis.

Limitations to Step 2: Exploratory Modelling

In this step of the method, the specified uncertainty ranges are sampled and their effect on the model under analysis is explored with the Exploratory Modelling and Analysis (EMA) Workbench.

In exploratory modelling a wide range of futures that could happen is explored to limit the bias of the modeller on the results and on the scenarios considered. Nevertheless, the use of exploratory modelling is no guarantee that the entire possible future uncertainty space is or can be explored. Also, the analyzed uncertainties, and their ranges, ultimately cannot be entirely *un*biased by the analyst or the model properties. Therefore, although exploratory of nature, an exploratory analysis will always remain limited and biased. As a result of this limitation, the identified (Energy System) Design characteristics cannot be considered a complete representation, neither of the complete set of possible designs in the model or of the total set of design characteristics present in the real-world.

Although the EMA Workbench reduces the analyst's workload by automated uncertainty sampling, model runs and output production, the model under analysis is still required to run the specified number of experiments. Therefore, the total computation time of performing an uncertainty analysis depends on the computational complexity of the model under analysis. A rule of thumb is that reducing a model's complexity to limit the computational requirements for solving the model, increases the number of parameters on which uncertainty analysis can be performed (Pfenninger et al., 2014). Therefore, to implement an exploratory modelling experiment set which is sufficiently large for a feasible sensitivity analysis, while taking up an acceptable computation time, optimization models that are large and computationally expensive require simplification or limitation of the number of experiment runs. Nevertheless, Pfenninger et al. (2014) state that complex energy models are often no better than simple ones in their predictive power, if prediction is the goal, so that reduced model complexity still allows for insightful exploratory modelling and analysis.

Limitations to Step 3: Results Analysis

In this step of the method, a novel approach is suggested which combines a cosine distance-based agglomerative hierarchical clustering algorithm with CART subspace partitioning, to identify clusters of experiments resulting in similar total Energy System Designs, from the high-dimensional exploratory modelling output space. Besides, several analysis tools are employed to spot Energy System Design trade-offs and general design characteristics resulting

from the uncertainty analysis.

Cosine Distance Measure
The cosine distance measure, which is used to quantify the dissimilarity between energy system designs, has a weak representation of the number of investments for individual design components. This weakness is aggravated in the presence of design component values which are disproportionately high across all experiments. Such presence results in the cosine distance measure to poorly register smaller value-differences across experiments. This weakness is demonstrated in the method proof of concept with the removal of the first time period from the total design, aggregated to time period, which resulted in much higher cosine distances (figure 6.2, note the changed cosine distance range).

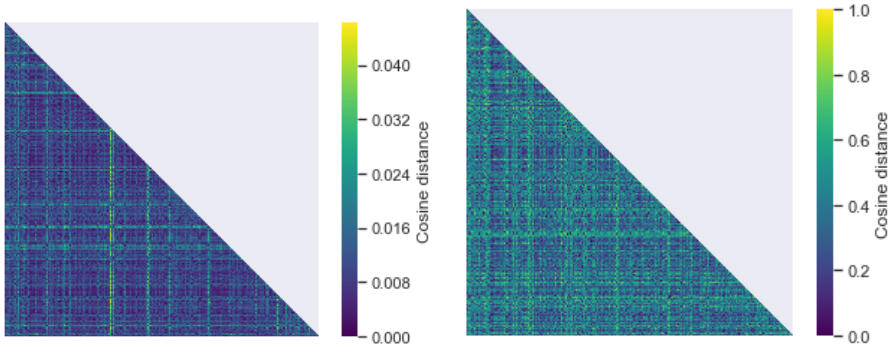

(a) Time period aggregation (b) Time period aggregation without 2018

Figure 6.2: Seaborn heatmap of the cosine distance values between all experiment outputs for the design aggregated to time period. (b) The 2018 time period counts are removed. The number of rows and columns is equal to the number of experiments (800).

The consequence of this weakness is that structurally higher valued design components have a larger influence on the cosine distance algorithm, and thus on the resulting clustering of experiments according to design similarity, than structurally lower valued components. To elaborate on the consequences of this weakness, imagine a case in which the number of investments varies around a value of 100 for the first technology unit and around a value of 4 for a second and third technology unit. In such designs with a consequently high variation between the design component values, the variation in value across experiments will be more poorly registered by the cosine distance algorithm for the lower-valued design components (the second and third technology units) than for the disproportionately high components (the first). To mitigate this limitation, the analyst can normalize the first technology unit values to be in the same order of size as the other two units. This measure would be implemented in constructing the cosine distance matrix only, and therefore, would not distort other results.

Clustering
First, a limitation to the specification of the number of clusters is the relatively arbitrary spec-

ification of the complete linkage distance threshold. It was chosen to maintain the default specification of the color_threshold (The SciPy community, 2019). It is recommended for analysts to maintain this default threshold value, unless the data set requires specification of a different threshold value to attain a different number of clusters that is deemed most indicative for the analysis. This threshold value definition remains up to the analyst.

A second limitation related to the clustering is the visual identification of the number of clusters from the dendrogram, which is expected to become increasingly challenging for a higher number of clusters and/or experiments. Hence, in cases with for example a high (desired) number of (smaller-sized) clusters, analysts are encouraged to explore different methods to determine the number of similar design clusters, other than employing a dendrogram. For instance, t-distributed Stochastic Neighbor Embedding (t-SNE) is an option. Other than pairing similar data from a high dimensional data set, this algorithm visualizes the isolation of dissimilar data. A quick application of this algorithm to the total design cosine distance matrix, with the apparent isolation of three clusters of designs which are dissimilar to the majority and to each other, is visualized in figure 6.3. Clearly, and as would be expected, this clustering algorithm results in different clusters and cluster sizes than the agglomerative clustering algorithm.

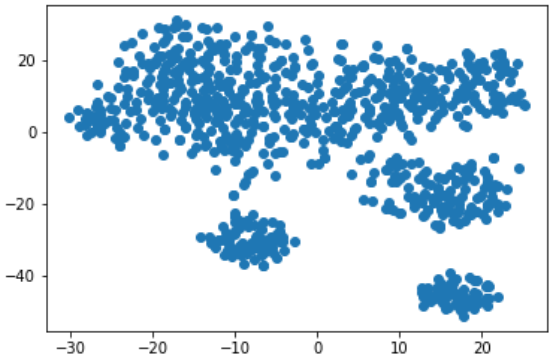

Figure 6.3: t-distributed Stochastic Neighbor Embedding performed with the total cosine distance matrix, with cosine distance values between all 800 experiments, as input distance values.

Characteristics of cluster designs appear increasingly unique and specific for clusters with a lower number of in-cluster experiments. This is as expected: with a higher percentage of in-cluster experiments, the cluster design characteristics are increasingly alike the 'average' design characteristics across all experiments. In this research, a number of in-cluster experiments of less than 10% of the total number of experiments is specified as cluster-size threshold with which specific design characteristics can be distinguished. Three clusters, 1, 2 and 5, were too large to draw specific design characteristic conclusions. In further research, it can be decided to lower the complete linkage threshold value to increase the number of clusters and subsequently decrease the number of in-cluster experiments per cluster.

Next, the Inter-Quantile Range (IQR) is used as sole representation of the in-cluster variability

and similarity. The specified complete (farthest-neighbor) linkage in the agglomerative clustering is assumed to result in densely similar design clusters. Nevertheless, this is just one method to assess in-cluster variability. This implies that a greater assurance in in-cluster variability is attained by employing a different or an additional measure, such as the comparison of the mean in-cluster distance with the mean distance of the in-cluster designs with the out-cluster designs.

6.2.2 Limitations of the Research

Limitations Related to the Model under Analysis

In this research, the functionalities of the proposed method are demonstrated by application to a single existing Energy System Design Optimization Model as proof of concept. The main limitation to this research is that the method has only been applied to one model, which in turn is applied to one specific case study. The functionalities, and limitations, of the method could have been demonstrated more fully if it would have been applied to more models or even to the same model using different case studies.

Like all models, the selected model for analysis has limitations (Box & Draper, 1987). However, the limitations of the model under analysis do not present a limitation to this research in demonstrating the method functionality. On the contrary, the model has been useful in demonstrating that the method is effective in identifying the model's strengths and weaknesses, as well as those of the input data. In other words, the proposed method could be fully demonstrated as proof of concept on the model and its case study of a medium-sized Dutch city.

A property of the model under analysis that does present a limitation to this research, is the fact that the model under analysis is specified in Python. Indeed, the EMA Workbench is a Python-based functionality as well. This facilitated the linking between the EMA Workbench and the model under analysis. Due to the shared Python-base, the proof of concept cannot demonstrate the functionality of applying the proposed method to an optimization model that is *not* Python-based. It is expected that the functional linking of the Workbench and a non-Python-based optimization model will be a challenge.

A second limitation to the proof of concept of the method is the aggregated character of case study simulated in the model under analysis. As described before, this model is actually applied to an aggregated case of 7 locations, which in reality is represented by at least 110 locations. Due to this aggregated character, the computational requirements of solving the model are low ($13 - 14$ seconds for an optimality gap of 7%). This has facilitated the running of 800 experiments within, still, a satisfactory total computation time. Even more so, the percentage of experiments solved to optimality was 100%, which easily validated comparison between experiment outcomes. It is expected that the total computation time of an experiment case for an optimization model with more computational requirements, due to for example a greater number of decision variables, will be much higher. Also, it is expected that the percentage of

experiments *not* solved to optimality for such a model will be non-zero unless the specified optimality gap is increased. This implies a less substantial base for comparison between experiment outcomes or the comparison between sub-optimal outcomes if the method is applied to models with higher computational requirements.

Furthermore, due to the aggregated character of case simulated by the model under analysis, aggregation of the total energy systems design to design specifics (technology type, location, time period), resulted in a reasonable amount of aggregated characteristics to be compared visually with the heatmaps (11 technology units, 7 locations and 21 edges, 17 time periods). Basically, the aggregated character of the case resulted in analysis of a subsystem of a system which shows different results.This could impact the usefulness of the uncertainty analysis for the model-owner. However, for a more computationally expensive case, with for example more locations, the number of aggregated characteristics grows as well, for example the number of edges connecting these locations. This is expected to complicate the analysis and comparison of the total energy system design characteristics across experiments.

As elaborated upon extensively in the section 'Implications for the use of (Optimization) Modelling for Energy Systems Design', the greenfield character of the case analyzed in the model under analysis limits the variation in investments across different uncertainty inputs, because of the large baseload of investments in the first time period. It is expected that application of the method to brownfield cases provides an even better insight into the variability of design outcomes resulting from uncertainties.

Limitations Related to the Method Application to the Model under Analysis

If more time would have been available to perform this research, energy system experts could have been interviewed to identify the most pressing uncertainties and their ranges. This has limited the exploratory character of the research, which portrays only a subsection of the feasible scope of uncertainties. On top of that, there is the risk of unknown unknowns: uncertainties of which it is not known they are uncertain or should be considered in the system. As a result, it is impossible to perform an uncertainty exploration which includes all unknowns.

The technological development rate, which is selected to represent the uncertainty in technological development, provides a limited representation of the real-world technological development. The mathematical definition of the development in the model under analysis is a cumulative change of the investment costs with the time as exponent. Yet, in the real-world technological development is usually s-shaped over time. The technological characteristics of the technology units, such as conversion efficiency and storage losses, could not be changed over time due to the mathematical model specification and the limited available time for this research. Instead, it was attempted to simulate this technological development in the s-shaped demand development scenario 11 ('Very fast change'). This was under the assumption that the energy demand directly adjusts to changing supply patterns due to technological development.

In the proof of concept, a particularly high sensitivity to the demand development uncertainty is portrayed. Therefore, the specified demand development scenarios are highly determining for most model outcomes, with the exception of the wind supply, heat storage and network investments. In the great majority of scenario development studies where only a subset of future uncertainties is captured, the analyst bias is expected to have impacted the model outcomes (Guivarch et al., 2017). Also, the inclusion of a multiplicity of uncertainties can lead to remarkable model behaviour. By specifying the demand development as scenarios and as categorical uncertainty, this is expected to have impacted the model outcomes in this research as well. For example, a particularly remarkable demand development scenario is scenario 11 ('Very fast change'). This scenario portrays a sharp drop in demand, owing to its mathematical formulation. The likeliness of the drop being this sharp in the real-world is small. Also, the specification of the demand development as categorical uncertainty is expected to have caused some discontinuity in the output space. A strategy to limit the effect of unrealistic uncertainty combinations is to include likelihood estimates to the uncertainty, which can result in a more reliable outcome space. However, caution must be taken in such strategies where uncertainties are attempted to be made less uncertain, as these can imply false certainty.

The optimality gap value specification is expected to impact the determining power of uncertainties to result in specific design outcomes. This is due to the relation between the height of the optimality gap value and the closeness of the 'optimized' outcome to the 'Best Bound': the lower the optimality gap, the closer to the 'Best Bound' as identified by the optimization algorithm (Appendix A.4). Resulting from the relatively high specified optimality gap of 7% is this research, and the capricious character of the branching algorithm, the exact same set of uncertainties could result in different design outcomes. Consequently, and in combination with the large cluster sizes, the model outcome behavior is ascribed to a small set of underlying uncertainties. It is hypothesized that the specification of a lower optimality gap results in more significantly underlying uncertainties.

6.3 Remarks for Analysts and Model-Owners to use the Method

It is encouraged to apply the method proposed in this study to different (Energy System) Design Optimization Models. Both to pave the way towards increased and facilitated insight on the impact of uncertainties on model outcomes and to further improve the method functionalities.

When applying the proposed method to an existing (Energy System) Design Optimization Model, it is important to consider the limitations mentioned in the previous section. Not only the limitations to the method should be regarded, but also the limitations to this research in which the method is applied to a model, that in turn is applied to a case study. This brings along limitations to the proof of concept as provided in this research. Being aware of the method limitations will allow successful method applications, additional to the proof of concept as provided in this research.

All three method steps should be executed each time the method is applied to a (different) model. This especially applies to the method step 1: Uncertainty Characterization. As mentioned before, the circumstances impacting the system considered change over time, which impacts the relevance of different uncertainties depending on the moment of analysis. Also, specific uncertainties and their ranges should not be generalized and copied to another case. Nevertheless, in case of repeated application to a specific non-changing model within a limited time frame, steps 2 and 3 can be replicated as fixed modelling sheets.

It is not recommended to try and repeat step 2: Exploratory Modelling for an analyst or model-owner with no experience in using the Exploratory Modelling and Analysis Workbench. Although the interface is user-friendly and the use of the Workbench are well-documented, some practice is required to be able to 'link' and run the Workbench to an existing model.

Although the design specifics for different (Energy System) Designs are expected to differ from the technology type, location and time period specifics in the proof of concept, most designs will be specified by location. This location can concern multiple scales, such as country, city, district, square meter or nanometer location design specifics. As mentioned before, as long as the specified scale or unit is used consequently, the method functionality is expected to be maintained.

It should be noted that with an increasing number of design specifics and possibilities per specific, the total outcome vector length (and thus outcome matrix) increases as well. The algorithm has been tested on maximum matrix size of $[3451, 800]$. The clustering-performance of the algorithm is expected to remain functional at higher dimensions, however, this should be explored in further research.

Lastly, the insights provided by applying the method to a Design Optimization Model, are valuable to communicate to clients and/or decision makers. This is demonstrated with two examples from the proof of concept method application in this research. First, the main cue to decision makers is to start by implementing measures towards the desired energy demand pattern. The demand development uncertainty is identified as the most determining uncertainty for the majority of the design components analyzed. It is hypothesized that if energy consumers can be urged to change their energy demand patterns, this could be a determining power for energy system investment (and potentially even technological development) patterns. A second cue to decision makers is the possibility of using the method to identify 'red flags' for adaptive decision making strategies. In this proof of concept application of the method, the PV development rate tipping point value of 5% and the determining character of the presence and duration of continued gas reliance, would be valuable as 'red flags' in a set design trajectory. Imagine a set design trajectory for which decision makers have planned high investments in PV supply. Then, if the PV development rate drops under a value of 5%, or has been below that value for a while, this would be a cue to review whether the design trajectory should be targeted more on wind supply capacity as well.

6.4 Conclusions

In this section, first the two questions posed in the introduction are answered for the proof of concept method application. Next, these conclusions are reflected upon to show that the aim of this research has been met. Thereafter, recommendations for further research are provided.

6.4.1 Answer to the Questions

Two questions were posed to be answered by applying the proposed method. Both questions are answered in this section, with respect to the proof of concept method application to an existing Energy System Optimization Model and its case study.

1. **How do the Energy System Designs vary resulting from underlying uncertainties?**
   The main energy system cluster-design variations relate to all model-specific design specifics: the technology units invested in, the time-period of investment and the location-specific placement of units. All three vary across the identified clusters. Similar to before, the total designs are described according to the three design specifics.

   The extent of variation per cluster design of each design specific, compared to the non-clustered design, is dependent on the underlying uncertainty composition. First, clusters portray the largest variation in *technology type* investments, compared to the non-clustered set of experiments, with the following underlying uncertainties: a PV development rate below 0.043, a demand development with a limited decrease in (relative) gas reliance in the demand mix, or a demand development with a delayed decrease in gas reliance towards electricity and heat. Second, the largest variation in *location*-specific investments is portrayed in clusters with a high amount of investments in technology types which are subject to locational constraints. Third, the largest variation in *time-period* of investment is demonstrated in cluster designs which are underlying by either demand development that changes very fast towards a different demand mix, or by demand development patterns without a decrease in the total gas demand.

   - **Technology type**
     PV supply technology is preferred over wind supply, due to the locational constraints of the latter and the absence of seasonality and day/night patterns. The PV development rate is the main determining factor in whether the model relies on PV, or on wind for electricity supply. A lower PV development rate renders the additional required network investments for transport of the supplied energy to constrained locations, in case of wind supply, relatively less expensive. Although

in most clusters the majority of capacity is invested in PV supply, the design in all clusters relies on *both* supply technologies for electricity generation. The strong reliance on PV supply is alleviated for a PV development rate below 0.05. The wind supply is preferred over PV supply for one small-sized cluster, with a PV development rate below 0.043 and in absence of a strong continued gas reliance or a delayed decreased gas reliance. This preference is expected to translate to other (urban) environments as well, because PV supply has relatively limited operational costs and is less subject to locational constraints than wind supply. Nevertheless, the presence of multiple different (electricity) supply techniques in the real-world is foreseen to limit this model-based dominance of PV supply.

The height of the future gas reliance drives the number of P2G conversion unit investments. If the total demand decreases as expected, but the demand mix does not change (enough) from gas towards electricity and heat reliance, a high number of P2G investments is required to meet this gas demand. Also, if the total demand and the demand mix remain unchanged, while the natural gas supply is decreased as intended, the gas demand is met with an exceptional amount of PV supplied electrical energy converted to gas.

The placement of P2G conversion and gas storage investments directly at the demanding locations is preferred, as opposed to investing in gas network capacity to later transport the gas. Consequently, there is no clear correlation between the P2G conversion and gas network investments, whereas the P2G and gas storage capacity investments are positively correlated and the gas network and gas storage capacity investments are negatively correlated (figure 6.4).

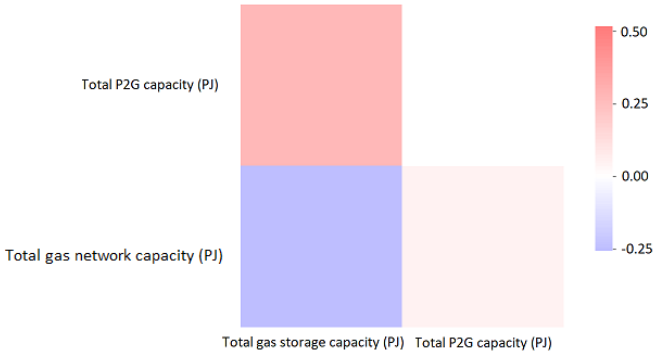

Figure 6.4: Correlation between the P2G conversion, gas network and gas storage capacity invested in. Red indicates a positive correlation, white absence of correlation and blue indicates a negative correlation.

– **Location**
The location-specific investments of non-network units is mainly determined by the height of the locations percentual demand in relation to the total demand across

all locations (figure 6.5a). Consequently, overall, investments are highest at the highest-demand locations 6, 2 and 7. The impact of uncertainties to this pattern is very limited, because the energy demand at each location must always be met and investments at the locations-of-demand are preferred over investing elsewhere and subsequently investing in additional network capacity.

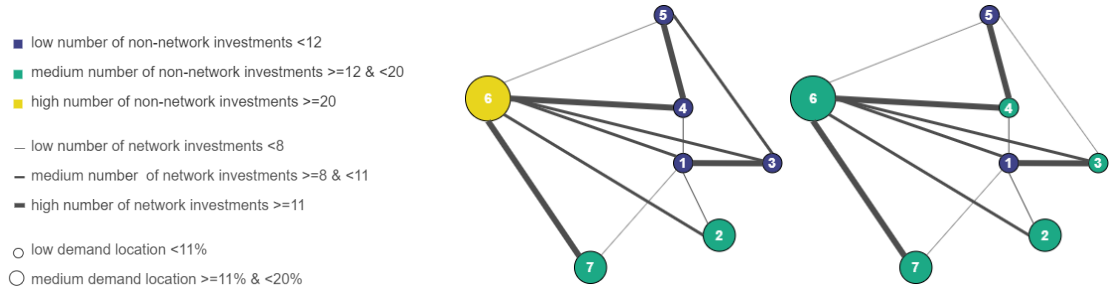

(a) Non-Clustered (b) Cluster 6

Figure 6.5: Visualization of the median number of investments aggregated to location of investment as a function of the relative demand per location and the edge distance.

The location-specific investments of network units are determined by a combination of the distance between the locations connected by the edge, which determines the network investment costs, and the relative demand of both locations. The locational placement of network investments is not much affected by underlying uncertainties, just like the non-network investments. All locations are connected to highest-demand location 6 regardless of the connecting distance or their own demand height. The two high-demand locations, 2 and 7, transport exclusively to highest demand location 6 and receive only from location 1, which is the nearest lower-demand location for both. Two lower-demand locations are only connected if the distance is sufficiently low to limit the required investment costs.

The location-specific placement of investments is performed according to the height of the demand and the distance between locations. This model behavior is only overruled if locational constraints apply to the technology units that are highly invested in. This is illustrated in cluster 6, in which the wind supply investments are preferred over PV supply due to the low PV development rate. In this cluster, the number of investments is lower in locations $1, 5$, and 6, where wind supply cannot enter the grid, as well as in the connecting edges (figure 6.5a and b).

– **Time Period**
Overall, the time-period specific pattern of investments is quite comparable across the clusters. However, two uncertain demand developments result in a significant variation in the time-period of investment. These are cluster design 3, which is underlying by a demand development with delayed, but very fast change towards

decreased gas reliance, and cluster 4, to which a demand development pattern without a decrease in the total gas demand is underlying (figure 6.6).

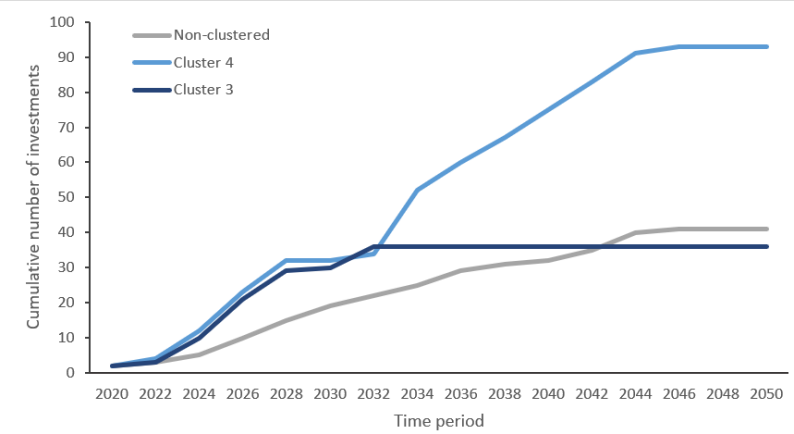

Figure 6.6: The time period of investment development for the non-clustered total set of experiments, and for clusters 3 and 4.

In case the expected shift from gas reliance to electricity and heat reliance is delayed to later time periods an eventually changes very fast, *earlier* and *lower* investments are required (figure 6.6, cluster 3). In this case, the extended period of gas reliance is met with: electricity to gas conversion with a few P2G units, and subsequent gas storage to bridge the (short-term) period of lacking gas supply. As the energy demand must always be met, the high investment costs and limited technological performance of P2G conversion units related to such early investments are a direct result from this scenario. In the real-world, it could be decided to investigate the import of gas from external sources or other sustainable sources such as biogas (if technologically feasible), to study if these might result in a better overall performance in low costs and meeting the demand. Because after the extended period of gas reliance, the shift to high electricity and heat reliance is made very fast in this scenario, the technology investments to meet these demands in later time periods are made early as well.

2. **What Energy System Design trade-offs are driven by which underlying uncertainties?**
   Two Energy System Design trade-offs are present in the proof of concept: first a consideration between PV and wind energy, and Combined Heat and Power (CHP) conversion and gas storage capacity. Both trade-offs are driven by the PV development rate and the demand development; specifically the shift from gas to electricity and heat reliance.

   A clear trade-off, in the form of a negative correlation, between investments in PV supply

versus wind supply capacity is distinguished. Naturally, if investments in the one electricity supply technology increase, less capacity of the other electricity supply technology is required. This trade-off and its underlying causes have already been elaborated upon more in-depth in the similar design cluster analysis.

The presence and duration of continued gas reliance towards the future are determining for the trade-off between investments in either CHP conversion technology or in gas storage units. In case of continued gas reliance, or a delayed decrease in gas reliance, additional gas is supplied with electricity supply which is converted to gas. Superfluous gas is stored to meet the gas demand in later time periods. This gas demand development induces high investments in P2G, PV and gas storage capacity, and low investments in CHP conversion capacity. Conversely, when the gas reliance decreases faster than the intended decrease in gas supply, superfluous gas is converted to meet the increased electricity and heat demand. In this scenario, the investments in CHP conversion capacity are high, as opposed to the low investments in P2G, PV and gas storage capacity.

6.4.2 Reflection on the Method Functionality and the Aim of this Research

The aim of this research is to *propose a **generically** applicable novel **method** with which **model-owners** can be provided insight into the **impact of uncertainties** on Energy System **Design** Optimization Model outcomes*. Next, the method functionality is reflected upon on the basis of these four parts of the aim: proposal of a method, generic applicability, insight into the impact of uncertainties on design outcomes and insight to model-owners.

1. **Proposal of a novel method** A method consisting of three steps is proposed: 1) Uncertainty Characterization, 2) Exploratory Modelling, 3) Results Analysis. The novelty of this method is in the structural coupling of these three steps to provide insight into Design Optimization Model behavior across a large number of uncertainty combinations. In addition, the method's novelty is in the innovative approach of combining the cosine distance measure with agglomerative clustering and subspace partitioning techniques to distinguish patterns of similar design outcomes and to relate these to the underlying uncertainties.

2. **Generic applicability of the method** The general applicability of the proposed method concerns two purposes: applicability of the method to Energy System Design Optimization Models and to Design Optimization Models in general. First, it is expected that the proposed method is applicable to other Energy System Design Optimization Models than the model used in the proof of concept. This is because of the model-specific selection of uncertainties, experiment design and design specifics, the open-source character of the EMA Workbench, which provides support for models developed in various modelling packages and environments, and the broad suitability and variety of the results analysis

tools. It is anticipated that the ease of applying the method to a model is influenced by: whether or not the model is specified in the same programming language as the EMA Workbench (Python), and the extent to which the modelled case is aggregated. Second, it is expected that the method, and the novel set of techniques to form clusters of similar outcomes in particular, is applicable to Design Optimization Models in general. This general applicability is constrained to (Energy System) Design Optimization Models where the optimized outcome, the design, can be formatted as a (high dimensional) vector which contains the value for all potential design components, including the zero values, in a fixed ordering over all experiment runs.

3. **Insight into the impact of uncertainties on design outcomes** The proposed method is useful in providing insight into the impact of uncertainties on design outcomes. In this research, the proposed method is employed to provide insight into the impact of 6 uncertainties on an existing Energy System Optimization Model and its simulated case. In 800 experiments, the provided uncertainty ranges are sampled with Latin Hypercube Sampling to produce 800 sets of underlying uncertainties and their associated model outcomes. In other words, the exploratory modelling resulted in 800 designs emerging from each uncertainty set. Clustering of the total outcome space, based on the cosine distances between all experiment-specific designs, allowed the identification and characterization of 6 distinct designs. Using the CART subspace partitioning algorithm, it was possible to relate these design characteristics back to the underlying uncertainties. Furthermore, PRIM subspace partitioning allowed the identification of uncertainty ranges that caused distinct model behavior, also in relying on either the one or the other technology for the resulting design. In addition, the results analysis made clear that for certain design elements, each experiment resulted in a separate line of investments over time. All in all, the results of this research imply that the analysis of uncertainties and their impact on (Energy System) Design Optimization Model outcomes is fundamental to design (energy) systems that are robust across a wide range of possible futures.

4. **Insight to model-owners** An optimization model expert described the method functionality of relating the impact of uncertainty in the model-input to the resulting model-output as very relevant to model-owners. This expert recognizes the general applicability of the method to Design Optimization Models and thought of a potential use case of the method to one of their own projects. Model-owners can use the insights to 1) identify model specifications (or the lack thereof) that are determining for the model output, and possibly take measures to limit these effects, and to 2) offer their clients (possibly decision-makers) strategy advice.

All in all, this implies that the proposed method is useful in providing insight to model-owners on the impact of uncertainties on the outcomes of their Design Optimization Models. This research has shown that numerous uncertainties play a role or potentially impact energy systems. The energy system is inevitably changing to meet the ambitious goals set in the energy

transition. The investment patterns revealed that investments towards a changing energy system should be performed on a short term and that supply, conversion and storage units are preferably located where the demand is high. Also, if the gas supply decreases as intended, but the gas demand does not follow, different sources of gas supply must be tapped. Finally, in urban regions, PV supply is expected to be preferred over wind supply in the absence of other electricity supply technologies.

6.4.3 Recommendations for Future Research

In this section, recommendations for future research are provided, based on this research and its associated implications and limitations.

This research offers a single proof of concept of the method functionality. As the method is expected to be applicable to Energy System Design Optimization Models and to Design Optimization Models in general, it is recommended to:

- Apply the method to other Energy System Design Optimization Models and cases to further test and improve the methods functionalities;
- Apply the method to Design Optimization Models, which do not specifically optimize for the energy system, to verify this general method applicability and to further test and improve the methods functionalities. Such models could concern the optimization of for example the design of water infrastructure or the design of mechanical units.
- Apply the method to an iterative optimization approach. As mentioned in the research limitations, extending a model to represent a more complete version of reality is not possible for optimization models that are already NP-hard. An alternative is to perform iterative optimization. There is scientific value in identifying how the proposed method could be implemented in an iterative optimization modelling approach. In which part of the iterations should the Exploratory Modelling be implemented and, how should the results of the uncertainty analysis be implemented into subsequent iterations?

The proof of concept of the method functionality is facilitated by the application to an Energy System Design Optimization Model that is written in Python, optimizes an aggregated case of the system under analysis and has a relatively high specified optimality gap of 7%. In order to attain a more complete picture of the ease of applying the method, the method should be applied to a broader spectrum of models:

- Apply the method to models that are *not* written in Python. Currently, the EMA Workbench offers connectors to Vensim, Netlogo, and Excel. Therefore, connecting the Workbench to models written in these languages is expected to be relatively straightforward as well. It is considered a challenge to apply the method to models specified in for example the AIMMS optimization software as currently there is no interface between this software and the EMA Workbench.

- Apply the method to a model in which a less aggregated version of a system is simulated. This could be the same model and the same case as in the proof of concept, but less aggregated, for example by considering more locations. The level of aggregation in this case is measured by the number of design components , which was 3451 in this proof of concept. It is expected that the computational requirements will increase, both to run the entire set of experiments and to analyse the higher-dimensional outcome space.
- Apply the method to the model that is used in this research, but with a lower optimality gap. It is important to also remove or up the maximum computation time, to prevent a resulting low percentage of experiments that is solved to optimality. As explained in the research limitations section, the height of the optimality gap is expected to influence the coherence in underlying uncertainties that result in similar design outcomes. This implies that applying the method to the model, with lower optimality gap, will result in more significant underlying uncertainties. This in turn will allow a more specific identification of the impact of specific demand development scenarios, other than the two most significant scenarios in this research' proof of concept.

Below, recommendations considering the uncertainties are listed.

- The scoping of this research was targeted specifically at external uncertainties. There is value in studying different external or internal uncertainties as well. Most specifically, Optimization Models usually have limited representations of societal factors such as stakeholder behavior. It is regarded an ambitious next step for the method to be applied to integrate such societal factors in the optimization modelling (Trutnevyte et al., 2019).
- Due to the determining power of the demand development, and the relative importance of some specific demand development scenarios, the determining power of the majority of scenarios could not be identified in the proof of concept. Therefore, relating the effect of the *individual* demand development scenarios to the outcomes is considered to be a valuable addition to the existing results analysis. To portray the influence of individual categorical uncertainty categories, it is recommended to start with performing a regional sensitivity analysis of specific design components to the uncertainties.

Next, to further substantiate the method's use of agglomerative hierarchical clustering to identify clusters of experiments that result in similar Energy System Design from the high-dimensional cosine distance matrix, it is recommended to explore the performance of different clustering choices.

- Although it is expected that the agglomerative hierarchical clustering with complete linkage results in the most 'dense' and similar clusters, there is scientific value in comparing the agglomerative clustering performance with that of divisive hierarchical clustering. Can another clustering algorithm result in clusters with a higher design similarity? Also, different linkage methods could be employed to compare the functionality. It is recommended to start with average linkage to define the shortest-link distance.

- In this research, the default value for the linkage distance threshold is used to determine the number of clusters. With a total number of 800 experiments clustered into 9 clusters, 3 clusters had a cluster size $< 1\%$ and 3 experiments had a cluster size $> 10\%$ of the total number of experiments. It appeared that a cluster size $> 10\%$ of the total number of experiments is too large to draw specific conclusions on the cluster-design characteristics and the underlying uncertainties. To explore the effects of the cluster sizing on the ability to draw distinct cluster-design conclusions in relation to the underlying uncertainties, it is recommended to lower the linkage distance threshold to analyze a larger number of smaller-sized clusters. For this proof of concept, lowering the threshold to 0.2, would already have resulted in approximately 30 clusters.

Lastly, the proof of concept model was set to a perfect foresight modelling approach. "The perfect foresight assumption means that the model can make massive investments in a single immature technology with a high learning rate without risk of failure" (DeCarolis et al., 2017).

- To analyze the effect of the chosen decision making approach in the model under analysis, it is relevant to perform the same uncertainty analysis on the model set to a limited foresight decision making approach.

- In the proof of concept, which simulates a greenfield case, a large baseload of energy system infrastructure is invested in in the first time period. This baseload serves to fill the model with infrastructure. However, in combination with the perfect foresight modelling, no distinction can be made between the baseload investments that represent 'existing' infrastructure and baseload investments that are invested in towards future requirements. An extension to this research could be to *produce* a brownfield starting point for the model, by running the greenfield model in 2018 with a limited foresight approach of two years. The investments required for that first time step are the 'existing' infrastructure, or the brownfield, which subsequently can be used as input to the remaining time periods 2020—2050, which are run with a perfect foresight modelling approach.

References

Almassalkhi, M. R., & Towle, A. (2016). Enabling city-scale multi-energy optimal dispatch with energy hubs. In *19th power systems computation conference, pscc 2016*. doi: 10.1109/PSCC.2016.7540981

Ashouri, A., Petrini, F., Bornatico, R., & Benz, M. J. (2014). Sensitivity analysis for robust design of building energy systems. *Energy*, *76*, 264–275. doi: 10.1016/j.energy.2014.07.095

Babiker, M., Gurgel, A., Paltsev, S., & Reilly, J. (2009). Forward-looking versus recursive-dynamic modeling in climate policy analysis: A comparison. *Economic Modelling*, *26*(6), 1341–1354. Retrieved from http://dx.doi.org/10.1016/j.econmod.2009.06.009 doi: 10.1016/j.econmod.2009.06.009

Bankes, S. (1993). Exploratory Modeling for Policy Analysis. *Operations Research*, *41*(3), 435–449. doi: 10.1287/opre.41.3.435

Bollen, J., & Brink, C. (2014). Air pollution policy in Europe: Quantifying the interaction with greenhouse gases and climate change policies. *Energy Economics*, *46*(2014), 202–215. Retrieved from http://dx.doi.org/10.1016/j.eneco.2014.08.028 doi: 10.1016/j.eneco.2014.08.028

Box, G., & Draper, N. (1987). *Empirical Model-Building and Response Surfaces (Wiley Series in Probability and Statistics)* (First ed.). New York: John Wiley & Sons.

Chong, A., Xu, W., & Khee Poh, L. (2015). UNCERTAINTY ANALYSIS IN BUILDING ENERGY SIMULATION : A PRACTICAL APPROACH. In *Bs2015: 14th conference of international building performance simulation association* (pp. 2796–2803). Hyderabad, India.

Cole, W., Mai, T., Logan, J., Steinberg, D., Mccall, J., Richards, J., ... Porro, G. (2018). 2018 Standard Scenarios Report : A U . S . Electricity Sector Outlook. (November). doi: NREL/TP-6A20-68548

Connolly, D., Lund, H., Mathiesen, B. V., & Leahy, M. (2010). A review of computer tools for analysing the integration of renewable energy into various energy systems. *Applied Energy*, *87*(4), 1059–1082. doi: 10.1016/j.apenergy.2009.09.026

DeCarolis, J., Babaee, S., Li, B., & Kanungo, S. (2016). Modelling to generate alternatives with an energy system optimization model. *Environmental Modelling and Software*, *79*, 300–310. doi: 10.1016/j.envsoft.2015.11.019

DeCarolis, J., Daly, H., Dodds, P., Keppo, I., Li, F., McDowall, W., ... Zeyringer, M. (2017). Formalizing best practice for energy system optimization modelling. *Applied Energy*, *194*, 184–198. Retrieved from http://dx.doi.org/10.1016/j.apenergy.2017.03.001

doi: 10.1016/j.apenergy.2017.03.001

DNV GL. (2018). *Regional Forecast Europe - Energy Transition Outlook 2018* (Tech. Rep.).

E3MLab/ICCS. (2017). *Prometheus Model - Model description* (Tech. Rep.). National Technical University of Athens. Retrieved from http://www.e3mlab.eu/e3mlab/PROMETHEUSManual/ThePROMETHEUSMODEL_2017.pdf

Gabrielli, P., Gazzani, M., Martelli, E., & Mazzotti, M. (2018). Optimal design of multi-energy systems with seasonal storage. *Applied Energy*, *219*(July 2017), 408–424. Retrieved from https://doi.org/10.1016/j.apenergy.2017.07.142 doi: 10.1016/j.apenergy.2017.07.142

Geidl, M., Koeppel, G., Favre-Perrod, P., Klöckl, B., Andersson, G., & Fröhlich, K. (2007). Energy hubs for the future. *IEEE Power and Energy Magazine*, *5*(1), 24–30. doi: 10.1109/MPAE.2007.264850

Guivarch, C., Lempert, R., & Trutnevyte, E. (2017). Scenario techniques for energy and environmental research: An overview of recent developments to broaden the capacity to deal with complexity and uncertainty. *Environmental Modelling and Software*, *97*, 201–210. doi: 10.1016/j.envsoft.2017.07.017

Gurobi Optimization. (n.d.). *MIPGap documentation.* Retrieved from https://www.gurobi.com/documentation/8.1/refman/mipgap2.html

Haasnoot, M., Kwakkel, J. H., Walker, W. E., & ter Maat, J. (2013). Dynamic adaptive policy pathways: A method for crafting robust decisions for a deeply uncertain world. *Global Environmental Change*, *23*(2), 485–498. Retrieved from http://dx.doi.org/10.1016/j.gloenvcha.2012.12.006 doi: 10.1016/j.gloenvcha.2012.12.006

Hallegatte, S., Lempert, R., & Brown, C. (2012). *Investment Decision Making Under Deep Uncertainty Application to Climate Change* (No. September 2012). doi: 10.1596/1813-9450-6193

Howells, M., Rogner, H., Strachan, N., Heaps, C., Huntington, H., Kypreos, S., ... Roehrl, A. (2011). OSeMOSYS: The Open Source Energy Modeling System. An introduction to its ethos, structure and development. *Energy Policy*, *39*(10), 5850–5870. Retrieved from http://dx.doi.org/10.1016/j.enpol.2011.06.033 doi: 10.1016/j.enpol.2011.06.033

Huber, C., Faber, T., Haas, R., Resch, G., Green, J., Olz, S., ... Lins, C. (2004). Green-X: Deriving optimal promotion strategies for increasing the share of RES-E in a dynamic European electricity market. *Final Report of the Project Green-X*, 1–186. Retrieved from http://www.green-x.at/downloads/FinalreportoftheprojectGreen-X.pdf

Hunter, K., Sreepathi, S., & DeCarolis, J. F. (2013). Modeling for insight using Tools for Energy Model Optimization and Analysis (Temoa). *Energy Economics*, *40*, 339–349. Retrieved from http://dx.doi.org/10.1016/j.eneco.2013.07.014 doi: 10.1016/j.eneco.2013.07.014

IIESI. (2016). *Energy Systems Integration: Defining and Describing the Value Proposition* (No. June). Retrieved from http://dx.doi.org/10.2172/1257674 doi: http://dx.doi.org/10.2172/1257674

Integrated Assessment Modeling Consortium. (2016). *IAMC documentation.* Retrieved from https://www.iamcdocumentation.eu/index.php/Model_concept,

_solver_and_details_-_DNE21%2B

IPCC. (2014). Climate Change 2014 Synthesis Report Summary Chapter for Policymakers. *Ipcc*. doi: 10.1017/CBO9781107415324

IPCC. (2019). *Special Report: The Ocean and Cryosphere in a Changing Climate* (Tech. Rep. No. September). Intergovernmental Panel on Climate Change. Retrieved from https://www.ipcc.ch/report/srocc/

Isaac, M., & Vuuren, D. P. V. (2009). Modeling global residential sector energy demand for heating and air conditioning in the context of climate change. *Energy Policy*, *37*(2), 507–521. doi: 10.1016/j.enpol.2008.09.051

Keirstead, J., & Calderon, C. (2012). Capturing spatial effects, technology interactions, and uncertainty in urban energy and carbon models: Retrofitting newcastle as a case-study. *Energy Policy*, *46*, 253–267. doi: 10.1016/j.enpol.2012.03.058

Keppo, I., & Strubegger, M. (2010). Short term decisions for long term problems - The effect of foresight on model based energy systems analysis. *Energy*, *35*(5), 2033–2042. Retrieved from http://dx.doi.org/10.1016/j.energy.2010.01.019 doi: 10.1016/j.energy.2010.01.019

Kim, H., Cheon, H., Ahn, Y. H., & Choi, D. G. (2019). Uncertainty quantification and scenario generation of future solar photovoltaic price for use in energy system models. *Energy*, *168*, 370–379. Retrieved from https://doi.org/10.1016/j.energy.2018.11.075 doi: 10.1016/j.energy.2018.11.075

Kononov, A., Kononova, P., & Gordeev, A. (2020). Branch-and-bound approach for optima localization in scheduling multiprocessor jobs. *International Transactions in Operational Research*, *27*(1), 381–393. doi: 10.1111/itor.12503

Krey, V., Guo, F., Kolp, P., Zhou, W., Schaeffer, R., Awasthy, A., ... van Vuuren, D. P. (2019). Looking under the hood: A comparison of techno-economic assumptions across national and global integrated assessment models. *Energy*, *172*, 1254–1267. doi: 10.1016/j.energy.2018.12.131

Kroposki, B., Garrett, B., Macmillan, S., Rice, B., Komomua, C., O'Malley, M., ... Kroposki, B. (2012). *Energy Systems Integration, A Convergence of Ideas* (No. July 2012). Boulder. Retrieved from www.nrel.gov/esi/pdfs/55649.pdf?

Kwakkel, J. H. (2017). The Exploratory Modeling Workbench: An open source toolkit for exploratory modeling, scenario discovery, and (multi-objective) robust decision making. *Environmental Modelling and Software*, *96*, 239–250. Retrieved from http://dx.doi.org/10.1016/j.envsoft.2017.06.054 doi: 10.1016/j.envsoft.2017.06.054

Kwakkel, J. H., & Jaxa-Rozen, M. (2016). Improving scenario discovery for handling heterogeneous uncertainties and multinomial classified outcomes. *Environmental Modelling and Software*, *79*, 311–321. Retrieved from http://dx.doi.org/10.1016/j.envsoft.2015.11.020 doi: 10.1016/j.envsoft.2015.11.020

Kwakkel, J. H., & Pruyt, E. (2013). Exploratory Modeling and Analysis, an approach for model-based foresight under deep uncertainty. *Technological Forecasting and Social Change*, *80*(3), 419–431. doi: 10.1016/j.techfore.2012.10.005

Larsson Ivanov, O., Honfi, D., Santandrea, F., & Stripple, H. (2019). Consideration of uncertainties in LCA for infrastructure using probabilistic methods. *Structure and Infras-*

tructure Engineering, *15*(6), 711–724. Retrieved from https://doi.org/10.1080/15732479.2019.1572200 doi: 10.1080/15732479.2019.1572200

Lempert, R. J., Popper, S. W., & Bankes, S. C. (2003). *Shaping the next one hundred years: New methods for quantitative long-term strategy analysis* (MR-1626-RP ed.). Santa Monica, CA: The RAND Pardee Center.

Li, Z., & De Rijke, M. (2017). The impact of linkage methods in hierarchical clustering for active learning to rank. *SIGIR 2017 - Proceedings of the 40th International ACM SIGIR Conference on Research and Development in Information Retrieval*, 941–944. doi: 10.1145/3077136.3080684

Loulou, R., Goldstein, G., Kanudia, A., Lettila, A., Remme, U., & Noble, K. (2016). Documentation for the TIMES Model PART I - Concepts and Theory. (July), 151. Retrieved from https://iea-etsap.org/index.php/etsap-tools/model-generators/timeshttps://iea-etsap.org/docs/Documentation_for_the_TIMES_Model-Part-I_July-2016.pdf

Maier, H. R., Guillaume, J. H., van Delden, H., Riddell, G. A., Haasnoot, M., & Kwakkel, J. H. (2016). An uncertain future, deep uncertainty, scenarios, robustness and adaptation: How do they fit together? *Environmental Modelling and Software*, *81*, 154–164. Retrieved from http://dx.doi.org/10.1016/j.envsoft.2016.03.014 doi: 10.1016/j.envsoft.2016.03.014

Mancarella, P. (2014). MES (multi-energy systems): An overview of concepts and evaluation models. *Energy*, *65*, 1–17. Retrieved from http://dx.doi.org/10.1016/j.energy.2013.10.041 doi: 10.1016/j.energy.2013.10.041

Marangoni, G., Tavoni, M., Bosetti, V., Borgonovo, E., Capros, P., Fricko, O., ... Van Vuuren, D. P. (2017). Sensitivity of projected long-term CO 2 emissions across the Shared Socioeconomic Pathways. *Nature Climate Change*, *7*(2), 113–117. doi: 10.1038/nclimate3199

Martinez Cesena, E. A., & Mancarella, P. (2019). Energy Systems Integration in Smart Districts: Robust Optimisation of Multi-Energy Flows in Integrated Electricity, Heat and Gas Networks. *IEEE Transactions on Smart Grid*, *10*(1), 1122–1131. Retrieved from https://ieeexplore-ieee-org.tudelft.idm.oclc.org/stamp/stamp.jsp?tp=&arnumber=8340876 doi: 10.1109/TSG.2018.2828146

Matrosov, E., Padula, S., & Harou, J. (2013). Selecting Portfolios of Water Supply and Demand Management Strategies Under UncertaintyContrasting Economic Optimisation and Robust Decision Making Approaches. *Water Resources Management*(27), 1123–1148. Retrieved from https://link.springer.com/article/10.1007%2Fs11269-012-0118-x#citeas doi: 10.1007/s11269-012-0118-x

Mavromatidis, G., Orehounig, K., & Carmeliet, J. (2018). A review of uncertainty characterisation approaches for the optimal design of distributed energy systems. *Renewable and Sustainable Energy Reviews*, *88*(September 2017), 258–277. Retrieved from https://doi.org/10.1016/j.rser.2018.02.021 doi: 10.1016/j.rser.2018.02.021

McCallum, P., Jenkins, D. P., Peacock, A. D., Patidar, S., Andoni, M., Flynn, D., & Robu, V. (2019). A multi-sectoral approach to modelling community energy demand of the built environment. *Energy Policy*, *132*(October 2018), 865–875. Retrieved from https://doi.org/10.1016/j.enpol.2019.06.041 doi: 10.1016/j.enpol.2019.06.041

Mcdowall, W., Trutnevyte, E., Tomei, J., & Keppo, I. (2014). UKERC Energy Systems Theme Reflecting on Scenarios. (June), 109. Retrieved from http://www.ukerc.ac.uk/publications/ukerc-energy-systems-theme-reflecting-on-scenarios.html

Moallemi, E. A., de Haan, F., Kwakkel, J., & Aye, L. (2017). Narrative-informed exploratory analysis of energy transition pathways: A case study of India's electricity sector. *Energy Policy*, *110*(August), 271–287. Retrieved from https://doi.org/10.1016/j.enpol.2017.08.019 doi: 10.1016/j.enpol.2017.08.019

Moallemi, E. A., Elsawah, S., Turan, H. H., & Ryan, M. J. (2019). Multi-objective decision making in multi-period acquisition planning under deep uncertainty. *Proceedings - Winter Simulation Conference*, *2018-Decem*(i), 1334–1345. doi: 10.1109/WSC.2018.8632316

Moallemi, E. A., & Köhler, J. (2019). Coping with uncertainties of sustainability transitions using exploratory modelling: The case of the MATISSE model and the UK's mobility sector. *Environmental Innovation and Societal Transitions*, *33*(March), 61–83. Retrieved from https://doi.org/10.1016/j.eist.2019.03.005 doi: 10.1016/j.eist.2019.03.005

Nejlaoui, M., Houidi, A., Affi, Z., & Romdhane, L. (2013). Multiobjective robust design optimization of rail vehicle moving in short radius curved tracks based on the safety and comfort criteria. *Simulation Modelling Practice and Theory*, *30*, 21–34. Retrieved from http://dx.doi.org/10.1016/j.simpat.2012.07.012 doi: 10.1016/j.simpat.2012.07.012

Netherlands Environmental Assessment Agency. (2014). *IMAGE documentation*. Retrieved from https://models.pbl.nl/image/index.php/Drivers/Model_drivers#Table_of_drivers

Netherlands Environmental Assessment Agency. (2016). *Energy transition scenarios*. Retrieved from http://themasites.pbl.nl/energietransitie/

Pfenninger, S., Hawkes, A., & Keirstead, J. (2014). Energy systems modeling for twenty-first century energy challenges. *Renewable and Sustainable Energy Reviews*, *33*, 74–86. doi: 10.1016/j.rser.2014.02.003

Pianosi, F., Beven, K., Freer, J., Hall, J. W., Rougier, J., Stephenson, D. B., & Wagener, T. (2016). Sensitivity analysis of environmental models: A systematic review with practical workflow. *Environmental Modelling and Software*, *79*, 214–232. Retrieved from http://dx.doi.org/10.1016/j.envsoft.2016.02.008 doi: 10.1016/j.envsoft.2016.02.008

Podani, J. (1989). Net combinational clustering methods. *Vegetatio*, *81*(1-2), 61–77. Retrieved from https://link.springer.com/article/10.1007/BF00045513#citeas doi: https://doi.org/10.1007/BF00045513

Pye, S., Sabio, N., & Strachan, N. (2015). An integrated systematic analysis of uncertainties in UK energy transition pathways. *Energy Policy*, *87*, 673–684. doi: 10.1016/j.enpol.2014.12.031

Qiu, B., Zhang, M., Li, X., Qu, X., & Tong, F. (2020). Unknown impact force localisation and reconstruction in experimental plate structure using time-series analysis and pattern recognition. *International Journal of Mechanical Sciences*, *166*(July). doi: 10.1016/j.ijmecsci.2019.105231

Radaideh, M. I., & Kozlowski, T. (2019). Combining simulations and data with deep learning

and uncertainty quantification for advanced energy modeling. *International Journal of Energy Research*, *43*(14), 7866–7890. doi: 10.1002/er.4698

Ranger, N., Reeder, T., & Lowe, J. (2013). Addressing deep uncertainty over long-term climate in major infrastructure projects: four innovations of the Thames Estuary 2100 Project. *EURO Journal on Decision Processes*, *1*(3-4), 233–262. doi: 10.1007/s40070-013-0014-5

Ren, H., Gao, W., & Ruan, Y. (2008). Optimal sizing for residential CHP system. *Applied Thermal Engineering*, *28*(5-6), 514–523. doi: 10.1016/j.applthermaleng.2007.05.001

Rice, K., Winkler, B., Jacobs, P., Skuce, A. G., Cook, J., Green, S. A., ... Anderegg, W. R. L. (2016). Consensus on consensus: a synthesis of consensus estimates on human-caused global warming. *Environmental Research Letters*, *11*(4), 048002. doi: 10.1088/1748-9326/11/4/048002

Shabanpour-Haghighi, A., & Seifi, A. R. (2016). An integrated steady-state operation assessment of electrical, natural gas, and district heating networks. *IEEE Transactions on Power Systems*, *31*(5), 3636–3647. doi: 10.1109/TPWRS.2015.2486819

Shobha, G., & Rangaswamy, S. (2018). Computational Analysis and Understanding of Natural Languages: Principles, Methods and Applications. In *Handbook of statistics* (38th ed., pp. 197–228). Elsevier B.V. Retrieved from https://www.sciencedirect.com/science/article/pii/S0169716118300191 doi: https://doi.org/10.1016/bs.host.2018.07.004

Statharas, S., Moysoglou, Y., Siskos, P., Zazias, G., & Capros, P. (2019). Factors Influencing Electric Vehicle Penetration in the EU by 2030: A Model-Based Policy Assessment. *Energies*, *12*(14), 2739. doi: 10.3390/en12142739

Steinbach, J., & Staniaszek, D. (2015). *Discount rates in energy system analysis* (Tech. Rep. No. May). Buildings Performance Institute Europe (BPIE). Retrieved from http://bpie.eu/publication/discount-rates-in-energy-system-analysis/

Stewart, T., & Durbach, I. (2016). Dealing with Uncertainties in MCDA. *Multiple Criteria Decision Analysis*, *233*, 467–496. Retrieved from https://link.springer.com/chapter/10.1007%2F978-1-4939-3094-4_12#citeas doi: https://doi.org/10.1007/978-1-4939-3094-4{_}12

Störmer, E., Truffer, B., Dominguez, D., Gujer, W., Herlyn, A., Hiessl, H., & Kastenholz, H. (2009). Technological Forecasting & Social Change The exploratory analysis of trade-offs in strategic planning : Lessons from Regional Infrastructure Foresight. *Technological Forecasting & Social Change*, *76*(9), 1150–1162. Retrieved from http://dx.doi.org/10.1016/j.techfore.2009.07.008 doi: 10.1016/j.techfore.2009.07.008

Sun, Y., Gu, L., Wu, C. F., & Augenbroe, G. (2014). Exploring HVAC system sizing under uncertainty. *Energy and Buildings*, *81*, 243–252. doi: 10.1016/j.enbuild.2014.06.026

The SciPy community. (2019). *scipy.cluster.hierarchy.linkage*. Retrieved from https://docs.scipy.org/doc/scipy/reference/generated/scipy.cluster.hierarchy.linkage.html#scipy.cluster.hierarchy.linkage

Thompson, E. L., & Smith, L. A. (2019). Escape from model-land. *Economics Discussion Papers*, *No 2019-23*(Kiel Institute for the World Economy). Retrieved from http://www.economics-ejournal.org/economics/discussionpapers/2019-23

Trutnevyte, E. (2016). Does cost optimization approximate the real-world energy transition? *Energy*, *106*, 182–193. Retrieved from http://dx.doi.org/10.1016/j.energy.2016.03.038 doi: 10.1016/j.energy.2016.03.038

Trutnevyte, E., Hirt, L. F., Bauer, N., Cherp, A., Hawkes, A., Edelenbosch, O. Y., ... van Vuuren, D. P. (2019). Societal Transformations in Models for Energy and Climate Policy: The Ambitious Next Step. *One Earth*, *1*(4), 423–433. doi: 10.1016/j.oneear.2019.12.002

Tsoukias, A., Montibeller, G., Lucertini, G., & Belton, V. (2013). Policy analytics: an agenda for research and practice. *EURO Journal on Decision Processes*, *1*(1-2), 115–134. Retrieved from http://link.springer.com/10.1007/s40070-013-0008-3 doi: 10.1007/s40070-013-0008-3

UNFCCC. Conference of the Parties (COP). (2015). ADOPTION OF THE PARIS AGREEMENT - Conference of the Parties COP 21. *Adoption of the Paris Agreement. Proposal by the President.*, *21932*(December), 32. Retrieved from http://unfccc.int/resource/docs/2015/cop21/eng/l09r01.pdf doi: FCCC/CP/2015/L.9/Rev.1

Van Beuzekom, I., Gibescu, M., Pinson, P., & Slootweg, J. G. (2017). Optimal planning of integrated multi-energy systems. *2017 IEEE Manchester PowerTech, Powertech 2017*, *1*, 1–6. doi: 10.1109/PTC.2017.7980886

van Beuzekom, I., Nijhuis, M., Hodge, B., Pinson, P., & Slootweg, J. G. (n.d.). Optimal Planning of Integrated Electricity , Gas and Heat Systems : a Multigrid Approach. , 1–11. doi: NP

Van Vuuren, D. P., Riahi, K., Moss, R., Edmonds, J., Thomson, A., Nakicenovic, N., ... Arnell, N. (2012). A proposal for a new scenario framework to support research and assessment in different climate research communities. *Global Environmental Change*, *22*(1), 21–35. doi: 10.1016/j.gloenvcha.2011.08.002

Welsch, M., Howells, M., Bazilian, M., DeCarolis, J. F., Hermann, S., & Rogner, H. H. (2012). Modelling elements of Smart Grids - Enhancing the OSeMOSYS (Open Source Energy Modelling System) code. *Energy*, *46*(1), 337–350. Retrieved from http://dx.doi.org/10.1016/j.energy.2012.08.017 doi: 10.1016/j.energy.2012.08.017

Witt, T., Dumeier, M., & Geldermann, J. (2020). Combining scenario planning, energy system analysis, and multi-criteria analysis to develop and evaluate energy scenarios. *Journal of Cleaner Production*, *242*, 118414. Retrieved from https://doi.org/10.1016/j.jclepro.2019.118414 doi: 10.1016/j.jclepro.2019.118414

Xu, L., Fuss, M., Poganietz, W.-R., Jochem, P., Schreiber, S., Zoephel, C., & Brown, N. (2019). An Environmental Assessment Framework for Energy System Analysis (EAFESA): The method and its application to the European energy system transformation. *Journal of Cleaner Production*, *243*, 118614. doi: 10.1016/j.jclepro.2019.118614

Yáñez, M., Ortiz, A., Brunaud, B., Grossmann, I., & Ortiz, I. (2019). *The use of optimization tools for the Hydrogen Circular Economy* (Vol. 46). Elsevier Masson SAS. Retrieved from https://doi.org/10.1016/B978-0-12-818634-3.50297-6 doi: 10.1016/b978-0-12-818634-3.50297-6

Zadeh, R. B., & Goel, A. (2013). Dimension independent similarity computation. *Journal of Machine Learning Research*, *14*, 1605–1626.

Zhang, J., Tang, H., & Chen, M. (2019). Linear substitute model-based uncertainty analysis of complicated non-linear energy system performance (case study of an adaptive cycle

engine). *Applied Energy*, *249*(March), 87–108. Retrieved from https://doi.org/10.1016/j.apenergy.2019.04.138 doi: 10.1016/j.apenergy.2019.04.138

Appendix A

Description of Energy System Optimization Model and the Case under Analysis

As a proof of concept of the applicability and functionalities of the proposed method, it is applied to a model that aims to aid decision-making regarding *integrated* energy system design and operation. This model, and the case that is modelled, are introduced in this chapter.

A.1 Integrated Energy Systems

In this research, an Energy System Optimization Model is used that optimizes for the design and operation of an *integrated* energy system.

The integration of energy systems is a promising approach to enable the transition from a fossil-based to renewable-based energy system (IIESI, 2016; Mancarella, 2014; Shabanpour-Haghighi & Seifi, 2016; Kroposki et al., 2012; Geidl et al., 2007). IIESI (2016) define Energy Systems Integration as the following:

Energy Systems Integration is the process of coordinating the operation and planning of energy systems across multiple pathways and/or geographical scales to deliver reliable, cost-effective energy services with minimal impact on the environment.

Energy Systems Integration connects energy systems, for example electricity, heat and fuels, by including interactions among these systems such as storage and conversion units and by coordinating these systems across infrastructures. These interactions can occur between multiple energy systems and on multiple scales: district, city, region, etc (figure A.1).

Through these interactions multiple energy systems can become one integrated energy system which is more flexible and reliable (Geidl et al., 2007). In case of a day without sun or wind, for

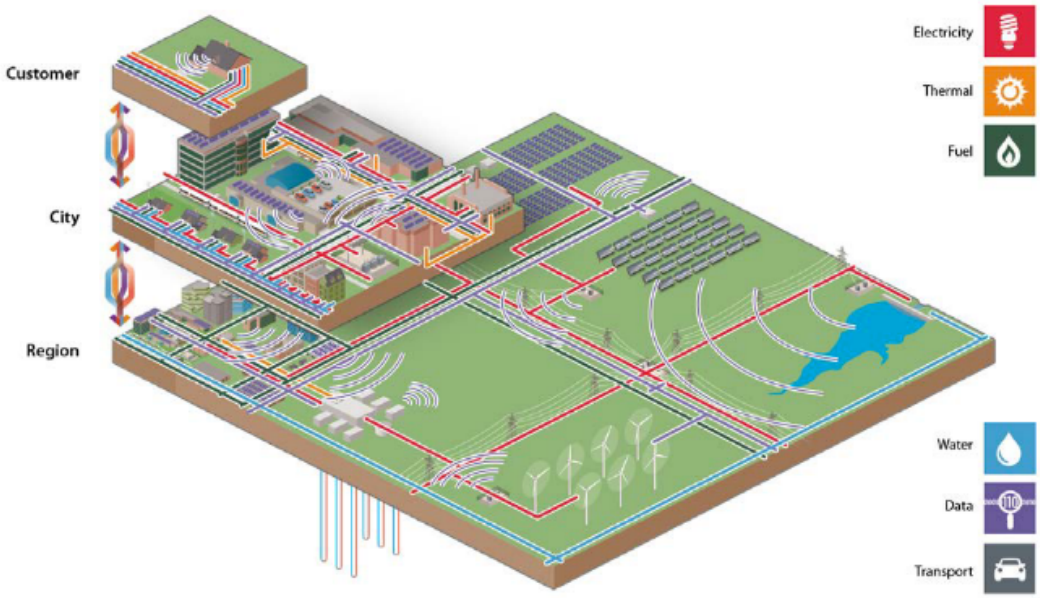

Figure A.1: Energy Systems Integration. Figure retrieved from IIESI (2016).

example, energy supply can be ensured by converting available energy in one energy system to the short-falling energy carrier in a connected energy system. For this purpose a conversion unit such as a Combined Heat and Power (CHP) unit could be used, which converts energy from one system (fuels) to another (heat and electricity).

All in all, an integrated energy systems allows to take advantage of the benefits in efficiency and performance of each of the connected energy systems, resulting in an improved technical, economic and environmental performance of the system (Mancarella, 2014; Gabrielli et al., 2018; Kroposki et al., 2012).

A.2 ORTEC Optimization Model

The model that is used in this research optimizes the investment planning up to 2050 for the integration of three energy systems at city-level. The medium-sized Dutch city that is modelled in this case represents Eindhoven. This ESOM is designed in the context of an ongoing PhD research at Eindhoven of Technology, Universitydepartment of Electrical Engineering, and ORTEC B.V. (Van Beuzekom et al., 2017; van Beuzekom et al., n.d.).

The model is intended to allow different decision-makers to see the effects of integrating the planning of multiple energy systems and the interactions between these systems (van Beuzekom et al., n.d.). When targeting decision makers, the following actors are meant: local

governments and energy system operators. The model could also be used to see the effects of for example policy measures or external events on the model outcome: optimized investment planning.

The modelled case considers the integration of: three energy systems: electricity (E), gas (G) and heat (H), with associated E, G, and H network and storage units; three types of conversion units; and two (renewable) energy generation units; at city-level, which is aggregated to seven locations (figure A.2). This brings the investment decision portfolio per location per time step to the following possibilities:

- Expansion of existing systems with network units: E network, G network, H network;
- Placement of energy storage units: E storage, G storage, H storage;
- Integrating systems using conversion units: combined heat and power (CHP), heat pump (HP), power-to-gas (P2G);
- Building renewable energy generation units: wind, photovoltaic (PV).

Each of these 11 investment possibilities can be invested in at each time step and location. Except for the wind turbines, which can only be invested in at four out of seven locations, due to real-world restrictions. Also, the network investment possibilities are not considered per location but per location pair, or edge, because a network *connects* locations. Per location, a node is present for each energy system, which sums the total of nodes to $3 * n$, with $n = 7$ the number of locations. The three energy systems (E, G and H), are fully coupled at each location. Therefore, the number of network investment possibilities per time-step equals $3 * n^2 = 147$. Due to the mathematical formulation edges connecting the same location are automatically assigned a value 0. Otherwise, the number of network investment possibilities per time-step would have been $3 * n * (n - 1) = 126$. The number of non-network investment possibilities per time-step equals $8 * n = 56$.

As briefly mentioned in the chapter introduction, the model optimizes the investment planning, which is a *combination* of the design and operation of the integrated energy systems at city scale. The design component of the investment planning consists of determining *how many* of which technology units are invested in (*what*) at which location (*where*) considering their operational characteristics and constraints (Mavromatidis et al., 2018). The operation component of the investment planning entails optimizing the operation of generation and storage technologies in the energy system along the time horizon (*when*) running from the year 2018 to 2050 in one-year time-steps. Please note that all technology units are assumed to have one capacity with associated costs and efficiency. Also, it should be noted that the model does *not* include economic parameters such as costs of operation or energy prices or actor parameters such as stakeholders or decision makers. Furthermore, the placement location of supply does not necessarily indicate the actual location of placement of the energy supply unit: it indicates where the energy enters the urban energy system. Consequentially, the output of the model is an optimized investment planning containing the number of units that should be invested in

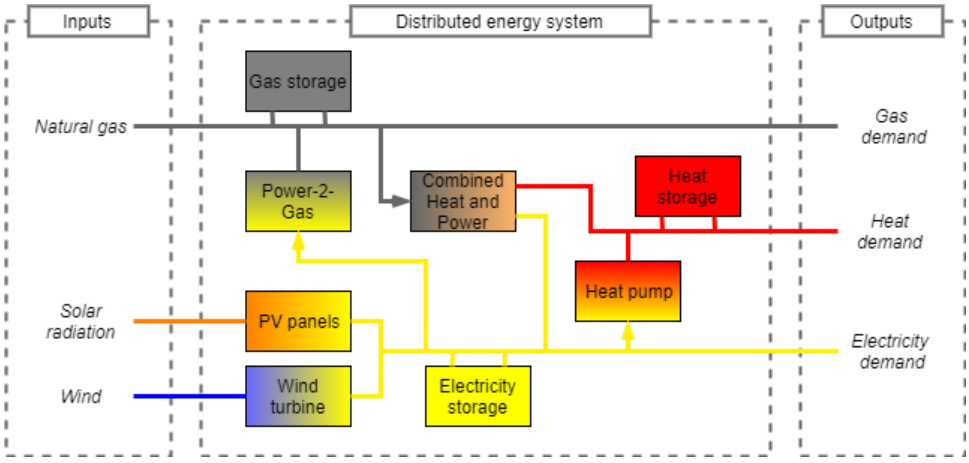

Figure A.2: Overview of the energy technologies considered in the integrated energy system of the model used in this research (adapted from Mavromatidis et al. (2018)).

per investment possibility (technology unit; location; year) (figure A.3).

A.3 Model Structure

The objective of this model is to minimize the total investment costs while meeting the specified constraints, which for example ensure that energy demand is met at each location and time step and that the amount of energy that is generated, converted or stored does not surpass the available capacity (figure 2.8). Climate goals are included in the model by reduction of gas supply according to the transition goal, and restriction of supply investments to wind and PV renewable energy sources.

To perform the optimization and deliver an 'optimal' investment planning up to 2050, the model makes use of the following external data. The precise values that were used as input to the model when testing the framework can be found in appendix B.

- Technology portfolio;
- Technical characteristics, such as the conversion efficiencies, standing losses of storage units and the projected technological development of the technological units.
- Economical parameters, including all investment costs and the discount rate;
- Supply parameter: the projected gas supply development profile, location specific;
- Projected energy demand development profile per location, energy carrier specific.

More detail on the model, including detailed desciptions of each equation and variable can be found in Van Beuzekom et al. (2017). Nevertheless, the next section features some more in-depth description of the models functionalities and modelling frameworks.

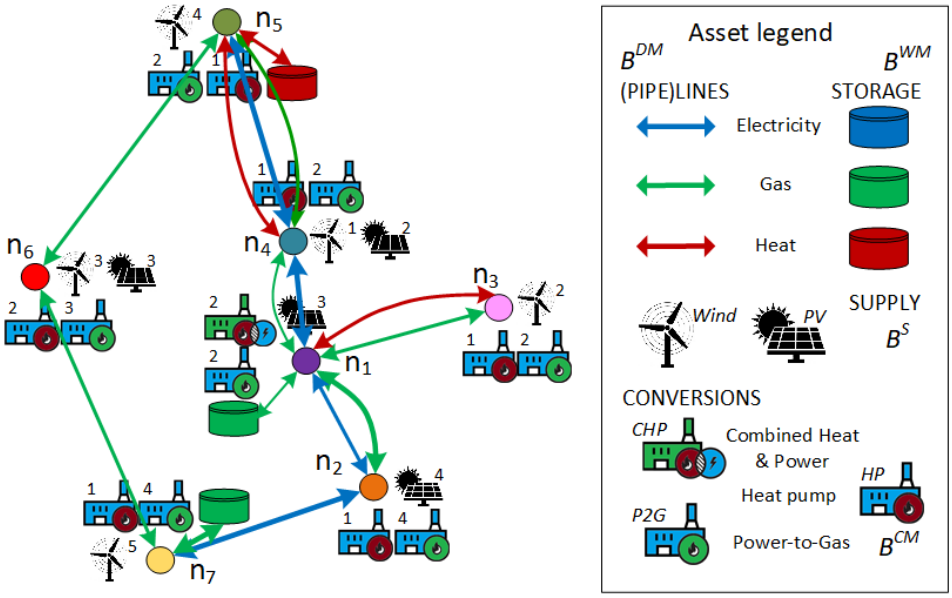

Figure A.3: Visualization of a model outcome (retrieved from van Beuzekom et al. (n.d.)). Example of an optimized solution for the investments to be made for an aggregated version of the model with 7 locations (n_x). The small number given at each invested asset denotes the proposed number to invest in over the time period of 2018-2050 per location.

A.4 Optimization Model Set-Up

The model employs a Mixed-Integer Linear Programming (MILP) technique (Van Beuzekom et al., 2017). This technique has been most favored in Integrated Energy System Optimization Models which model the design and/or operation of IESs (Gabrielli et al., 2018; Martinez Cesena & Mancarella, 2019; Ashouri et al., 2014; Yáñez et al., 2019). This is because MILP combines integer investment decisions with operation constraints (van Beuzekom et al., n.d.), which sufficiently represents the system features, and does so under acceptable computational requirements.

The optimization model is written in Python. To employ optimization, the Python Optimization Modeling Objects (Pyomo) library is used (Hunter et al., 2013; DeCarolis et al., 2016). Pyomo is an open source Python library that provides optimization capabilities which are associated with for example AIMMS. It also embeds a number of supporting libraries. Pyomo also supports a link to the used mixed-integer linear solver Gurobi (Gurobi Optimization, n.d.).

A.4.1 Branch and Bound Optimization

The model uses a Branch and Bound algorithm design paradigm for mathematical optimization (Kononov, Kononova, & Gordeev, 2020). The algorithm constitutes of a tree in the solution space with the full set of candidate solutions at the root. Each branch of the tree represents a

subset of the solution space. Each candidate solution embodies a set of integer values. In order to qualify whether candidate solutions approach the optimal solution, the algorithm *estimates* the value of the optimal solution with linear programming (LP) relaxation. In LP relaxation, the mathematical problem is solved by ignoring the integrality constraint $x_i \in \{0, 1\}$ and using a collection of linear constraints $0 \geq x_i \geq 1$ instead, for each variable present in the mathematical problem. The LP relaxation provides the upper or lower bound on the optimal solution, depending on whether the objective function is to be maximized or minimized. This solution is called the *best bound*. Subsequently, the candidate solutions (with integrality constraints) are systematically enumerated by comparing them with the estimated *best bound*. A candidate solution is discarded if it cannot provide a solution that better approaches the *best bound* than the candidate solutions previously enumerated. This process, of recursively splitting the solution space, is called *branching*. The goal of the branch and bound algorithm is to identify the optimal result: the candidate solution that best maximizes or minimizes the specified objective function of the mathematical problem.

Optimality gap

The Gurobi optimization solver computes the relative mixed integer programming (MIP) *optimality gap* (MIPgap) to determine whether the result is solved to optimality (Gurobi Optimization, n.d.). The MIP solver will terminate when the optimal result is achieved. The optimal result is reached when the absolute gap between the *best bound* and the best candidate solution found so far (*best integer*) is less than the MIPgap times the absolute value of*best integer* (A.1).

$$MIPGap = \frac{|BestBound - BestInteger|}{1e^{-10} + |BestInteger|} \tag{A.1}$$

The MIPGap value is specified by the user and can have any value between 0 and 1.0. The default value is $1e^{-4}$, which corresponds to a gap of 0.01%. At this tolerance, the identified optimal result is guaranteed to be within 0.01% of the *best bound*. The lower the MIPGap value is specified, the closer the best candidate solution (*best integer*) has to approach the *best bound* before the result is considered to be optimal. This results in higher optimality, but also in extended computation time. Thus, if a model can accept greater optimality tolerance, a bigger MIPGap value should be specified.

Appendix B

Model Input

In this Appendix, the original model input is described. The uncertainty ranges for the parameters that are considered as uncertainties in this research (energy demand development, development rates and discount rate) are specified in Appendix D. As visualized in figure 2.8, the model input consists of five components: technology portfolio, technical characteristics, economical parameters, supply parameters and end-use parameters. Each of these are specified in the next sections.

B.1 Technology Portfolio

In this section, the set and type of technology units is specified, also, the locations and the location-specific energy demand mix and contribution to the total demand are introduced. Furthermore, the distances are specified for each edge and this section concludes with the listing of time periods.

Table B.1: Technology portfolio

Technology unit	**Type**
PV	Supply
Wind	Supply
Electricity	Storage
Heat	Storage
Gas	Storage
CHP	Conversion
HP	Conversion
P2G	Conversion
Electricity	Network
Heat	Network
Gas	Network

Table B.2: Listing of the 7 locations in which the medium-sized Dutch city is aggregated. The percentages of the electricity, gas and heat demand per location is provided. Also, the allocation of the demand to residential, commercial, industrial and transport purposes are provided.

Node	**Electricity**	**Gas**	**Heat**	**Res.**	**Comm.**	**Ind.**	**Transp.**	**Total**
1	8.61%	9.71%	8.87%	1.2%	4.7%	0.0%	3.1%	9.0%
2	17.10%	18.08%	14.25%	2.3%	7.1%	3.6%	3.1%	16.1%
3	8.61%	9.71%	8.87%	1.2%	4.7%	0.0%	3.1%	9.0%
4	9.23%	9.71%	11.02%	4.7%	2.4%	0.0%	3.1%	10.1%
5	9.23%	9.71%	11.02%	4.7%	2.4%	0.0%	3.1%	10.1%
6	30.11%	25.00%	31.72%	2.3%	18.8%	2.4%	6.2%	29.7%
7	17.10%	18.08%	14.25%	2.3%	7.1%	3.6%	3.1%	16.1%
check	100.0%	100.0%	100.0%	18.7%	47.1%	9.5%	24.6%	100.0%

Table B.3: The network distance in kilometers between all seven locations.

[km]	**1**	**2**	**3**	**4**	**5**	**6**	**7**
1	0						
2	2.8825	0					
3	2.3394	3.1535	0				
4	1.9911	4,8737	3.4704	0			
5	4.461	7.3088	5.2187	2.5366			
6	5.0739	7.1747	7.3157	4.2135	5.139	0	
7	3.4563	3.2841	5.3733	4.7446	7.1819	4.778	0

Table B.4: Listing of the time periods.

	Time Period
1	2018
2	2020
3	2022
4	2024
5	2026
6	2028
7	2030
8	2032
9	2034
10	2036
11	2038
12	2040
13	2042
14	2044
15	2046
16	2048
17	2050

B.2 Technical Characteristics

In this section the technical characteristics for all technology units are provided. This concerns the conversion efficiencies, the conversion, storage, supply and network capacities, the standing and transport losses and the development rates.

Table B.5: The conversion efficiency values specified for all conversion units and energy types.

Energy type 1	Energy type 2	Conversion unit	Efficiency
Electricity	Electricity	CHP	0
Electricity	Gas	CHP	0.36
Electricity	Heat	CHP	0
Gas	Electricity	CHP	0
Gas	Gas	CHP	-1
Gas	Heat	CHP	0
Heat	Electricity	CHP	0
Heat	Gas	CHP	0.54
Heat	Heat	CHP	0
Electricity	Electricity	HP	-1
Electricity	Gas	HP	0
Electricity	Heat	HP	0
Gas	Electricity	HP	0
Gas	Gas	HP	0
Gas	Heat	HP	0
Heat	Electricity	HP	4
Heat	Gas	HP	0
Heat	Heat	HP	0
Electricity	Electricity	P2G	-1
Electricity	Gas	P2G	0
Electricity	Heat	P2G	0
Gas	Electricity	P2G	0.55
Gas	Gas	P2G	0
Gas	Heat	P2G	0
Heat	Electricity	P2G	0
Heat	Gas	P2G	0
Heat	Heat	P2G	0

Table B.6: The maximum storage charge capacity and the standing losses factor specified for all three storage unit types, with which the stored capacity is multiplied to calculate the stored capacity after a one-year time period.

Storage type	Max. storage charge capacity (PJ)	Standing loss factor
Electricity	0.0000288	0.04
Gas	0.36	0.998
Heat	0.0108	0.9

Table B.7: The development rates specified for all technology unit types. The development rates with a value > 0.02 are considered as uncertainty. The uncertainty value input is specified in Appendix D.

Technology unit	Development rate
Wind supply	0.022
PV supply	0.05
Electricity storage	0.05
Gas storage	0
Heat storage	0.016
CHP conversion	0
HP conversion	0.01
P2G conversion	0.079
Network (E,G,H)	0

Table B.8: The maximum transport capacity and transport loss factor per one-year time period specified for all three pipeline network types.

Network type	Max. transport capacity (PJ)	Transport loss factor
Electricity	0.179	0.025
Gas	0.123	0.001
Heat	0.284	0.05

Table B.9: The maximum conversion capacity per one-year time period specified for all three conversion units.

Conversion unit	Max. conversion capacity (PJ)	Energy carrier
CHP	0.426	Gas
HP	0.02664	Electricity
P2G	0.397	Electricity

Table B.10: The maximum supply capacity per one-year time period specified for both supply units.

Supply unit	Max. supply capacity (PJ)	Energy carrier
PV	0.309	Electricity
Wind	0.54	Electricity

B.3 Economical Parameters

In this section the initial investment costs for each technology unit are specified. The model does not concern other economical parameters, such as energy price or operation and maintenance costs.

Table B.11: Investment costs per technology unit.

Technology unit	Type	Initial investment costs (MEur)
PV	Supply	3
Wind	Supply	4.5
Electricity	Storage	1.12
Heat	Storage	0.8
Gas	Storage	6
CHP	Conversion	8.19
HP	Conversion	0.75
P2G	Conversion	18
Electricity [MEur/m]	Network	0.65E-4
Heat [MEur/m]	Network	5.5E-4
Gas [MEur/m]	Network	1E-4

B.4 Supply Parameters

The source of supply that is included in the model, besides the renewable energy PV and wind supply that can be invested in, is the natural gas supply. To meet the energy transition goal, this supply is decreased over time to zero in 2050. Due to the real-world constraints of energy entering the (medium-voltage) grid, both the gas supply and the wind supply can only enter the system at locations $2, 3, 4$ and 7.

Table B.12: Total gas supply per location per time period. The locations with gas supply are in correspondence with the real-world situation of this case study.

Time Period	Gas supply [PJ/year] Nodes 2,3,4,7	Gas supply [PJ/year] Nodes 1,5,6
2018	3.13	0
2020	2.86	0
2022	2.61	0
2024	2.37	0
2026	2.13	0
2028	1.91	0
2030	1.69	0
2032	1.48	0
2034	1.28	0
2036	1.09	0
2038	0.91	0
2040	0.73	0
2042	0.57	0
2044	0.41	0
2046	0.27	0
2048	0.13	0
2050	0	0

B.5 End-use Parameters

The end-use parameter for the model is the energy demand specified as the amount of Peta-Joules per energy carrier and time period. The baseline energy demand development, as provided in table B.13, considers a linear change per modelled time step.

Table B.13: The energy demand development. The start- and end year demand over all locations is provided in combination with the percentual change per time-step.

	Change (%/Time-step)	2018	2050
Electricity [PJ/yr]	-0.07%	4.41	4.31
Gas [PJ/yr]	-2.54%	7.01	1.31
Heat [PJ/yr]	0.13%	4.21	4.38
Total [PJ/yr]	-1.13%	15.63	10

Appendix C

Uncertainty Characterization

This Appendix provides more in-depth information of both the top-down analysis and the bottom-up analysis that are executed to characterize uncertainties for the exploratory modelling. This is described in chapter 3.

C.1 Top-Down Analysis

In this section, as part of the top-down analysis, first the three renowned energy system models are introduced that are analyzed. Second, a table is provided which provides an overview of the scenario key themes that are identified from the analysis of the referenced scenario planning studies.

C.1.1 Introduction to IMAGE, PROMETHEUS and TIMES

- **IMAGE**
  IMAGE (Integrated Model to Assess the Global Environment) is an Integrated Assessment Model (IAM) which has been developed under the authority of PBL Netherlands Environmental Assessment Agency, who describe the model as follows: "IMAGE is an ecological-environmental model framework that simulates the environmental consequences of human activities worldwide. It represents interactions between society, the biosphere and the climate system to assess sustainability issues such as climate change, biodiversity and human well-being. The objective of the IMAGE model is to explore the long-term dynamics and impacts of global changes that result from interacting socio-economic and environmental factors." (Netherlands Environmental Assessment Agency, 2014).

  The main drivers of the model are: population, economy, policies, technology, lifestyle and resources. The model is developed at a global scale with a geographic resolution of 26 regions (Marangoni et al., 2017). Different time-steps can be used and the model is run up to 2050 or 2100 depending on the modelling objectives. To explore future

scenarios, exogenous assumptions are made for a range of factors that shape the development of key model variables and results. IMAGE explicitly considers data uncertainty in 21 categories, of which 6 are potentially relevant for the model under analysis (table 3.1). Due to IMAGE being a non-energy system specific global model that describes a set of global environmental issues and sustainability challenges, the remaining categories mainly concern (aquatial) biodiversity, land-use and atmospheric composition uncertainties, which are out of the scope of this research.

- **PROMETHEUS**
  The PROMETHEUS model is developed by the E3MLab/ICCS at National Technical University of Athens. It is designed to provide medium (up to 2050) and long term (up to 2100) energy system projections. The model covers the global energy system, but can support impact assessment of specific energy and environment policies and measures applied at the regional and global level. This is thanks to the identification of 10 regions. The PROMETHEUS model incorporates a recursive dynamic (limited-foresight) decision-making time horizon with annual resolution (E3MLab/ICCS, 2017).

  PROMETHEUS is a self-contained large-scale world stochastic energy demand and supply model consisting of a large set of stochastic equations describing the time evolution of key variables, which are of interest in the context of a general analysis of the energy-environment-economic system (table 3.1).

- **TIMES**
  TIMES (The Integrated MARKAL-EFOM1 System) is an economic model generator for local, national, multi-regional, or global energy systems (Loulou et al., 2016). The model provides a technology-rich basis for estimating energy system dynamics over a multi-period time horizon (2010−2100), without necessarily being able to say anything about the likeliness of these evolutions (Pfenninger et al., 2014). TIMES evolved from the MARKAL model, which was used by the UK government to assess various scenarios in both explorative and normative contexts, following integration of MARKAL with a related optimization model (McCallum et al., 2019). TIMES remains the principal tool for energy planning in the UK and Pfenninger et al. state that it is possibly the most widely used general purpose energy systems model. The entire MARKAL/TIMES family is developed by the IEA ETSAP, which is a consortium of researchers from IEA member countries, with the mission to maintain energy systems modeling capacity amongst its members (Pfenninger et al., 2014).

  TIMES is an originally linear, but now also including MILP, optimization model to minimize total energy system cost. Of the energy systems are included; the supply sector, power generation sector and demand sectors. The scope of the model extends beyond purely energy-oriented issues, to the representation of environmental emissions, and perhaps materials, related to the energy system. In addition, the model is suited to the

analysis of energy-environmental policies (Loulou et al., 2016). In this TIMES documentation, four types of uncertainty scenario inputs are described (table 3.1).

C.1.2 Scenario Planning Studies Key Themes

Table C.1 provides an overview of the scenario key factors resulting from the analysis of scenario planning studies as part of the top-down analysis.

C.2 Bottom-Up Analysis

In this section, table C.2 lists the model-parameters that are considered to be subject to uncertainty as part of the bottom-up analysis.

Table C.1: The scenario key factors resulting from analysis of nine scenario analysis studies.

Scenario Key Factor	Description	Source
Topology of power plants	Spatial distribution and size of power plants.	Witt et al. (2020)
Energy mix	The shares of renewable and fossil energies in the net electricity generation.	Witt et al. (2020); Cole et al. (2018); Mcdowall et al. (2014)
Levelized cost of electricity	The future development of the levelized costs of electricity for both renewable and fossil energies.	Witt et al. (2020); Cole et al. (2018); Mcdowall et al. (2014); Xu et al. (2019); Huber et al. (2004)
Power grid	The nature of the power grid (power lines or controllable equipment etc.)	Witt et al. (2020)
Digitization in the distribution grid	The level of digitization in the distribution grid	Witt et al. (2020)
Energy management	The diffusion of energy management systems in private households and industry.	Witt et al. (2020); Mcdowall et al. (2014); Huber et al. (2004)
Energy demand	The energy demand from private households. Is dependent on the consumer behavior and number of electric devices per capita.	Witt et al. (2020); Mcdowall et al. (2014); Huber et al. (2004); Van Vuuren et al. (2012)
Economy and its energy demand	The energy intensity and growth of the economy.	Witt et al. (2020); Mcdowall et al. (2014); Huber et al. (2004); Van Vuuren et al. (2012); Xu et al. (2019)
Energy policy and international coordination	Reflects national and international developments in energy policy.	Witt et al. (2020); Cole et al. (2018); Mcdowall et al. (2014); Xu et al. (2019); Huber et al. (2004); Van Vuuren et al. (2012); Bollen and Brink (2014)
Knowledge and perceived control	The knowledge of individuals about and perceived opportunities to control renewable energy technologies in the smart home or smart grid.	Witt et al. (2020); Mcdowall et al. (2014)
Acceptance	The acceptance of renewable energy technologies on both individual and societal levels as a function of cost-benefit ratios.	Witt et al. (2020); Mcdowall et al. (2014)
Population		Mcdowall et al. (2014); Xu et al. (2019); Van Vuuren et al. (2012)
RES technology advancements beyond PV & wind	The potential for RE technologies beyong solar photovoltaics (PV) and land-based wind.	Cole et al. (2018); Mcdowall et al. (2014)
Technology development	Energy intensity, energy efficiency, conversion technology, storage capacity etc.	Van Vuuren et al. (2012); Mcdowall et al. (2014)
GHG emission		Van Vuuren et al. (2012); Mcdowall et al. (2014)

Table C.2: Model inherent parameters of which the value is potentially subject to external uncertainties.

Parameter	Description	Type	Unit
Energy demand	Energy demand per timeslot per node per carrier. Influenced by the demand energy mix and the demand share per node.	Timeseries	PJ/year
Development rate	The rate with which the initial investment costs change in addition to the standard discount rate representing the decreased cost/technological performance ratio as a result from technology-specific technological development.	Constant	dmnl
Conversion potential	The maximum production per conversion unit as a result from one investment made.	Constant	PJ/year
Storage potential	The maximum energy that can be stored per storage unit as a result from one investment made.	Constant	PJ
Supply potential	The energy supply that is generated from a wind or PV supply unit per node as a result from one investment made.	Constant	PJ/year
Transport potential	The maximum capacity of a pipeline specified per energy carrier as a result from one investment made.	Constant	PJ/year
Transport losses	The loss factor of pipeline energy transport specified per energy carrier.	Constant	dmnl
Gas supply	The energy supplied in the form of gas per node.	Timeseries	PJ/year
Conversion efficiency	The conversion efficiency per conversion unit.	Constant	PJout/PJin
Standing losses	Loss of energy per storage unit	Constant	%/year
Discount rate	The rate used to determine the present value of future cash flows.	Constant	dmnl

Appendix D

Uncertainty Model Input

In this appendix, the uncertainty ranges for the parameters that are considered as uncertainties are specified. This concerns the energy demand development, the discount rate and the development rates for PV and wind supply, electricity storage and P2G conversion technology. The 'original' values for these uncertain model input parameters are provided in appendix B.

D.1 Demand Development Scenarios

The energy demand development scenarios are established based on three aspects: the height of the total demand in 2050, the energy mix in 2050 in terms of the reliance on gas, electricity and heat respectively, and the curve of the demand development towards 2050 (figure tab:QualDemand). This analysis resulted in 12 specified demand development scenarios of which the properties are provided in table D.2. The actual implications of these demand development scenario properties are quantitatively provided in table D.3 and are visualized in figure D.1.

Table D.1: Qualitative description of the demand scenarios.

	Scenario	Demand development	Energy mix	Demand development curve
1	Baseline	Baseline demand decrease. Increased population and energy efficiency.	Phase-out of gas reliance. Increased heat and electricity reliance due to shift from gas to heat and shift to electrical vehicles.	Currently existing climate and energy policy targets and actions are realized with no new policy measures introduced.
2	Very high demand	No demand change. Increased population and limited increased energy efficiency.	Phase-out of gas reliance.	Currently existing climate and energy policy targets and actions.
3	Very low demand	Very high demand decrease. Decreased population and high increased energy efficiency.	Phase-out of gas reliance.	Currently existing climate and energy policy targets and actions.
4	High demand	Some demand decrease. Some increase in population and energy efficiency	Phase-out of gas reliance.	Currently existing climate and energy policy targets and actions.
5	Low demand	High demand decrease. Some decrease in population and increased energy efficiency.	Phase-out of gas reliance.	Currently existing climate and energy policy targets and actions.
6	High E, Low G, Low H	Baseline demand decrease.	Strong phase out of gas reliance. Limited heat reliance. Strong shift to electrical vehicles.	Currently existing climate and energy policy targets and actions.
7	Low E, Low G, High H	Baseline demand decrease.	Strong phase out of gas reliance. Strong heat reliance. Limited shift to electrical vehicles.	Currently existing climate and energy policy targets and actions.
8	Low E, High G, Low H	Baseline demand decrease.	Limited phase-out of gas reliance. Limited shift from gas to heat or to RES.	Currently existing climate and energy policy targets and actions.
9	Very low E, Very high G, Very low H	Baseline demand decrease.	Continued gas reliance. No shift from gas to heat or to RES.	Currently existing climate and energy policy targets and actions.
10	Fast change	Baseline demand decrease.	Fast phase-out of gas reliance towards heat and electricity.	Currently existing climate and energy policy targets and actions are realized and implemented quicker due to societal/politcal pressure.
11	Very fast change	Baseline demand decrease.	Very fast phase-out of gas reliance towards heat and electricity.	Currently existing climate and energy policy targets and actions are realized and implemented very quickly due to large societal/politcal pressure.
12	No change compared to 2018	No demand change.	Continued gas reliance. No shift from gas to heat or to RES.	No curve

Table D.2: Quantitative description of the demand development scenarios.

Scenario	Total demand (2050) [PJ/y]	Demand energy mix (2050) [%]	Demand curve
1 (Original)	10	Elec 43%, Gas 13%, Heat 44%	Linear
2	15	Elec 43%, Gas 13%, Heat 44%	Linear
3	5	Elec 43%, Gas 13%, Heat 44%	Linear
4	12.5	Elec 43%, Gas 13%, Heat 44%	Linear
5	7.5	Elec 43%, Gas 13%, Heat 44%	Linear
6	10	Elec 54%, Gas 11%, Heat 35%	Linear
7	10	Elec 35%, Gas 11%, Heat 55%	Linear
8	10	Elec 33%, Gas 34%, Heat 33%	Linear
9	10	Elec 27%, Gas 45%, Heat 28%	Linear
10	10	Elec 43%, Gas 13%, Heat 44%	Exponential
11	10	Elec 43%, Gas 13%, Heat 44%	S-shaped
12	16	Elec 28%, Gas 45%, Heat 27%	Constant

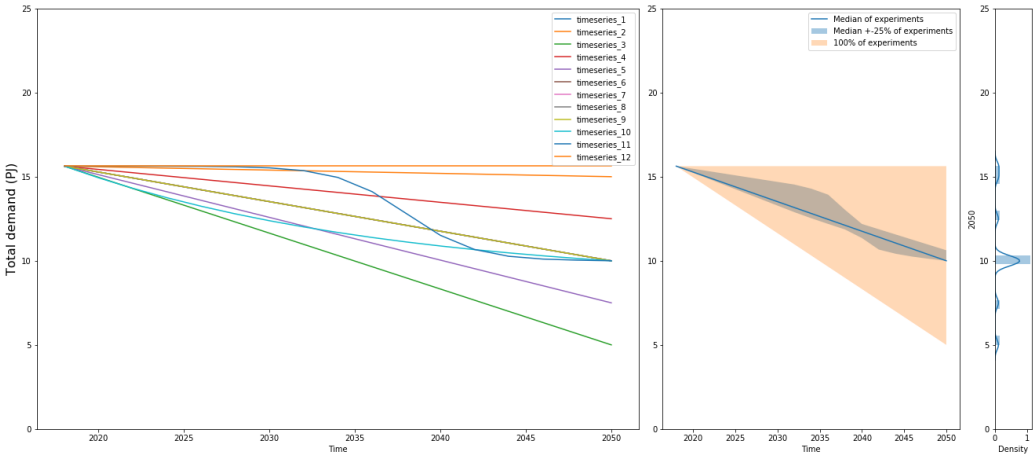

Figure D.1: Line plot of the demand development over time for each timeseries used in the experiments. The middle figure is an envelope plot and the right figure shows the probability density plot.

Table D.3: The demand development scenarios. Provided are the start- and final total demands for all locations and the percentual change per time-step.

Scenario 1: Baseline	**Change (%/Time step)**	**2018**	**2050**
Scenario 2: Very high demand			
Electricity	1.46%	4.41	6.47
Gas	-2.25%	7.01	1.97
Heat	1.75%	4.21	6.57
Total [PJ/yr]	-0.13%	15.63	15
Scenario 3: Very low demand			
Electricity	-1.60%	4.41	2.16
Gas	-2.83%	7.01	0.66
Heat	-1.50%	4.21	2.19
Total [PJ/yr]	-2.13%	15.63	5
Scenario 4: High demand			
Electricity	0.69%	4.41	5.39
Gas	-2.39%	7.01	1.64
Heat	0.94%	4.21	5.48
Total [PJ/yr]	-0.63%	15.63	12.5
Scenario 5: Low demand			
Electricity	-0.83%	4.41	3.23
Gas	-2.69%	7.01	0.98
Heat	-0.69%	4.21	3.29
Total [PJ/yr]	-1.63%	15.63	7.5
Scenario 6: High E, Low G, Low H			
Electricity	0.69%	4.41	5.39
Gas	-2.65%	7.01	1.06
Heat	-0.49%	4.21	3.55
Total [PJ/yr]	-1.13%	15.63	10
Scenario 7: Low E, Low G, High H			
Electricity	-0.83%	4.41	3.23
Gas	-2.43%	7.01	1.56
Heat	0.74%	4.21	5.21
Total [PJ/yr]	-1.13%	15.63	10
Scenario 8: Low E, High G, Low H			
Electricity	-0.79%	4.41	3.29
Gas	-1.63%	7.01	3.36
Heat	-0.64%	4.21	3.35
Total [PJ/yr]	-1.13%	15.63	10
Scenario 9: Very low E, Very high G, Very low H			
Electricity	-1.19%	4.41	2.74
Gas	-1.13%	7.01	4.48
Heat	-1.06%	4.21	2.78
Total [PJ/yr]	-1.13%	15.63	10
Scenario 10: Fast change	Exponential		
Electricity		4.41	4.31
Gas		7.01	1.31
Heat		4.21	4.38
Total [PJ/yr]		15.63	10
Scenario 11: Very fast change	S-shaped		
Electricity		4.41	4.31
Gas		7.01	1.31
Heat		4.21	4.38
Total [PJ/yr]		15.63	10
Scenario 12: No change compared to 2018			
Electricity	0%	4.41	4.41
Gas	0%	7.01	7.01
Heat	0%	4.21	4.21
Total [PJ/yr]	0%	15.63	15.63

D.2 Development Rates and Discount Rate

The specified uncertainty ranges for the development rates and the discount rate are provided in table D.4. As pointed out before, the development rates are technology-specific. It was decided to only incorporate the development rates with a 'base'-value of >= 2% (table B.7). Following the example of Moallemi et al. (2017), a range of minus-plus 50% of the estimated (base) value is assumed as the uncertainty range for the development rates. For the discount rate, the range of minus-plus 50% of the estimated (base) value (Moallemi et al., 2017) is expanded to a range between 1% and 15%.

Table D.4: The 'base values' and lower and upper bound for the uncertainty ranges for the uncertain development rates (DR) and for the discount rate.

Uncertainty	**'Base value'**	**Lower bound**	**Upper bound**
DR wind supply	0.022	0.022	0.033
DR PV supply	0.05	0.025	0.075
DR E storage	0.05	0.025	0.075
DR P2G conversion	0.079	0.0395	0.1185
Discount Rate	0.04	0.01	0.15

Appendix E

Experiment Set-Up

E.1 Optimality Gap

First, due to the different uncertainty input combinations per experiment run, the computation time to reach a specified optimality gap varies between experiments (figure E.1). This figure clearly depicts that the specification of a *lower* optimality gap, thus *improved* results in terms of distance between the 'optimal' result and the best bound, results in *extended* computation time and a *decreased* percentage of all experiment runs which are solved to optimality.

The comparability of experiments is vital in the proposed method. It is argued that comparing experiment outcomes which have reached the same optimality gap value, and thus have comparable relative deviation from the *best bound*, is better substantiated than comparing experiment outcomes with varying optimality gaps. Therefore, it is important to reach an as high as possible percentage of experiments solved to optimality.

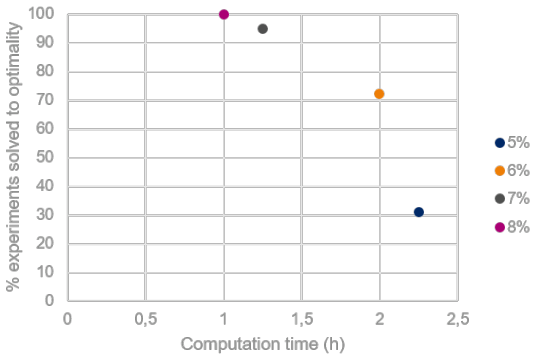

Figure E.1: The % of experiments solved to optimality under what total computation time for 100 experiments with a stopping condition of the specified optimality gap in combination with a maximum computation time of 300 s. per experiment.

Appendix F

Supporting Material: Energy System Design Clusters

In this appendix, supportive figures are given for the proof of concept method application to an existing Energy System Optimization Model, as described in chapter 5. The results of the global sensitivity analysis are not provided here, as the feature scoring visualization in figure 5.10 provide sufficient insight.

F.1 Visualization of the Cosine Distance Matrices

As elaborated upon in chapter 2 and section 5.1, the similarity between the total designs resulting from the experiments is represented with a cosine distance measure. In this section the number of investments per design component represents the amount of energy invested in, because this value is causally related to the capacity [PJ] invested in.

The functionality of the cosine distance measure is presented by calculating the cosine distance between experiments for the total modelling output (figure F.1a), and the total output aggregated to each specific design component: technology type (figure F.1b), location (figure F.1c) and time period (figure F.1d). The cosine distance matrices, that contain the cosine distance value between all 800 experiments, is presented in the form of a seaborn heatmap (figure F.1). A higher distance is depicted more 'yellow' on the heatmap. Thanks to this color coding, the existence of potential clusters of experiments with a low distance to each other is distinguished.

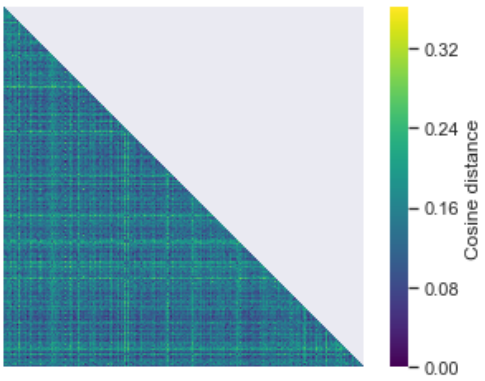

(a) Total model output

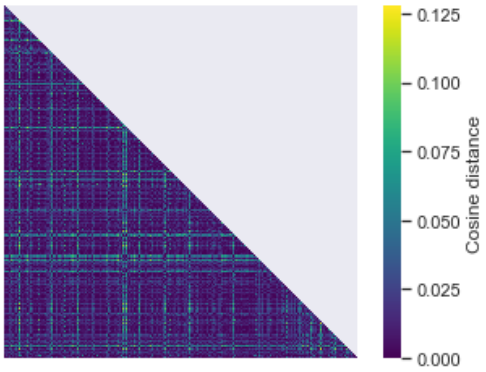

(b) Technology unit aggregation

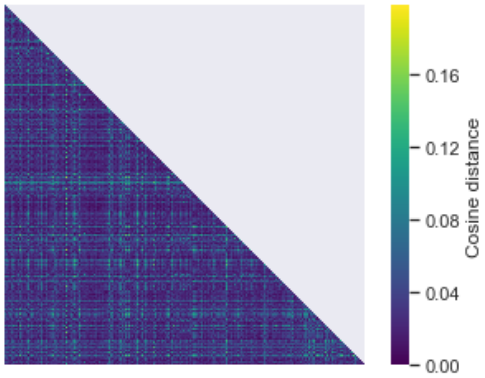

(c) Location aggregation

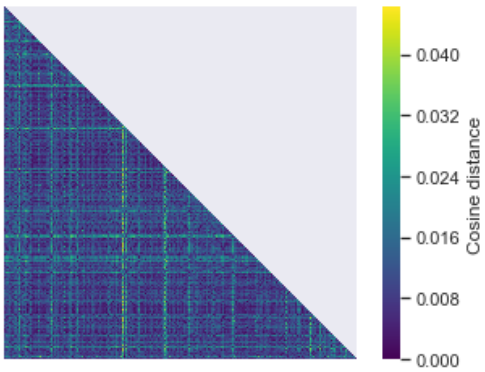

(d) Time period aggregation

Figure F.1: Visualization of the cosine distance values between all experiment outputs for the total design (a) and the total design aggregated to each design specific: technology type (b), location (c) and time period (d).

The low value of the highest cosine distance in the design aggregated to time period indicates that the experiments portray the lowest variation in time period of investment. This is however due to the distorting character of the high number of investments in the first time period, which diminishes the variation between the number of investments in the following time periods.

F.2 Agglomerative Hierarchical Clustering

Each of the four produced cosine distance matrices, of the total output (figure F.2a), and of the total output aggregated to each specific design component: technology type (figure F.2b), location (figure F.2c) and time period (figure F.2d), are clustered with an agglomerative clustering algorithm. The resulting clusters are visualized as a dendrogram (figure F.2). For the visualization of the number of clusters, the default linkage distance value threshold is used, as

explained in section 5.1.

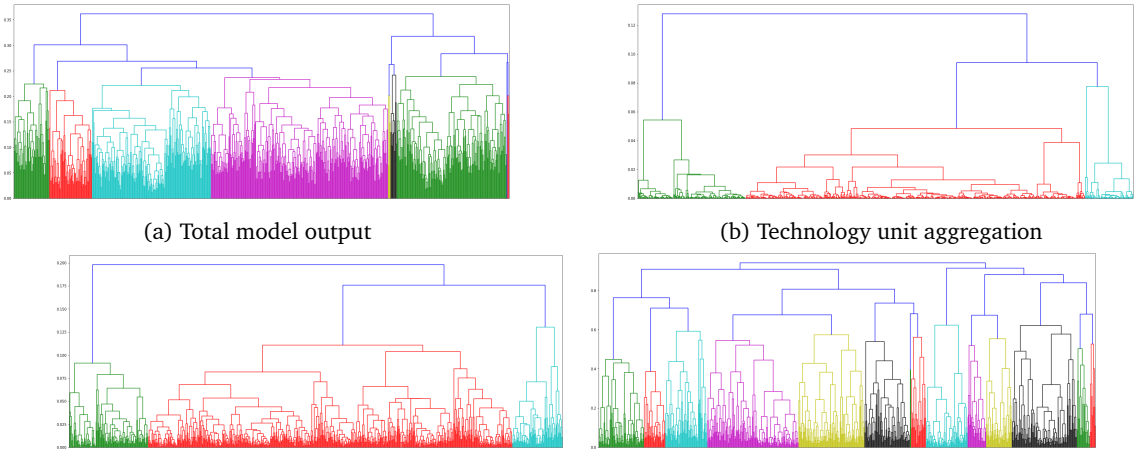

(a) Total model output

(b) Technology unit aggregation

(c) Location aggregation

(d) Time period aggregation

Figure F.2: Visualization of the hierarchical agglomerative clustering of the cosine distance matrices with 'complete' linkage between all experiment outputs for the total design (a) and the design aggregated to each specific design component: technology type (b), location (c) and time period without 2018 (d).

F.3 CART Tree of the Cluster Subspace Partitioning

In this section, a detailed version of the CART Tree is provided (figure F.3). A simplified version of this tree is visualized in figure 5.4. This tree reveals the underlying uncertainty input ranges resulting in the total of nine clusters of similar designs. This tree is the result of the CART subspace partitioning algorithm in CLASSIFICATION mode. This algorithm relates the uncertainty input of each of the 800 experiment runs to the resulting 800 experiment outputs, to which a cluster label $(1, 2, ..., 9)$ is assigned.

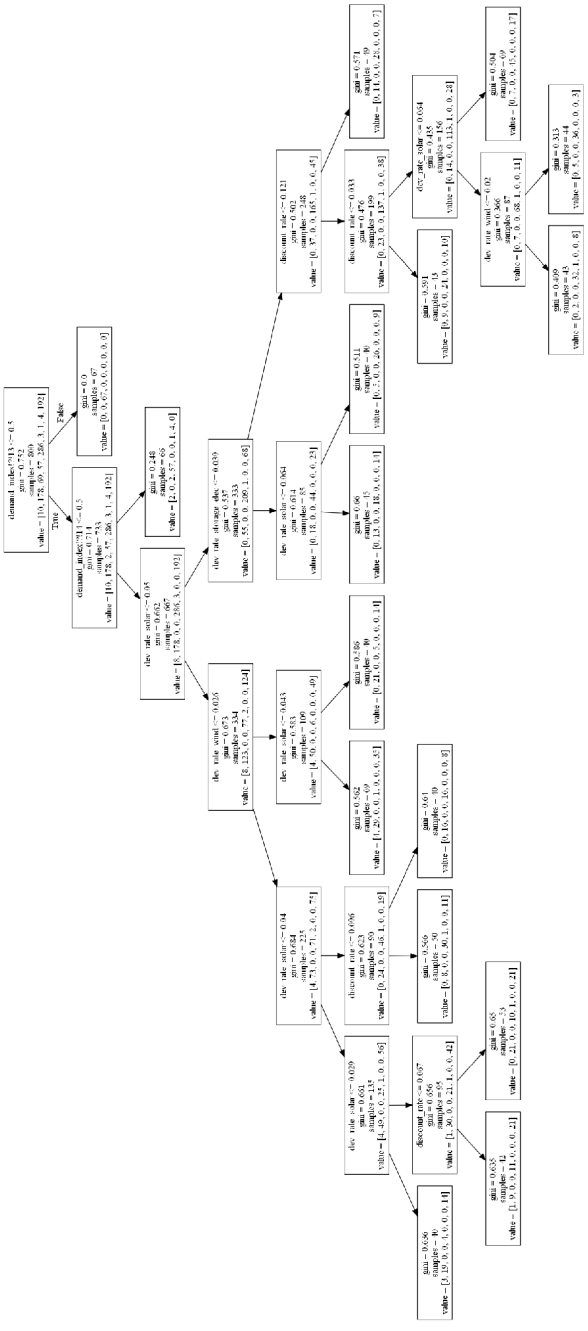

Figure F.3: CART tree resulting from subspace partitioning in CLASSIFICATION mode on the similar energy system design clusters.

Appendix G

Similar Design Cluster Characterization

In this Appendix, an elaborate characterization of the similar cluster designs is provided, according to which the total outcome space of 800 experiments is clustered. This clustering is performed based on a cosine distance matrix, which is provided as input into an agglomerative hierarchical clustering algorithm with complete linkage. The underlying uncertainties that result in the clusters, are identified with CART subspace partitioning (figure 5.4).
The specific cluster design characteristics are identified by aggregating the total design to the three design specifics. The difference in median values between the clusters is visualized with seaborn heatmaps (technology type (figure 5.5), location (figure 5.6) and time period (figure 5.7)). Remarkable cluster design characteristics are interpreted by comparing the median values between the clusters and with the non-clustered characteristics.

Each of these clusters characterizations is presented briefly in table 5.1.

Cluster 1

Cluster 1 contains 178 experiments and it stems from all but two demand scenarios (not 11 and 12) and a PV development rate of lower than or equal to 0.05. *It is characterized by high CHP and low gas storage and network investments.* Also, the P2G and PV are lower than usual and the wind supply investments are slightly increased. Corresponding with the sensitivity analysis, the wind supply development rate is of less importance to the higher wind and lower PV supply investments compared to the PV development rate. Network investments are especially high between locations $1-2$, which is due to the high number of CHP conversion unit investments. Non-network investments are relatively low at location 6, which is conform the higher wind investments and the locational constraints associated with this (figure 2.8). Otherwise, the location-wise and time-wise investment distributions are similar to the non-clustered total design.

Cluster 2

Cluster 2 is the largest cluster, with 268 in-cluster experiments. The main underlying uncertainties shaping this cluster are all but two demand scenarios (not 11 and 12), which is similar to cluster 1, yet for this cluster the PV development rate is higher than 0.05. *The main characteristic of cluster* 2 *is the slightly increased PV supply investments.* Although the HP conversion investments are increased as well, this characteristic is less reliable due to the high HP-specific Inter Quantile Range. Also, the electrical storage development rate is above 0.039. This high PV development rate range induces the higher PV supply investments. The demand scenarios underlying this cluster, mostly concern a decrease in gas reliance. Consequently, the electrical energy supply is required to meet the electricity demand and is not to be converted to gas. Despite the high electricity storage development rate range underlying this cluster, investments are not performed in electrical storage units, due to its unprofitable assets (section 5.2.2). Locational and period-of-investment distribution for this cluster are comparable to that of the non-clustered total design. Except for the relatively high investments at location 6, which corresponds to the high electricity demand at that location and the high PV electricity supply investments (table 5.2).

Cluster 3: Early investments

Cluster 3 consist of 69 experiments arises from demand development scenario 11: 'Very fast change'. This scenario represents a delayed and s-shaped change from gas reliance towards electricity and heat reliance. *This design is mainly characterized by the high number of investments performed in* 2024, 2026, 2028 *and* 2032 *after which no more investments are performed.* Also, it is characterized by low investments in P2G and CHP conversion and PV supply and high investments in gas storage. This scenario, where the gas reliance decreases slower than the gas supply, causes increased investments in electricity supply, P2G conversion and gas storage in earlier time periods. These ensure sufficient gas supply to meet the demand, until the gas reliance drops after 2032 (figure D.1). The investment peak between 2024 and 2032 is visible in the wind supply investment development over time (figure H.4aa). The P2G investment developments over time portray the cluster of early P2G investments, which remain low (figure H.3a). Location-specific investments for this cluster do not deviate from the non-clustered experiments.

Cluster 4: High gas production with P2G electrical energy conversion from PV supply

Cluster 4 consists of 57 experiments and arises from demand development scenario 12: 'No change compared to 2018'. *This cluster is especially characterized by very high P2G conversion and PV supply investments.* The strongly increased P2G and PV unit investments in this cluster are overwhelmingly placed at location 6 and at locations 2 and 7, with a remarkably low in-cluster variability. This placement corresponds with the percentual demand distribution across locations (table 5.2). The number of investments is relatively high at all locations, approxi-

mately multiplied 1.5 times compared to the non-clustered total design, which is required to meet the continued high energy demand. In order to keep meeting the high future gas demand, electrical PV energy is converted to gas with P2G units, which is stored. Conversely, the investments in CHP conversion units are low, because all produced gas is required to meet the demand. The continued high energy demand in this demand scenario is supported by higher (electricity) network investment located between locations $1-4$ and $5-6$. The seemingly limited placement of network investments compared to the non-clustered total design indicates that the increased technology unit investments is are mainly focused on meeting the increased energy demand at the locations. The high number of investments are predominantly performed in the 2034 time-step, but also in $2024, 2026, 2028$ and $2036-2044$. When comparing this to the investment trajectories over time, the high PV supply unit investments are performed in the first time-period cluster, $2024, 2026, 2028$ (figure H.2a) and the P2G conversion in 2034 and the following time-steps (figure H.3a). This corresponds with the technological P2G development pattern.

Cluster 5

Cluster 5 consists of 192 experiments and, similar to cluster 1, it stems from all but two demand scenarios (not 11 and 12) and a PV development rate of $<= 0.05$. *This design is characterized by high investments in the gas network and low investments in HP conversion units.* It should be noted that one third of the in-cluster experiments arises from a PV development rate > 0.05. It is hypothesized that the underlying demand development scenario for this cluster considers a low heat demand, which would explain the low investments in Heat Pumps and a regular gas demand. The high number of gas network investments in combination with a regular number of P2G investments cannot be explained. Potentially, the cluster size is too large for these demand scenarios to appear dominant with the CART algorithm, whereas the resulting design characteristics do appear. The locational distribution of non-network investments is similar to that of the non-clustered total design. Also, the investment trajectory over time is quite similar to that of the non-clustered total design.

Cluster 6: High wind supply, low PV supply investments

Cluster 6 consists of only 10 experiments and arises mainly from a PV development rate $<= 0.043$ and all but two demand scenarios (not 11 and 12). *This design cluster is characterized by very high wind supply and high P2G investments in combination with low HP, Gas network, PV supply and high Heat network investments*. Three of the in-cluster experiments even arise from the PV development rate $<= 0.029$. The high investments in P2G conversion and the electricity network indicate a high gas demand, which in this exceptional set of experiments is met with wind supply instead of PV supply. This is due to the low PV development rate. It is hypothesized that the underlying demand development scenarios for this cluster are 8 ('Low E, High G, Low H') and 9 ('Very low E, Very high G, Very low H'), which would explain the low investments in Heat Pumps (due to the low heat demand) and the high P2G

investments (due to the high gas demand). The low gas network investments imply that the P2G units are located at the locations with high gas demand. The investment trajectory over time shows strong 'bulks' of investment in 2020, $2026-2030$ and $2036-2044$. Considering the locational placement of non-network investments, the placement is low at locations 1, 5 and 6. This corresponds with the locational constraints for the placement of wind supply units (figure 2.8). It was expected that the number of network investments to especially these constrained locations would increase for high-wind supply reliance. The demand at location 1 is met with increased transport from locations 3 and 4. Due to its low percentual demand, location 5 does not require additional network investments (table 5.2). The high percentual (electricity) demand at constrained location 6 is met with increased transport from location 7. As expected, the network investments between the constrained locations, $1-6$ and $5-6$ are decreased as well.

Appendix H

Supporting Material: Energy System Design Trade-offs

H.1 Correlation Pair plot

In this section, a detailed version of the correlation between design components that are considered to be of interest is visualized (figure H.1). This is a more exact representation of correlation by depicting all experiment data points in the scatter plots. An aggregated version of this correlation matrix is portrayed in figure 5.12. This figure provides additional insight by clearly portraying the discrete character of the following Outcomes of Interest: gas storage capacity invested in, heat storage capacity invested in, Combined Heat and Power capacity invested in, and the HP capacity invested in, to a lesser extent.

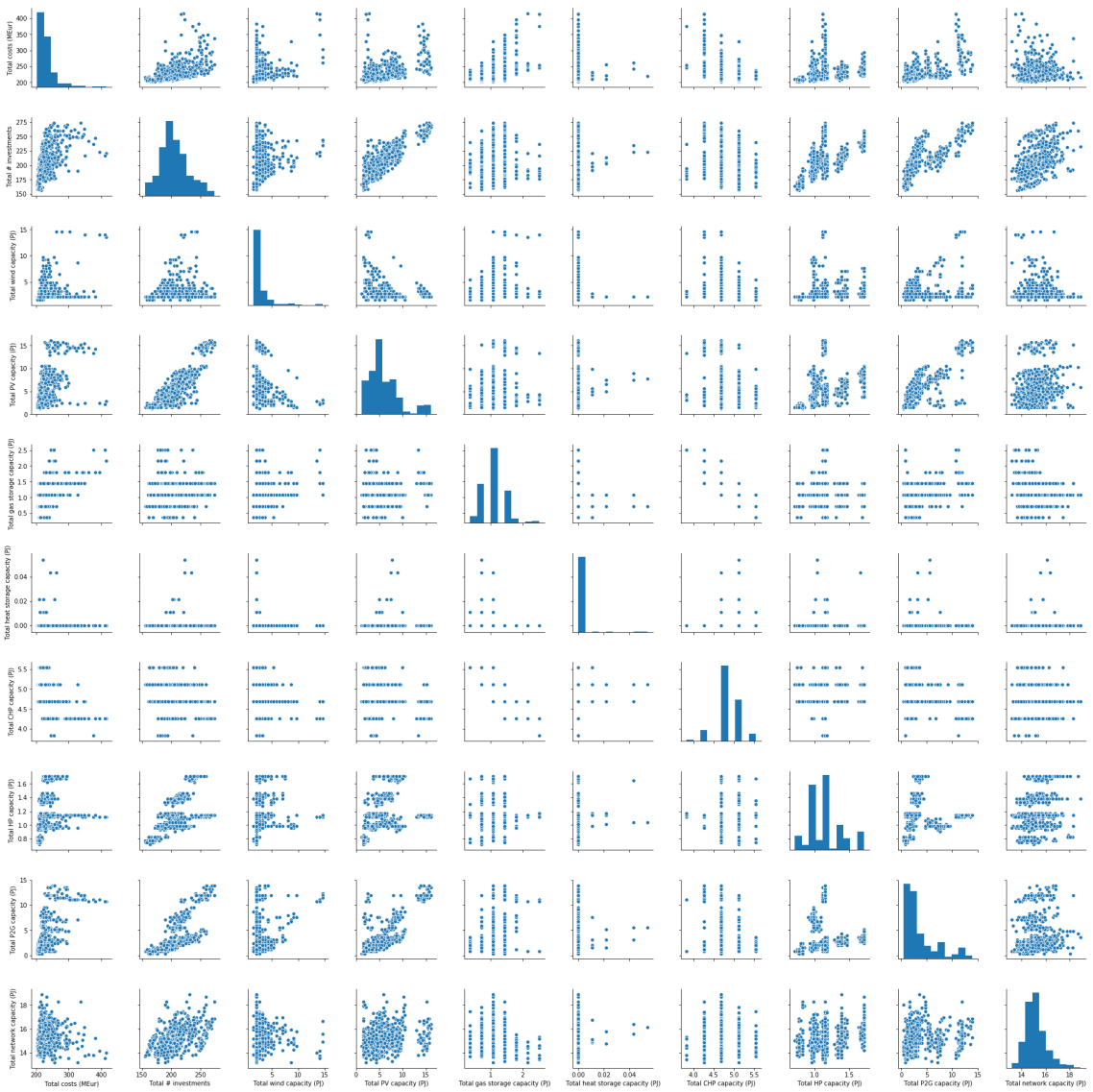

Figure H.1: Pairplot between the outcomes of interest.

H.2 Line Plots and Probability Density Plots for Outcomes of Interest

In addition to the analysis tools used to identify the Energy System Design Trade-offs that are described in section 5.2, line plots and probability density plots are used for this characterization of the technology types present in this proof of concept. Both techniques facilitate the visual identification of interesting patterns for each technology type outcome. Thus this section describes the: PV and wind supply units, network and storage units: electricity, gas and

heat, and the conversion units: Combined Heat and Power (CHP), Power-2-Gas (P2G), and Heat Pump (HP).

The technology type specific design outcomes are visualized as 'zoomed-in' kernel density estimate probability density plots. This probability density plot shows the histogram in combination with the kernel density estimate for the cumulative outcome values over all experiments in the final time period 2050. This visualization is performed to show the *distribution* of cumulative, costs, capacities or number of units invested in per technology type specific design outcome. The probability densities of all plots are capped at a density value of 3 to facilitate comparison across Outcomes of Interest.

In addition to the 'zoomed-in' probability density plots, the Outcomes of Interest are visualized as investment trajectories over time with line plots. This visualization is performed to illustrate *how many* (resulting in what costs and capacity) of *what* (which technology unit) is invested *when* (in which time period). For all line plot visualizations described in this section, the left figure shows the investment trajectory for each experiment over time. The middle figure is an envelope plot visualizing the median, middle 50% (IQR), lower 25% and upper 75% quantiles of the investment trajectory across all experiments to give an impression on the spread of the data. It should be noted that the envelope visualizations give a distorted view of the data distribution and apparent patterns due to its continuous coloring within the quantiles. The right figure shows a (small-sized) probability density plot of the cumulative proportions in the final time period 2050. The upper line plot set depicts the cumulative *costs* over time, the lower set shows the cumulative *capacity* invested in. The costs of investment are visualized because of their importance to decision makers using this model, as part of the objective function to be minimized (figure 2.8). The cumulative costs plots are capped at 40 MEur and the cumulative capacity plots are capped at 25 PJ to facilitate comparison. It should be noted that the median CHP conversion capacity investment costs equals 90 MEuro. This is too high for the general y-axis limit and therefore falls off the axis (figure H.8(a)).

Now, the two technology types showing much variation in their 'final' outcome dispersion are analysed: PV supply and P2G conversion. First, the PV capacity invested in shows a larger variation than the wind supply capacity invested in, which can be recognized by the broad middle 50% quantile range (figure H.2). This is in correspondence with the wide IQR range and the large dependence on the the demand development scenario (table 5.4).

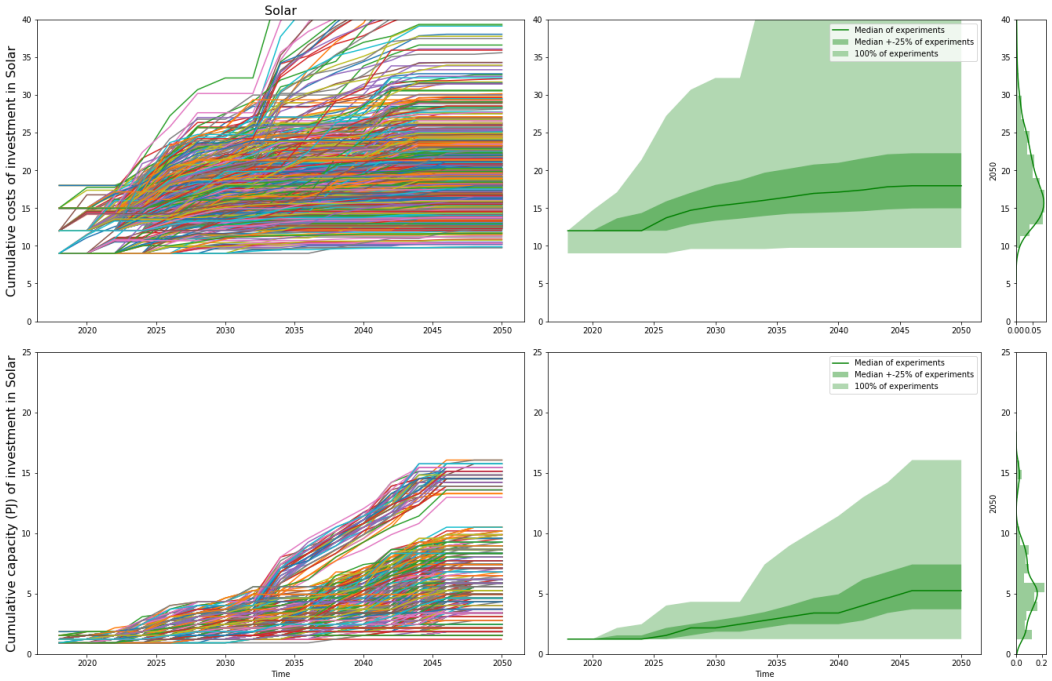

(a) Line plots of the PV investments cumulative costs and capacity over time.

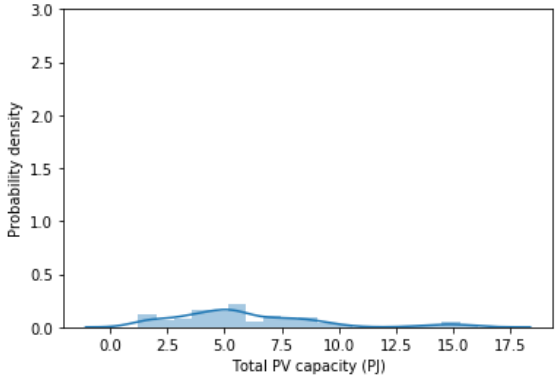

(b) Probability density plot of the cumulative capacity of PV energy.

Figure H.2: Line plots (a) and probability density plot (b) of the PV investments cumulative costs and capacity over time over all experiments.

The P2G conversion unit capacity invested in portrays a continuous distribution with a large variability across experiments (figure H.3(b)). The median capacity value invested in is 2.38 PJ. An interesting observation is that investments in P2G usually start in time period 2030. This is expected to be due to the development rate, which at that time will have reached an acceptable price-performance ratio.

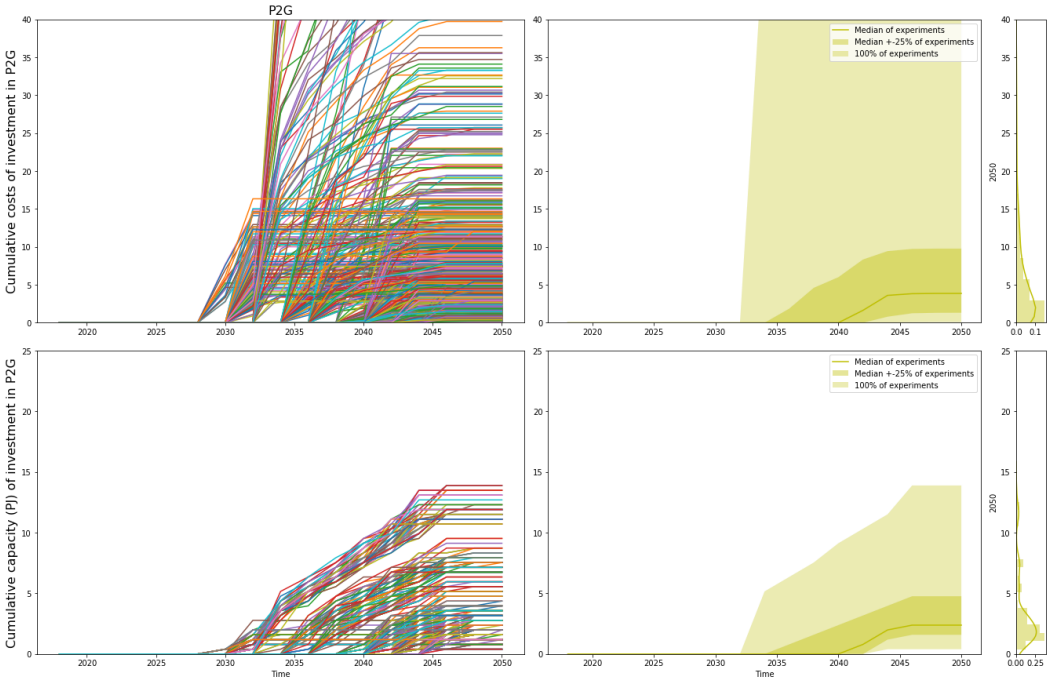

(a) Line plots of the P2G conversion investments cumulative costs and capacity over time.

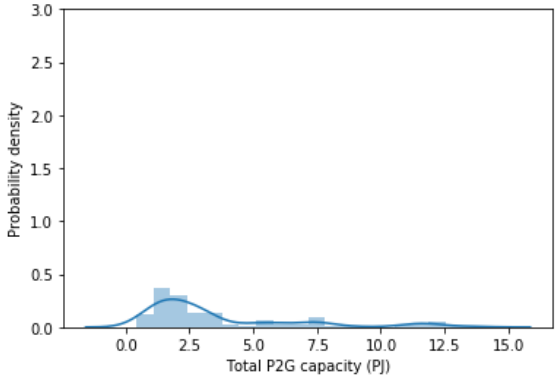

(b) Probability density plot of the cumulative capacity of P2G conversion.

Figure H.3: Line plots (a) and probability density plot (b) of the P2G conversion investments cumulative costs and capacity over time over all experiments.

Now, the Outcomes of Interest portraying very little variation in their 'final' outcome dispersion are discussed: wind supply, gas storage, heat storage, electricity storage, CHP conversion, and HP conversion capacity. Most of these technology units portray investment trajectories that show limited to no development over time: the 'baseload' investments. First, although the wind capacity invested in shows large dispersion in the line plots, the middle 50% experiment outcomes are not higher than the starting value. Consequently, the required wind capacity seems to be quite constant across all experiments. The seven cumulative gas storage capacity

values (figure H.5) exhibit mostly 'flat' capacity developments which are mostly performed in the first time period. The heat storage capacity is non-developing over time as well (figure H.6). Just five cumulative capacity values result from all 800 experiments. The far most prevalent value is 0 PJ, or in other words, no investments made. Lastly, most network investments are 'baseload' investments as the line plots are non-developing (figure H.10(a:c)).

The capacity of wind energy supply invested in peaks quite strongly on a value of around 2 PJ (figure H.4). This is in accordance with the median value of 2.16 PJ and the small data spread (table 5.4). In most experiments, regardless of the uncertainty input, the required wind supply capacity invested in is 2.16 PJ. At least, the required wind supply capacity is 1.62 PJ.

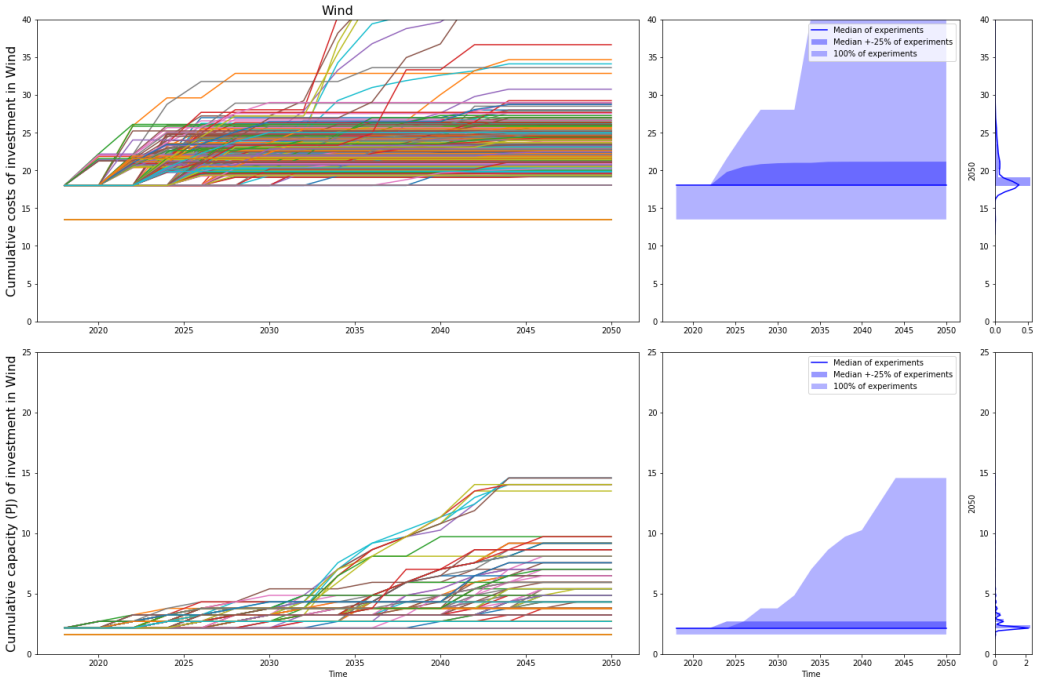

(a) Line plots of the wind investments cumulative costs and capacity over time.

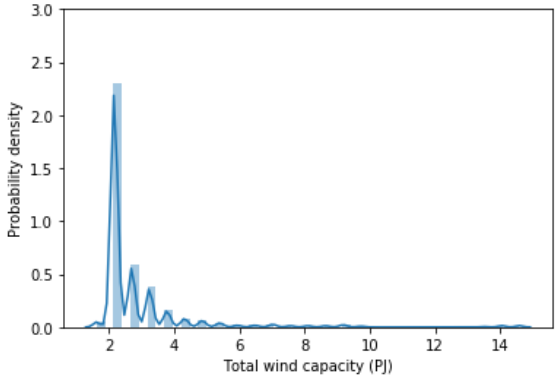

(b) Probability density plot of the cumulative capacity of wind energy.

Figure H.4: Line plots (a) and probability density plot (b) of the wind investments cumulative costs and capacity over time over all experiments.

Second, the gas storage capacity invested in (figure H.5) exhibits a quite discretely distributed probability density plot with only seven cumulative capacity values result from all 800 experiments. The values with the highest probability density being 0.72, 1.44 and especially 1.08 PJ, which is the median value and the Q3 border value as well. Apparently, regardless of the uncertainty values, a gas storage capacity of between 0.72 and 1.44, but mostly 1.08 PJ is required.

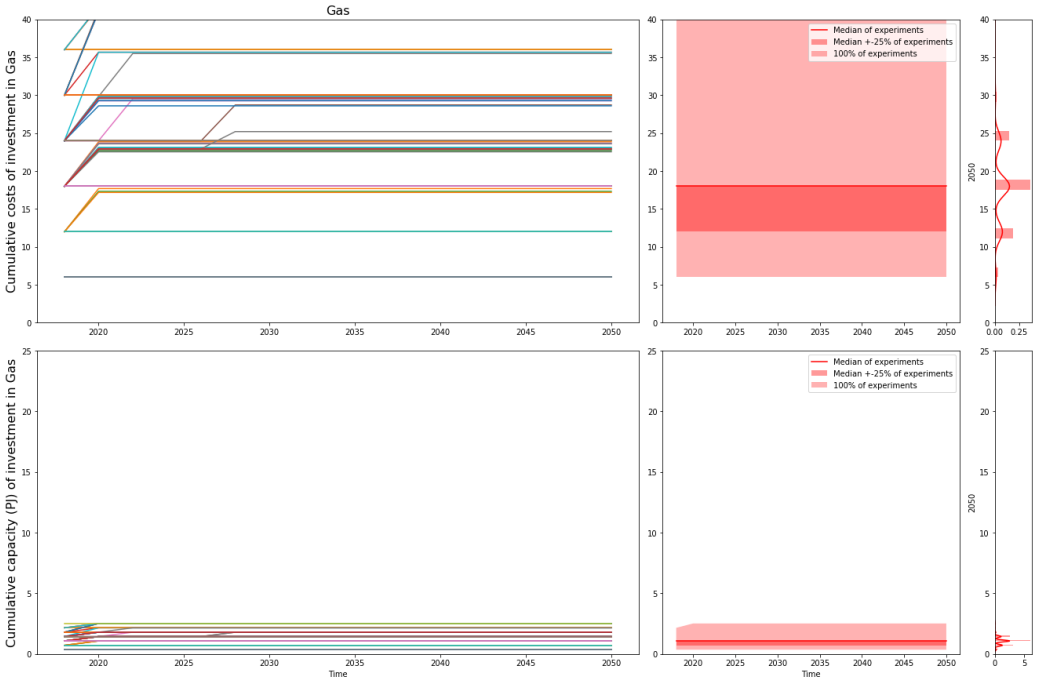

(a) Line plots of the gas storage investments cumulative costs and capacity over time.

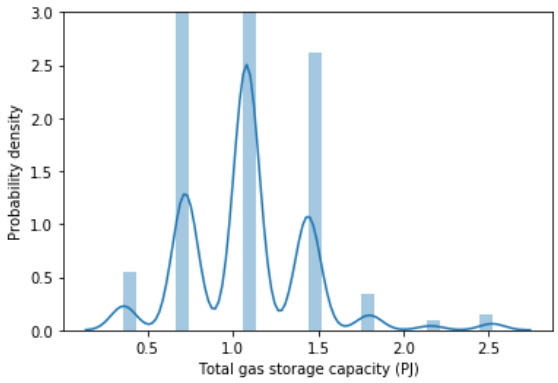

(b) Probability density plot of the cumulative capacity of gas storage.

Figure H.5: Line plots (a) and probability density plot (b) of the gas storage investments cumulative costs and capacity over time over all experiments.

Similar to the gas storage capacity distribution, the heat storage capacity is quite discretely distributed portraying just five cumulative capacity values (figure H.6). The far most prevalent value is 0 PJ, or in other words, no investments made.

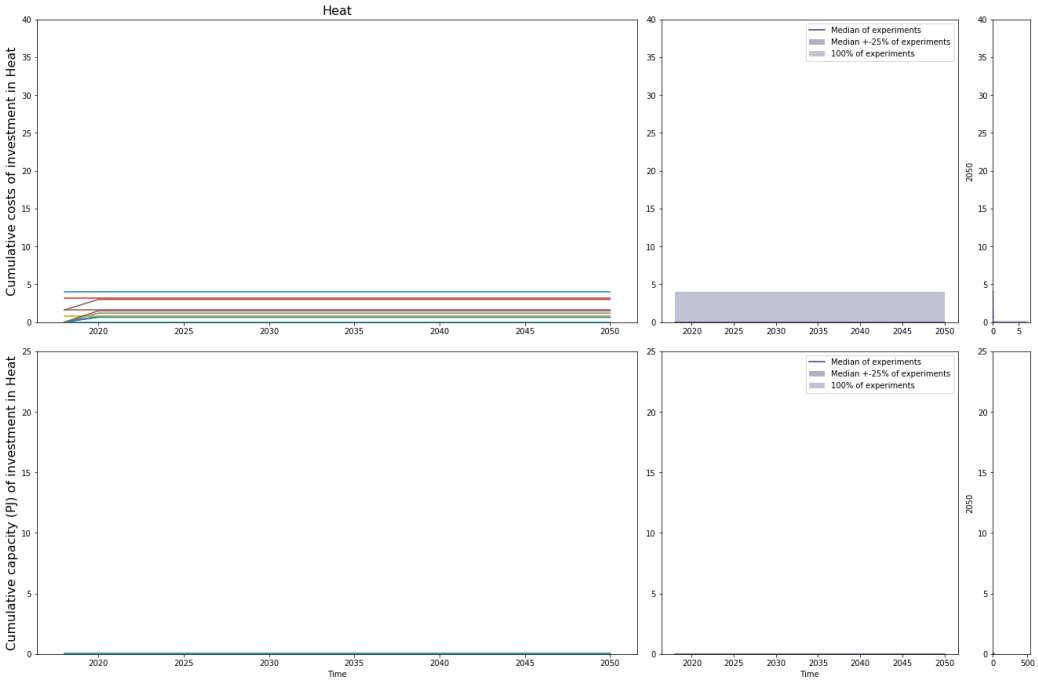

(a) Line plots of the heat storage investments cumulative costs and capacity over time.

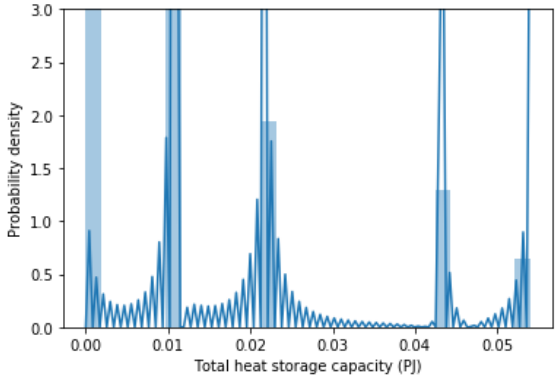

(b) Probability density plot of the cumulative capacity of heat storage.

Figure H.6: Line plots (a) and probability density plot (b) of the heat storage investments cumulative costs and capacity over time over all experiments.

Even more so, the electricity storage capacity invested in portrays the most limited variation in 'final' outcome value across all experiments: no investments are made (figure H.7). Therefore, the electricity storage outcome is excluded from further analysis. The absence of investments in E storage capacity was expected due to the one-year time step used by the model. This causes the storage losses to be 99% over a year, whereas for smaller time steps the storage losses would be smaller. This leaves the electricity storage as a too inefficient unit to invest in.

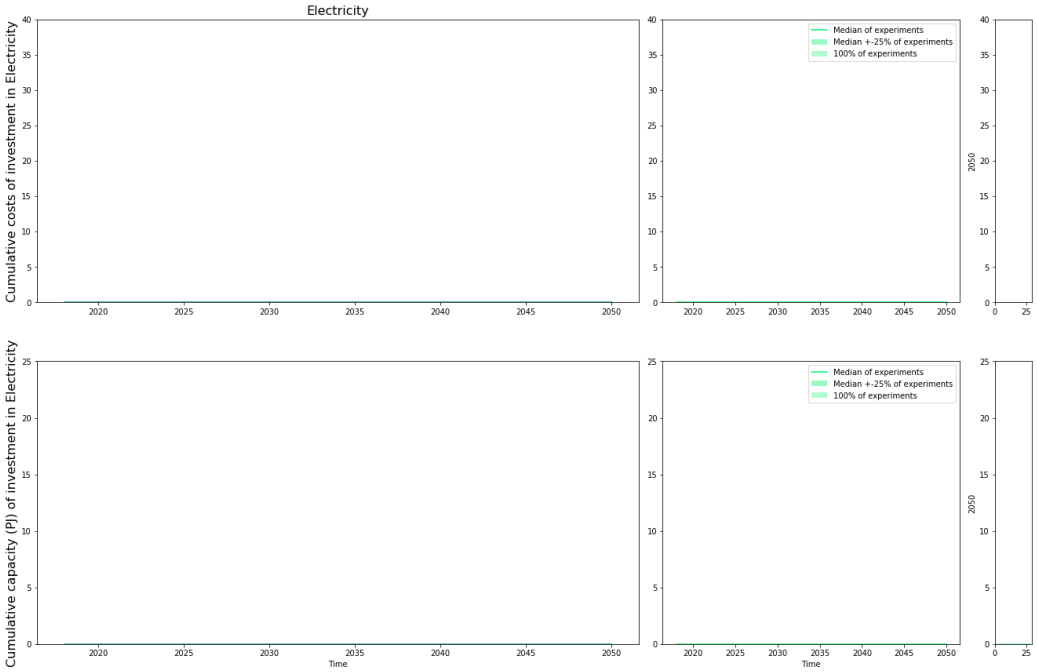

(a) Line plots of the electricity storage investments cumulative costs and capacity over time.

Figure H.7: Line plots (a) of the electricity storage investments cumulative costs and capacity over time over all experiments.

Furthermore, the CHP conversion capacity investment pattern is discretely distributed. In almost all experiments, regardless of the uncertainty input, a CHP capacity of 4.69 PJ is required. Less prevalent, but still highly occurring is the required CHP capacity investment of 5.11 PJ. Regardless, the minimum CHP capacity required is 3.83 PJ.

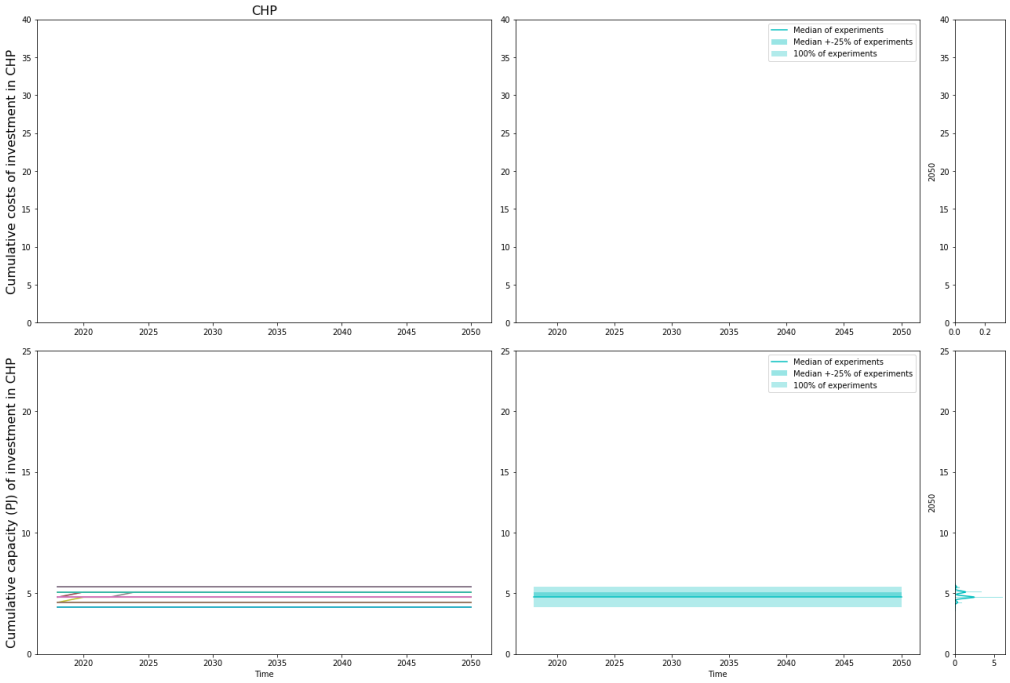

(a) Line plots of the CHP conversion investments cumulative costs and capacity over time.

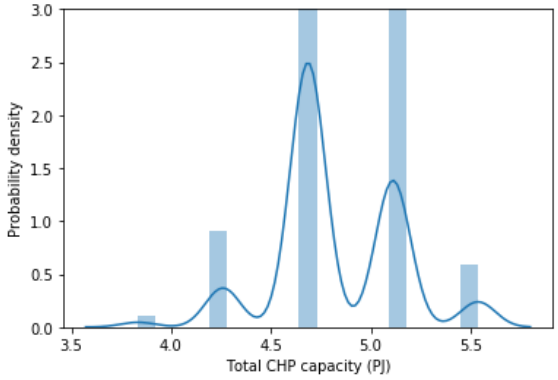

(b) Probability density plot of the cumulative capacity of CHP conversion.

Figure H.8: Line plots (a) and probability density plot (b) of the CHP conversion investments cumulative costs and capacity over time over all experiments.

Also, the HP conversion capacity invested in across all experiments portrays a discrete distribution with limited variance. The lowest and highest capacity invested in differ with only 1 PJ.

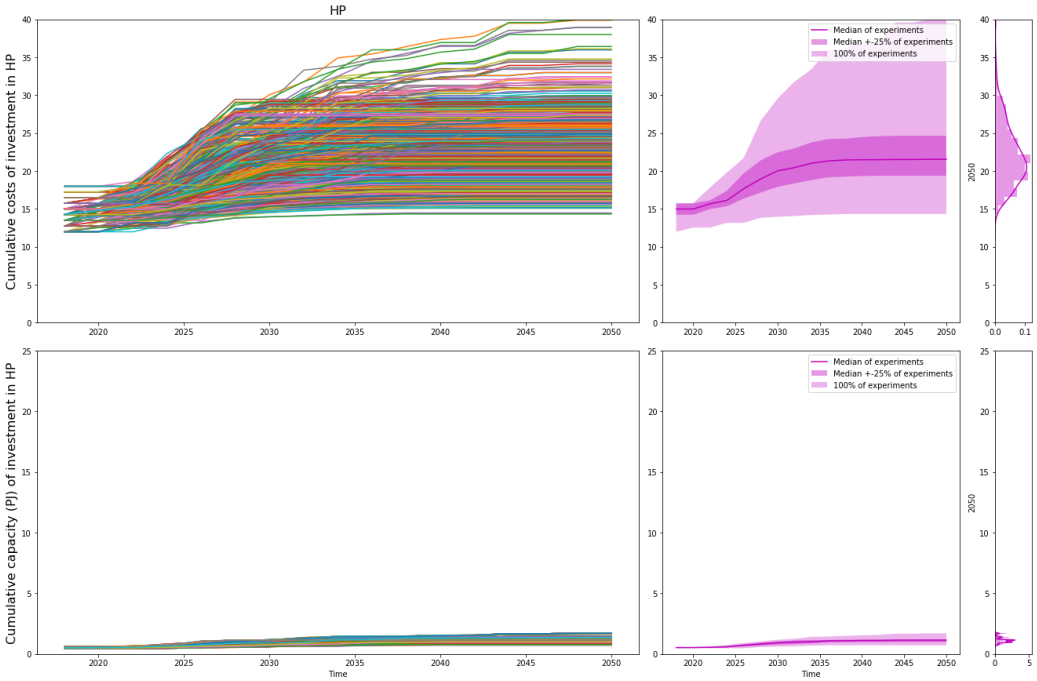

(a) Line plots of the HP conversion investments cumulative costs and capacity over time.

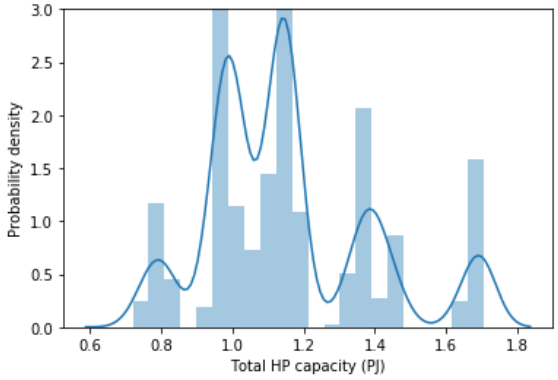

(b) Probability density plot of the cumulative capacity of HP conversion.

Figure H.9: Line plots (a) and probability density plot (b) of the HP conversion investments cumulative costs and capacity over time over all experiments.

Finally, the cumulative network capacity invested in is continuously distributed and does not show large outliers (figure H.10).

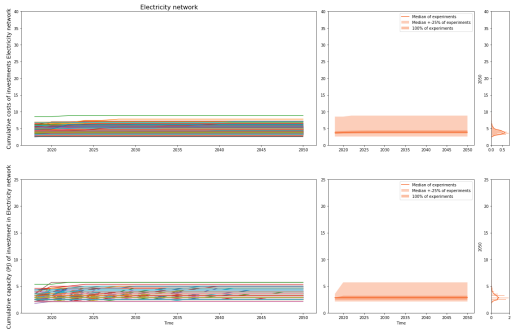

(a) Line plots of the electricity network investments cumulative costs and capacity over time.

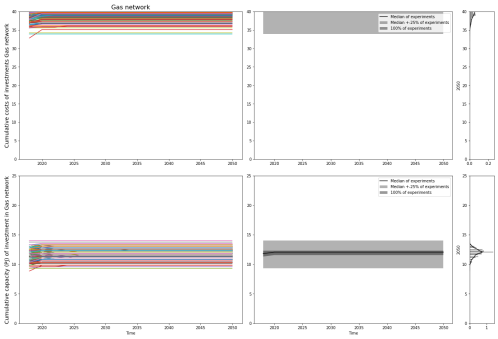

(b) Line plots of the gas network investments cumulative costs and capacity over time.

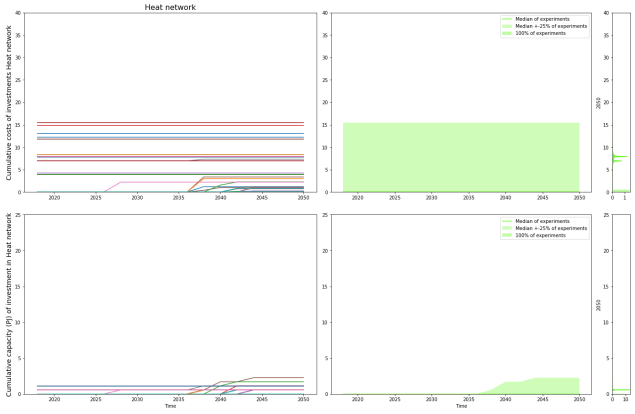

(c) Line plots of the heat network investments cumulative costs and capacity over time.

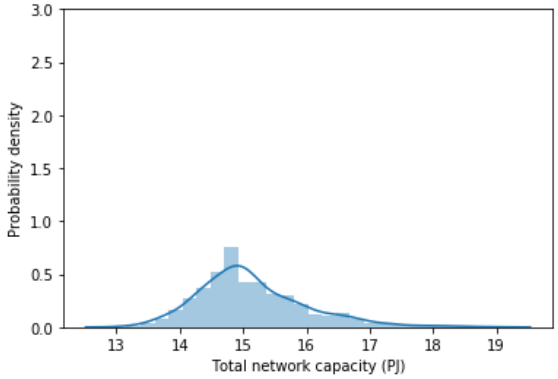

(d) Probability density plot of the cumulative capacity of the network.

Figure H.10: Line plots (a) and probability density plot (b) of the E, G and H network investments cumulative costs and capacity over time over all experiments.

From these line plots, some behavioral patterns are distinguished. First, even though the wind capacity investments data spread is quite small, a small set of very high experiment outcomes

with a value above 13 PJ is identified from both the line plot and the probability density plot. This is the cluster of experiments that corresponds to cluster 6, in which due to the low PV development rate, the investments in wind supply capacity are extraordinarily high. The PV supply capacity invested in portrays a set of experiments with a value above 12.5 PJ as well, also a second 'peak' with a value of 11 PJ can be identified. The P2G conversion capacity line plot patterns correspond with that of the PV supply. This is in accordance with the strong positive correlation between PV and P2G technology investments. Also, the P2G investment trajectories clearly portray pattern-like behavior. These clusters are most easily identified from the starting year of investments in P2G conversion. The first cluster starting in 2030, the second in 2032 (ending with a cumulative capacity $>$ 10 PJ), then 2034 and 2036 (ending with a cumulative capacity $>$ 5 and $<$ 10 PJ) and then the median cluster starting in 2040, 2042 and finally 2044 and ending with a cumulative capacity $>$ 1 and $<$ 5 PJ. These patterns are expected to correlate with the underlying demand development scenarios and the P2G development rate.

H.3 Supply Composition

The figure portrayed in this section (figure H.11) demonstrates the modelled decrease in gas supply to meet the energy transition goal, the energy demand development scenarios, and the PV supply and wind supply capacities invested in. The envelope plots are implemented to facilitate distinction between the four modelled supply and demand factors. However, it should be noted that these envelopes distort the visualization of the actual distribution, as these seemingly portray a continuous distribution across the colored outcome space. The reader is referred to the individual plots of the demand development scenarios (figure D.1), PV supply (figure H.2) and wind supply (figure H.4) for the actual distribution across the outcome space.

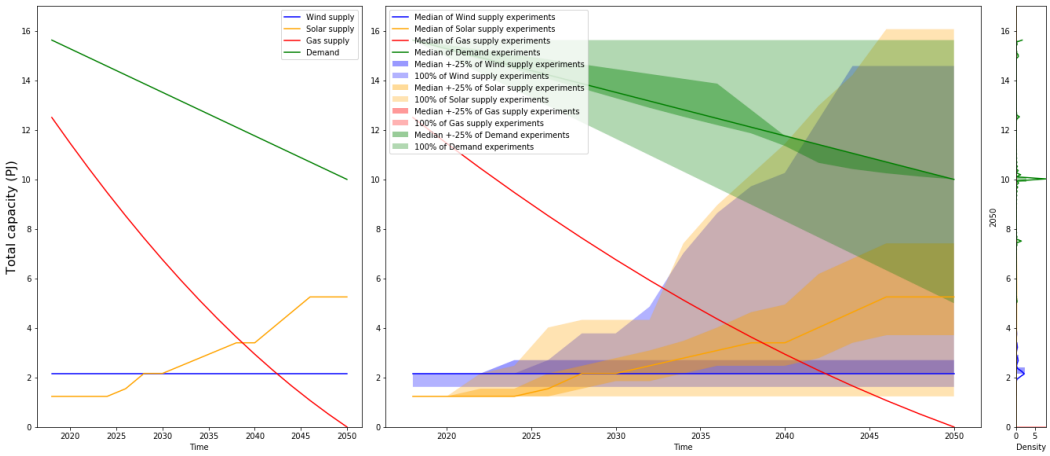

Figure H.11: Line plot of the median supply composition over time over all experiments. The middle figure is an envelope plot and the right figure shows the probability density plot.

H.4 PRIM Subspace Partitioning: Design Trade-offs

In this section, the uncertainties underlying Energy System Design component trade-offs are identified with PRIM subspace partitioning. For uncertainties to be considered 'underlying of' or 'significant to' the behavior, the quasi-p threshold must have a value equal to or higher than 0.05. Consequently, 'non-significant' underlying uncertainties are portrayed in the figures as well, with a qp-value below 0.05, whereas these are not used in this analysis.

H.4.1 Design Trade-off: PV versus Wind Supply

A small pattern of wind capacity experiments that results in an invested capacity higher than 12.5 PJ is distinguished from both the line plot and the probability density plot (figure H.12). Such a set of experiments exists for the PV supply as well, with a capacity invested in above 12.5 PJ.

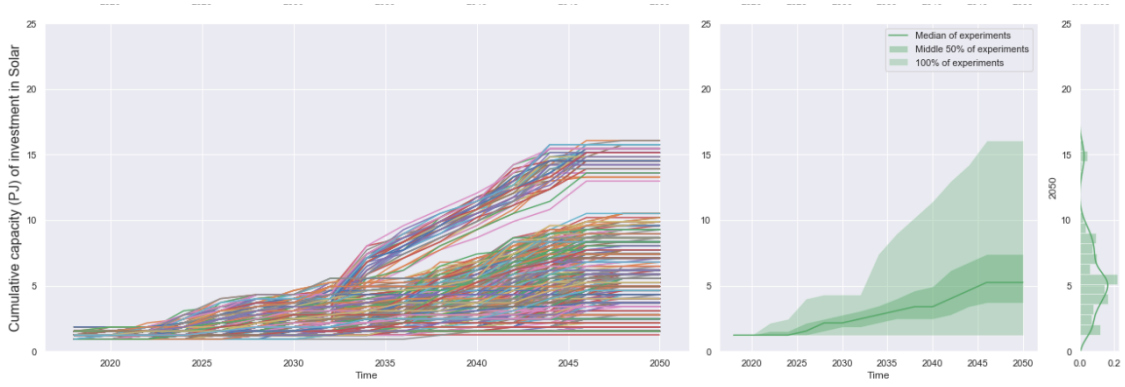

(a) PV supply investments

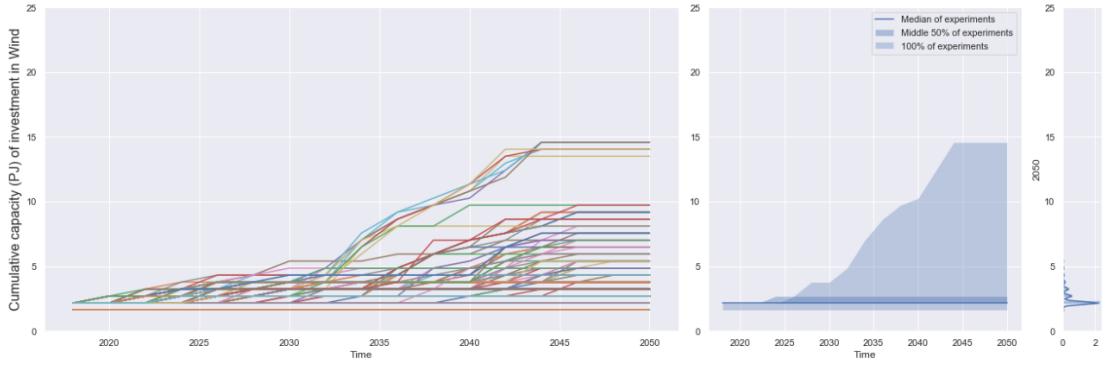

(b) Wind supply investments

Figure H.12: Line plots of the PV supply (a) and Wind supply (b) investments cumulative capacity over time over all experiments.

First, the origin of this high wind capacity cluster is analyzed and compared with the origin of

experiments resulting in similarly high PV supply capacity (figure H.13). Because the number of experiments resulting in a wind capacity invested in > 12.5 PJ is only 7, the minimal mass of the PRIM box is decreased to 0.5% (corresponding to $800 * 0.005 = 4$ experiments).

Both the high PV and wind clusters arise from the demand development scenario 'No change compared to 2018'. Remarkably, for the PV capacity, the second significantly underlying uncertainty range is the PV development rate range $[0.032, 0.075]$. However, marking the negative correlation and a potential tipping point in the PV development rate, for the wind capacity this second range is the PV development rate range $[0.026, 0.032]$. In other words, if the demand development scenario is 11 and the PV development rate has a value below 3.2%, the investments in wind supply capacity are higher, whereas if the PV development rate is valued higher than 3.2%, the investments are high in PV supply capacity.

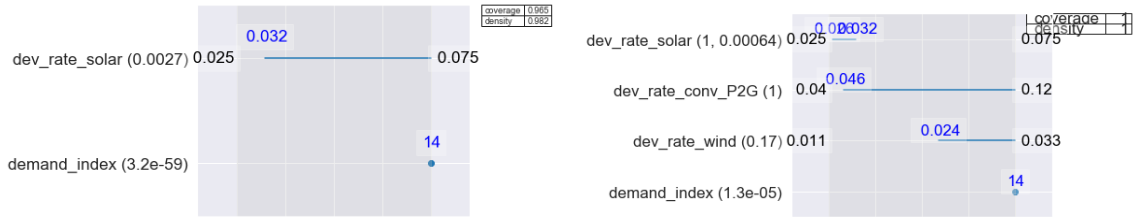

(a) PV supply capacity > 12.5 PJ

(b) Wind supply capacity > 12.5 PJ

Figure H.13: PRIM output of underlying uncertainty ranges resulting in the highest cluster of supply capacity for both the PV supply (a) and wind supply (b) invested in.

Now, to further explore the trade-offs between investing in PV versus Wind supply capacity, the underlying uncertainties for one more range are compared: the outcome space $> Q3$ and < 12.5 PJ (figure H.14a,b). For PV supply, the demand scenario 'Very low E, Very high G, Very low H' is most determining. Followed by the PV development rate range $[0.04, 0.075]$. For wind supply, the experiments resulting in this capacity 'cluster' arise mainly from a PV development rate range $[0.025, 0.04]$. In addition, the demand development scenario 'Very high demand' is determining for these relatively high wind capacity investments. Again, the PV development rate marks a tipping point in the negative correlation between PV and wind supply investments. In other words, if the PV development rate is below 4% and the total demand is very high, the wind supply investments are relatively high. However, if the PV development is above 4%, relatively high PV supply investments are preferred.

H.4.2 Design Trade-off: P2G Conversion & PV Supply

Both the PV supply and the P2G conversion capacity invested in portray a large variation in outcomes and experiment trajectory across experiments (figure H.15). The strong positive correlation between P2G and PV capacity invested in can be perceived from the similar experiment trajectory shapes as well. Even more so, a similar cluster of investment trajectories over

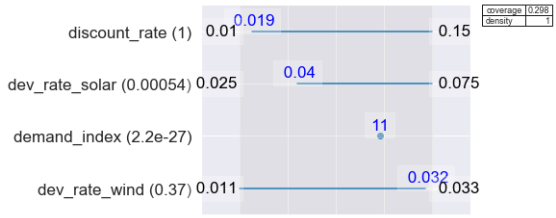

(a) PV supply capacity $Q3 < PJ < 12.5$

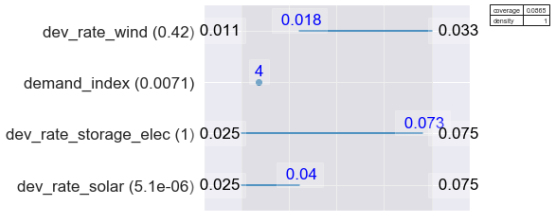

(b) Wind supply capacity $Q3 < PJ < 12.5$

Figure H.14: PRIM output of underlying uncertainty ranges resulting in the cluster of supply capacity $Q3 < PJ < 12.5$ for both the PV supply (a) and wind supply (b) invested in.

time, ending with a capacity value > 12.5 PJ, can be distinguished in both plots. In addition, both Outcomes of Interest portray a 'cluster' of experiments with a cumulative capacity value under the $Q1$-bound (table 5.4).

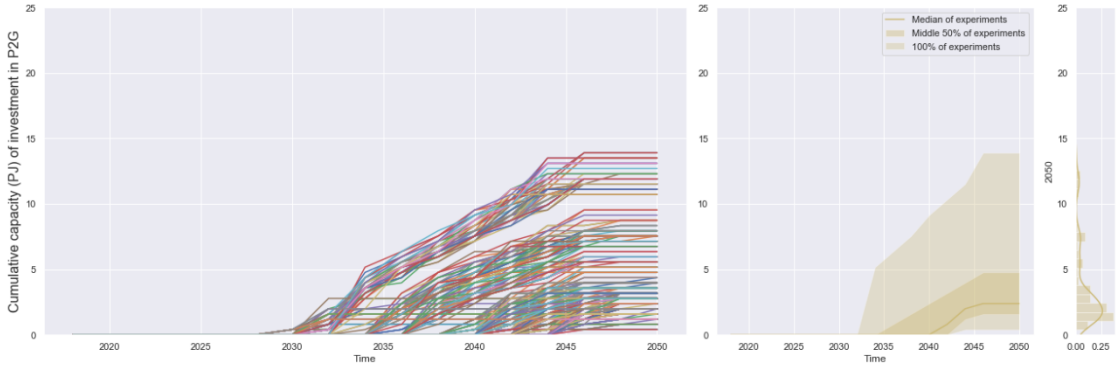

(a) P2G conversion investments

(b) PV supply investments

Figure H.15: Line plots of the P2G conversion (a) and PV supply (b) investments cumulative capacity over time over all experiments.

The origin in uncertainty input for both clusters is identified with PRIM subspace partitioning (figure H.16).

Both the PV supply (57 experiments) and the P2G conversion (66 experiments) experiments resulting in a cumulative capacity invested in above 12.5 PJ arise from the demand development scenario 'No change compared to 2018'. For the PV capacity, the second significantly underlying uncertainty range is the PV development rate range $[0.032, 0.075]$. More specifically, for the PV supply capacity to reach a value above 12.5 PJ invested in, the PV development rate should be higher than 3.2%, in combination with demand scenario 12.

The experiments resulting in a cumulative capacity invested in $< Q1$ PJ, arise from the demand development scenario 'Very low demand'. For the PV supply capacity, this scenario is supplemented with significant determining power of the 'Low demand' scenario and a discount rate range of $[0.01, 0.091]$.

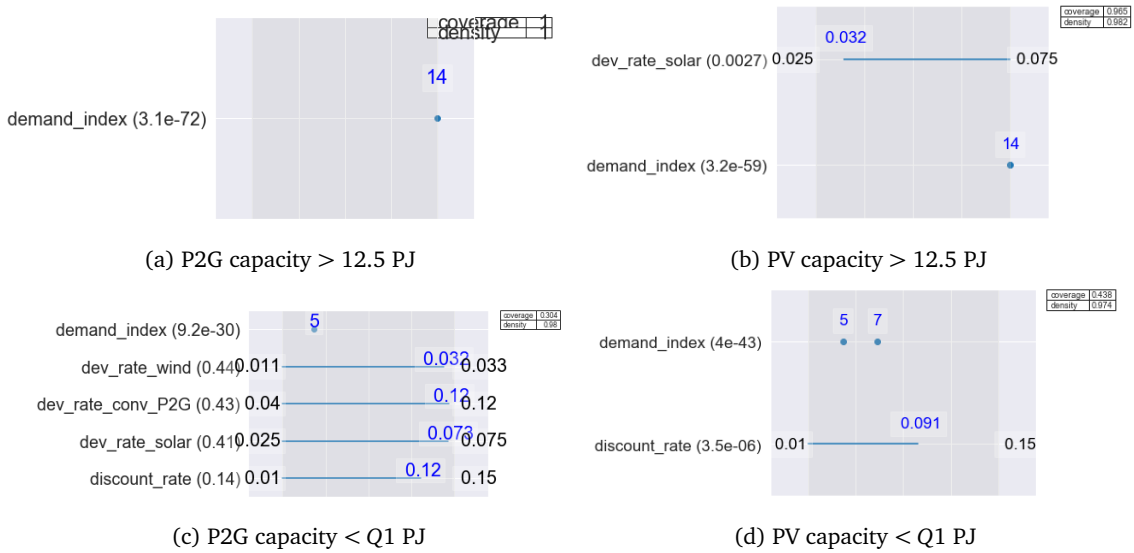

(a) P2G capacity > 12.5 PJ

(b) PV capacity > 12.5 PJ

(c) P2G capacity < Q1 PJ

(d) PV capacity < Q1 PJ

Figure H.16: PRIM output of underlying uncertainty ranges resulting in similar P2G conversion (a,c) and PV supply (b,d) capacities invested in.

H.4.3 Design Trade-off: CHP Conversion versus Gas Storage

Both the CHP conversion and the gas storage investments are discretely distributed across experiments (Appendix H.2). Therefore, the uncertainty input causing opposing investment trade-offs is not identified with visually identified clusters from the line plots. Instead, the Q1 and Q3 borders are used to identify the uncertainty input resulting in high CHP and low gas storage capacities and vice versa, as the CHP conversion and gas storage capacity invested in are negatively correlated (figure H.18).

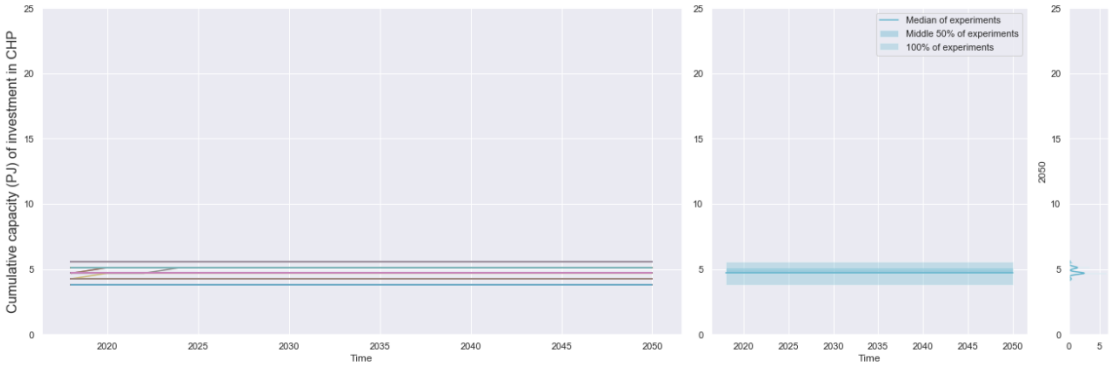

(a) CHP conversion investments

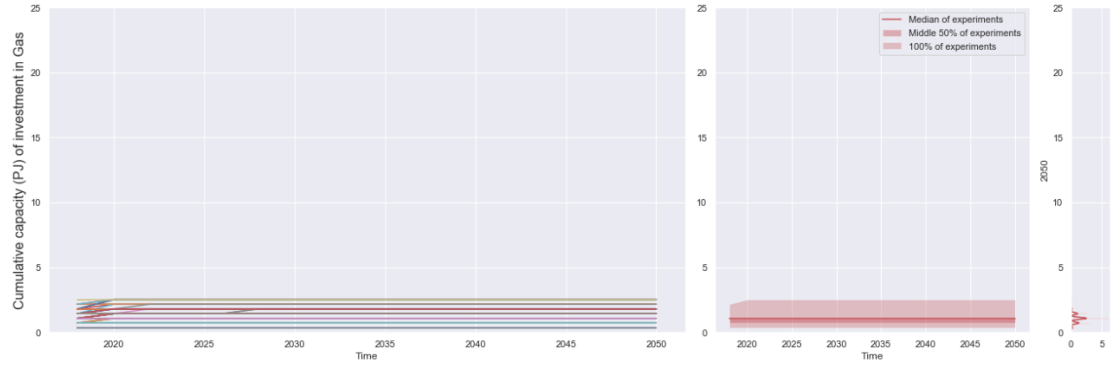

(b) Gas storage investments

Figure H.17: Line plots of the CHP conversion (a) and Gas storage (b) investments cumulative capacity over time over all experiments.

The sample sizes of the two 'clusters': CHP $>$ $Q3$ & gas storage $<$ $Q1$ and CHP $<$ $Q3$ & gas storage $>$ $Q1$ are too small to maintain the default minimum mass threshold of the PRIM boxing algorithm. Therefore, the minimum mass is decreased from the default 5% to 2% (corresponding to $800 * 0.02 = 16$ experiments) to retrieve accurate subspace partitioning results.

The demand scenario 'Fast change', with exponential change, results in the 42 experiments with the highest CHP and the 34 lowest gas storage capacities invested in.
The 73 experiments with lowest CHP and the 36 experiments with highest gas storage capacities arise from the demand scenarios 'Very fast change' and 'No change compared to 2018'. A discount rate range of $[0.01, 0.11]$ is responsible for the lowest quantile CHP capacity investments. The lowest quantile gas storage investments however, are determined by a discount rate range of $[0.047, 0.15]$.

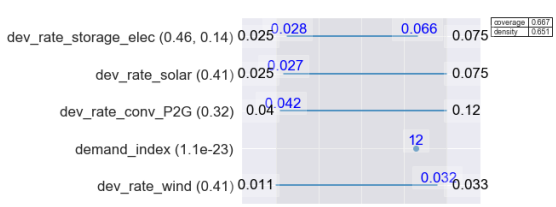

(a) CHP conversion capacity > $Q3$ PJ

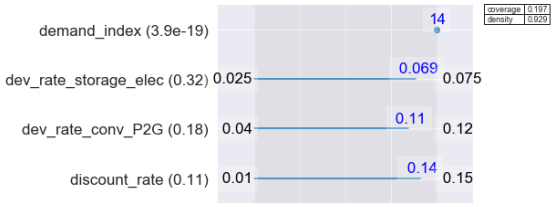

(b) Gas storage capacity > $Q3$ PJ

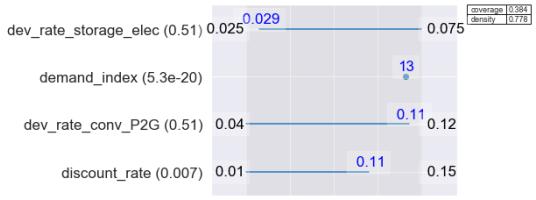

(c) CHP conversion capacity < $Q1$ PJ

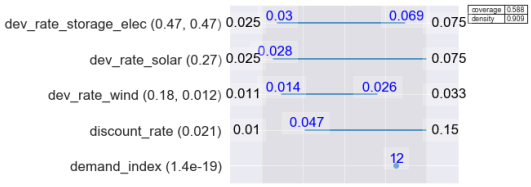

(d) Gas storage capacity < $Q1$ PJ

Figure H.18: PRIM output of underlying uncertainty ranges resulting in opposing CHP conversion (a,c) and gas storage (b,d) capacities invested in.

Appendix I

Code

The Python files that are used in this research are made accessible in a GitHub folder. All files concern the proof of concept method application to an existing Energy System Optimization Model and its modelled case. The two Python files that concern the specific model specification are not included, because it is confidential. When interested in these, the model-owner can be contacted via: `i.v.beuzekom@tue.nl`. Please note that a lot of changes in the code are required to link the Workbench to a different model. Also, the codes to process the data are tailored to the proof of concept. Model-owners and analysts that desire to apply the proposed method to their own model are referred to the documentation of the EMA Workbench: `https://emaworkbench.readthedocs.io/en/latest/` and `https://github.com/quaquel/EMAworkbench`.

The following link leads to all the files used for this research: `https://github.com/HelloYoulie/exploratory-modelling-optimization-models`.

This concerns the following files:

- Linkage between the EMA Workbench and the Energy System Optimization Model. This includes the specification of the uncertainties and their ranges.
- The linked Energy System Optimization Model which is run from the Workbench. The lower part of the code entails the specification of what is exported as output back to the Workbench.
- Results Analysis
  - Importing the Exploratory Modelling output data.
  - Calculate the percentage of experiments that is solved to optimality.
  - Preprocessing of the entire output data set.
  - Calculating the number of investments, and share of investments of the preprocessed output data aggregated to different desired design specifics.

  - Calculate the energy capacity that is invested in (in PetaJoules) for the design specifics.

- Energy System Design Clustering
  - Function to Produce the Cosine Distance Matrices
  - Cosine Distance Matrix and Visualization
  - Cosine Distance-based Agglomerative Clustering
  - Cluster-based CART Subspace Partitioning
  - Cluster Characterization

- Energy System Design Trade-offs
  - Specification of Outcomes of Interest
  - Characterization of the Outcomes of Interest
  - Density Plots
  - Boxenplot
  - Correlation matrix
  - PRIM Subspace Partitioning
  - Sensitivity Analysis
  - Development over Time across Experiments
  - Various lineplots

Hello, here is some text without a meaning. This text should show what a printed text will look like at this place. If you read this text, you will get no information. Really? Is there no information? Is there a difference between this text and some nonsense like “Huardest gefburn”? Kjift – not at all! A blind text like this gives you information about the selected font, how the letters are written and an impression of the look. This text should contain all letters of the alphabet and it should be written in of the original language. There is no need for special content, but the length of words should match the language.